(Swim) water quality modelling in the city of Amsterdam

MSc thesis by Amber van den Tillaart

February 2017

Environmental Systems Analysis Group

WAGENINGEN UNIVERSITY
WAGENINGEN UR

(Swim) water quality modelling in the city of Amsterdam

Master thesis at the Environmental Systems Analysis Group submitted in partial fulfilment of the degree of Master of Science in Environmental Sciences at the Wageningen University, the Netherlands

Study program:
MSc Environmental Sciences

Student registration number:
940808832080

ESA-80436

Supervisors:
WU Supervisor: Nynke Hofstra
Deltares supervisor: Bas van der Zaan and Erwin Meijers
Waternet supervisor: Liesbeth Hersbach

Examiners:
Prof. Rik Leemans
WU Supervisor: Nynke Hofstra

Date: February 15th, 2017

Environmental System Analysis Group, Wageningen University

Abstract

Increasingly people enjoy swimming in Amsterdam's canals. Yet the canal's water quality is questionable. After the Amsterdam City Swim of 2015, one third of the people who answered the questionnaire of the municipal health agency (GGD, response rate 50%), suffered from gastrointestinal illness in the week after the City Swim. Gastroenteritis symptoms are diarrhoea, indigestion, nausea and stomach-ache. Water quality is monitored every second week during the swimming season (mid April – end September) by Waternet. Analysing those samples takes, however, three days. This means that the actual situation is not available and peaks can be easily missed. Waternet would like to improve the water quality information that they provide to swimmers.

Modelling provides opportunities to achieve this. This research therefore focusses on water quality modelling of Amsterdam's canals to enhance Waternet's ability to better predict actual water quality and Gastroenteritis risks. The research area is the un-official swim location Somerlust. Here the waters of the Amstel and Weespertrekvaart converge and enter the city.

The faecal indicator *Escherichia Coli* is used as a proxy for microbial water quality. Modelling is done with the modelling software SOBEK that includes Waternet's 'Boezemmodel.' The 'Boezemmodel' covers all water ways and their discharges from Utrecht to IJmuiden. SOBEK also comprises the water-quality model DELWAQ. To set up DELWAQ for Somerlust, I reviewed the literature for information on sources of faecal bacteria in surface waters and their loads and decay rates. The model output is validated using Waternet's water quality measurements from 2013 and 2015. The calibrated variables are the best typical concentrations per source and the variables in the decay formula. The water fractions, age and *E coli* loads were computed to determine how Somerlust's hydrological system behaves and what its *E coli* sources and concentrations are.

The model results for 2013 compare 'sufficiently' and for 2015 almost 'good' to observations. The upstream Waste Water Treatment Plant of Amstelveen causes the highest loads of *E coli* concentration at Somerlust throughout the year. The *E coli* peaks during the summer season are caused by the discharges of the separated sewer overflows as a result of rainfall events on the other side of the canal. Somerlust's water quality is not strongly affected by the polders and the combined sewer overflows just downstream of Somerlust. The decay of *E coli* in surface waters is strongly dependent on the water temperature.

The model is used to estimate the risk of to get gastroenteritis. The literature review related *E coli* concentrations and this risk. The resulting formula that links water quality to the chance of getting gastrointestinal problems indicated that this risk was low (i.e. less than six percent) during 66, 54 and 34 summer days in 2013, 2014 and 2015 respectively.

This research offers a good basis to forecast actual water-quality values. This system can be operational for the summer of 2017. To do this, the 'Boezemmodel' has to be cut into a smaller area. This is most relevant for calculating Somerlust's *E coli* concentrations during the swimming season. Enhancing this part of the model into a 2D or 3D model probably results in more reliable water mixing and therefore more accurate concentrations and risks estimates.

My study showed that the impact of separated sewer overflows in Somerlust is substancial in summer. This impact can be reduced by correcting faulty connections in sewer systems. Amstelveen's treatment plant also majorly affects the water quality at Somerlust, but its exact effluent concentration is unknown. Sampling its effluent to obtain better model inputs likely leads to better predictions. Finally, more water quality measurements at Somerlust would increase the calibration's reliability.

My study is a first step towards an early warning system for Gastroenteritis risks in city swims and seasonal swimming in Amsterdam's canals. These risks are not nil on most swimming days. This research provides a sound basis for operationalization of estimating the actual risks during the swimming season.

Contents

1 Introduction 10
1.1 Water recreation in Amsterdam 10
1.2 Impact of weather conditions 10
1.3 Current water quality monitoring practices 10
1.4 Research area 11
1.5 Objective 11
1.6 Reading guide 12
2 Methods 14
2.1 Why modelling 14
2.2 SOBEK2 14
2.3 Hydrological system around Somerlust 14
2.4 Water quality modelling 15
2.5 Calibration, sensitivity analysis and validation of the model 20
2.6 Risk assessment 21
3 Results 25
3.1 Hydrological analysis using fractions and age tracers 25
3.2 Sensitivity analysis 28
3.3 Calibration and validation 35
3.4 Model results 43
3.5 Typical concentrations of faecal bacteria per source 45
3.6 Influence of weather conditions 48
3.7 Assessment of human health risks 52
4 Recommendations for making an actual forecast 53
5 Discussion 55
6 Conclusion 57
References 58
Annexes i

List of Tables

Table 1 Areas of interest related to product line SOBEK River (Part of a table of Deltares, 2016) 14
Table 2 The spectra of concentrations per source of faecal indicator bacteria in urban waters used in the model 17
Table 3 Swim water quality scales as decided by the European Bathing Water Directive (EP, 2006). 22
Table 4 Results of previous epidemiologic studies in one table 23
Table 5 Fractions and age of the water during summer season for several bigger sources for location Somerlust (2015) 27
Table 6 Variables tested in the model and the values used in the sensitivity analyses 28
Table 7 The spectra of concentrations per source of faecal indicator bacteria in urban waters used in the model (Chapter 2.4.1), including the initial concentrations used in the calibration and the typical concentration for this water system 35
Table 8 Constants in the decay formula of Mancini with the initial values and the typical values for this model 35
Table 9 Output of the target diagram of location AMS009 with the exact values for the biases, RMSD's and distances to the centre for the WWTP 37
Table 10 Output of the target diagram with the exact values for the biases, RMSD's and distances to the centre for the WWTP 38
Table 11 Output of the target diagram with the exact values for the biases and RMSD's of a SSO with an effluent of 1.10^5 or 7.10^4 *E coli* (CFU/100mL) 38
Table 12 Output of the target diagram with the exact values for the biases, RMSD's and distances to the centre for Mrt/ K_0 39
Table 13 Output of the target diagram with the exact values for the biases, RMSD's and distances to the centre for FrUV 40
Table 14 Output of the target diagram with the exact values for the biases, RMSD's and distances to the centre for cfRAD 40
Table 15 Output of the target diagram with the exact values for the biases, RMSD's and distances to the centre for extinction 41
Table 16 Output of the target diagram with the exact values for the biases, RMSD's and distances to the centre for temperature coefficient 42
Table 17 Concluding table with the constants in the decay formula and the typical values used in this model 42
Table 18 Output of the target diagram with the exact values for the biases, RMSD's and distances to the centre for the final model result 43
Table 19 Minimum and maximum concentration per source as was found in literature (Table 2) together with the final typical concentrations used in the model 45
Table 20 The numbered tracers with the associated sources 45
Table 21 Precipitation, water temperature and radiation over the same week as Figure 46 51
Table 22 Summary of the summers of 2013 and 2015 and its water quality linked to the chance of getting GI problems 52
Table 23 Daily values of water temperature and radiation, used as model and decay input ii
Table 24 Additional mortality rate due to difference in radiation xii
Table 25 Measurements of *E coli* bacteria during the City Swim of 2015 xiii
Table 26 Concluding table corresponding to the final Figure 10 in Chapter 2.6 xiii
Table 27 Concentrations per day per polder xiv

Table 28 Calculation table for Duivendrecht polder as example to show how to transformation of numbers is done xv
Table 29 Runoff areas per separated sewer overflows obtained from QGIS, numbers corresponding with Figure 55. xv
Table 30 Runoff areas and width per combined sewer overflows obtained from QGIS, names corresponding with Figure 56. xvi
Table 31 Detailed table with fraction and ages of the water corresponding (2013).....xix
Table 32 Results of the q-PCR analysis for source determination of faecal bacteria at Somerlust (2016) xix

List of Figures

Figure 1 Map showing the waters of Amsterdam and the track of the ACS in relation to the location of Somerlust 11
Figure 2 Process steps as a guideline for this research linked to the different research questions. The solid lines provide inputs for the other boxes, the dotted line shows that the boxes are linked and the dashed line shows that the system analysis is used to conduct a hindcast and sensitivity analysis but that the system analysis is grasped by the hindcast and sensitivity analysis. 13
Figure 3 Example of a fraction calculation at location Somerlust 15
Figure 4 Schematisation showing the sources of faecal indicators (filled arrows) contaminating the urban surface water. 16
Figure 5 Overview of the sources included in this research with the minimum and maximum values in CFU/100mL in the upper right corners 17
Figure 6 Mortality rate of *E coli* at location Somerlust plotted over the three years 19
Figure 7 Added combined and separated sewer overflows close to location Somerlust 19
Figure 8 The selected branches to which the dispersion coefficient of 1 is applied 20
Figure 9 Calibration of the water flow in the 'Boezemmodel' with Chloride concentration as bench-mark (Erwin Meijers, 2016). With 'Huidige situation' the model output is aimed. 21
Figure 10 Curve which links the water quality to the chance of getting GI problems, as a conclusion of the concluding studies, ACS 2015 and the chance to get GI problems in general. 24
Figure 11 Simplified map of the water ways around Amsterdam (Boezemmodel), including numbers corresponding to the fractions 25
Figure 12 Fraction calculation of origin from the water at Somerlust (year 2015) 26
Figure 13 Line graph showing the fraction of WWTP Amstelveen and the precipitation 26
Figure 14 Graph showing the duration of the water of WWTP Amstelveen until it reaches Somerlust (2015) 27
Figure 15 Testing different concentrations for the WWTPs and their effect on Somerlust over time 29
Figure 16 Testing different concentrations for the WWTPs and their effect on Somerlust for the summer of 2013 (zoomed into Figure 15) 29
Figure 17 Effect of different input values for the combined sewer overflow on the *E coli* concentration at Somerlust 30
Figure 18 Impact of the different input values for the separated sewer overflows on Somerlust over time 30
Figure 19 The impact of applying a decay rate on the *E coli* concentration at Somerlust or not applying a decay rate 30
Figure 20 Different runs for k_0 values for the decay rate of *E coli* in Amsterdam 31
Figure 21 Different runs for fractionUV values for the decay rate of *E coli* in Amsterdam 31
Figure 22 Different runs for conversion factor radiation to mortality (m2/W/d) for the decay rate of *E coli* in Amsterdam 32
Figure 23 Four different runs for extinction of UV radiation (m-1) in the city of Amsterdam 32
Figure 24 Different runs for the salinity (mg/L) in the water of Amsterdam 32
Figure 25 Different salinity coefficients for the decay rate of *E coli* in the city of Amsterdam 33
Figure 26 Four different runs with different decay rate due to temperature deviation from 20 degrees Celsius 33
Figure 27 Simplification of the water system around Somerlust with measurement location AMS009 included 36

Figure 28 Target diagrams of both Somerlust and AMS009 in relation to different WWTP effluent concentrations 37
Figure 29 Target diagrams of two runs. One with an input value for the WWTPs of 2.10^4 CFU/100mL and one with 3.10^4 CFU/100ml. 37
Figure 30 Target diagram with different *E coli* concentrations in the effluent of the SSOs and their effect on Somerlust 38
Figure 31 Target diagram with only the plots of SSO loads of 1.10^5 and 4.10^7 *E coli* [CFU/100mL] 39
Figure 32 Target diagram for different k_0 values for the decay rate of *E coli* in Amsterdam 39
Figure 33 Target diagram for fractionUV values for the decay rate of *E coli* in Amsterdam 40
Figure 34 Target diagram for conversion factor radiation to mortality (m2/W/d) for the decay rate of *E coli* in Amsterdam 40
Figure 35 Four different runs for extinction of UV radiation (m-1) in the city of Amsterdam 41
Figure 36 Target diagram with four different runs with different decay rate due to temperature deviation from 20 degrees Celsius 41
Figure 37 Final model output of *E coli* concentration CFU/100mL over time at location Somerlust compared to the measurements 43
Figure 38 Representation of the root-mean square difference of the model results with respect to the observations 43
Figure 39 *E coli* concentration at Somerlust in the period 2013-2015 with the shares of each source of pollution shown and the measurements 46
Figure 40 *E coli* concentration at Somerlust in the summer of 2015 with the shares of each source of pollution shown and the measurements (zoomed into Figure 39) 46
Figure 41 Figure with percent of each of the defined fractions in the *E coli* concentration at Somerlust 46
Figure 42 Precipitation, water temperature, radiation and the *E coli* concentration at Somerlust of 2013 plotted in one diagram 49
Figure 43 Precipitation, water temperature, radiation and the *E coli* concentration at Somerlust of 2015 plotted in one diagram 49
Figure 44 *E coli* concentration at Somerlust in the summer of 2015 with fractions and precipitation 49
Figure 45 Line chart with the *E coli* concentration and water temperature at Somerlust for years 2013 and 2015 50
Figure 46 *E coli* concentration and its fractions at Somerlust over one week in the summer of 2015 50
Figure 47 Simplified graph of the process time needed for a forecast 53
Figure 48 Schematisation of the water system around Somerlust 54
Figure 49 Day length over time used in this model xi
Figure 50 Water depth over time at location Somerlust xi
Figure 51 Temperature and Salinity mortality rates plotted against the water temperature xii
Figure 52 Decay rates per day of *E coli* modelled in SOBEK over time xiii
Figure 53 Discharges at the Berlage-brug of the new and initial datafile xiv
Figure 54 Explanation of swim-runoff-season, designed by Mol *et al.* (2005) xiv
Figure 55 Location and numbers of separated sewer overflows xvi
Figure 56 Location and names of the different combined sewer overflows xvii
Figure 57 All the data combined for calculating the discharges of the combined SO in as example Weesperzijde69 xvii
Figure 58 Fraction calculation for location Somerlust year 2013 xviii

Figure 59 Fraction calculation for location Somerlust year 2014 xviii
Figure 60 Travel time from the water of WWTP Amstelveen till Somerlust plotted together with the rainfall (2015) xix
Figure 61 Location tHuis aan de Amstel compared to Somerlust xx
Figure 62 Figure with percent of each of the defined fractions in the *E coli* concentration at Somerlust including precipitation xx
Figure 63 Hourly discharges in 2014 at the Berlagebrug close to the locations of the CSOs xxi
Figure 64 Daily discharges at the Berlagebrug close to the locations of the CSOs xxi
Figure 65 *E coli* concentration at Somerlust in the summer of 2013 with fractions and precipitation xxii

List of abbreviations

ACS	Amsterdam City Swim
CFU	Colony Forming Units
CSO	Combined sewer overflow
GI	Gastrointestinal Illness
HDSR	'Hoogheemraadschap De Stichtse Rijnlanden'
E coli	*Escherichia Coli*
IE	Intestinal Enterococcus
NAP	'Normaal Amsterdams Peil'
SSO	Separated sewer overflow
UV	Ultraviolet
WWTP	Waste Water Treatment Plant

1 Introduction

1.1 Water recreation in Amsterdam

Nowadays, an increasing number of people enjoy recreational swimming within cities. Especially in Amsterdam, a city that is surrounded by water and is famous for her canals, people like to swim in the canals during summertime. They are then exposed to the canal waters (Schets *et al.,* 2008). The willingness of Amsterdam's citizens to swim evolved together with the feeling that Amsterdam's water quality had improved, the latter is confirmed by Waternet and OIS (pers. comm. Hersbach, 2016; OIS, 2015). The connection of the houses along the canals to the sewer system in 1987, the relocation of the waste water treatment plant in Amsterdam West in 2006 and the connection of most houseboats to the sewer made sure that the water quality indeed increased (Amsterdam Marketing, 2015; OIS, 2015). Moreover, flushing the canals of Amsterdam with water from the IJ was, after implementing those measures, also not needed anymore and this rapidly improved the water quality even further (pers. comm. Hersbach, 2016).

Currently nine official swim areas exist in Amsterdam and over forty un-official places within the city and the last number is still increasing (OIS, 2015). Next to that, the study of OIS (2015) showed that 37 percent of the citizens does swim in open waters within the city and 5 percent swims actually in the canals of Amsterdam.

Although Amsterdam Marketing (2015) and OIS (2015) both state that "the water in the canals of Amsterdam is now cleaner than ever," the quality can still not be guaranteed and does not always meet safety standards (pers. comm. Hersbach, 2016). This can negatively affect health and thus raises questions. For example, during the week after the Amsterdam City Swim of 2015, 31 percent of the swimmers, that answered the questionnaire of the Gemeentelijke Gezondheidsdienst (GGD, response rate 50%), got gastrointestinal health complaints (GGD Amsterdam, 2016).

1.2 Impact of weather conditions

Weather conditions do also play a role in the quality of the water. Previous studies show an increase in 'faecal indicators in surface waters after heavy rainfall events, due to sewer overflow and surface runoff' (Rechenburg *et al.,* 2006 and Goyal *et al.,* 1977). And those heavy rainfall events within cities are expected to increase in the future due to climate change which induces more intense rainfall (Lenderink and Meijgaard, 2008). Urbanisation and imperviousness of urban areas increases inflow to urban drainage systems (ten Veldhuis *et al.,* 2010) resulting in earlier overflows. Next to that, temperature and UV radiation also play a role in the growth or destruction of faecal bacteria in water (van de Wal *et al.,* 2012; Moresco *et al.,* 2016; Liu *et al.,* 2006).

1.3 Current water quality monitoring practices

Currently measurements related to water quality are done by Waternet, although, as the Amsterdam canals are not official European bathing sites, the water quality is not always routinely monitored (Schets *et al.,* 2008). At some specific locations, samples tested for *Escherichia Coli* and intestinal enterococcus are taken once every two weeks during the summer period (mid-April to October), yet on other locations those measurements are taken only once per summer and some locations are not even tested at all (pers. comm. Hersbach, 2016). Moreover, this testing method takes three days to get the results (pers. comm. Hersbach, 2016), this means that the available data are always behind the actual situation and that there is a chance that events of bad water quality are missed. Modelling the water system in such a way that enables to timely indicate water quality, would in this case provide a solution. Hereby is un-official swim location Somerlust taken as research location.

1.4 Research area

Location 'Somerlust' in Amsterdam was selected as research area for the water quality modelling in this study. Somerlust is located along the river Amstel and is an unofficial swim location in front of the headquarters of Waternet. It is an often used swim location, especially after cleaning the 'underwater bottom' in early summer this year (pers. comm. Hersbach, 2016). The picture on the cover page of this thesis is made at the location at August 23th 2016. As Waternet recognized this location as a possible swim location already several years ago, the concentrations (in CFU/100ml) of *E coli* and intestinal enterococcus are already measured there over the last summers and can therefore be used for calibration. Via this location (Figure 1), water from the Amstel River enters the canals of Amsterdam. The location of the plot is 52°20'27.0" N latitude and 4°55'01.1"E longitude and has an elevation of 0.3 meters NAP (AHN, n.d.).

The water system around Somerlust was already mapped by Waternet in the so-called 'Boezemmodel.' This model covers all the water ways and their discharges from Utrecht to IJmuiden.

If the water quality modelling at Somerlust is successful, the expansion of this research to other locations within the canals of Amsterdam on the track of the Amsterdam City Swim is a likely follow-up (Figure 1).

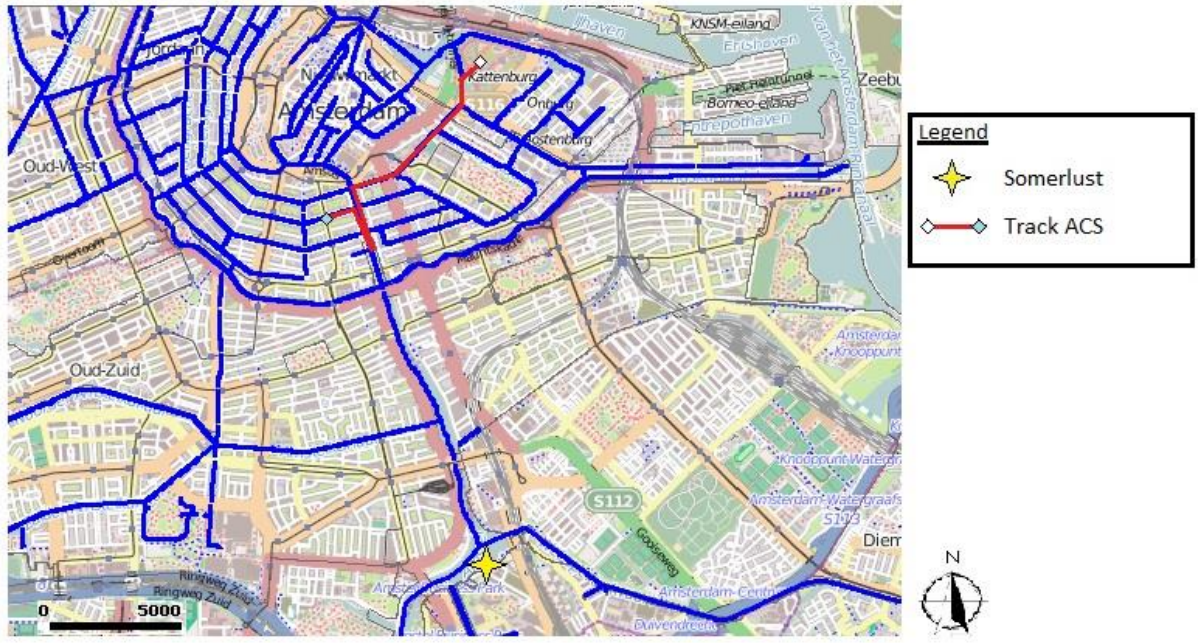

Figure 1 Map showing the waters of Amsterdam and the track of the ACS in relation to the location of Somerlust

1.5 Objective

Therefore, the research aims to model the water quality in the urban surface water at Somerlust in Amsterdam and to link the water quality to health risks of participants of swim-event. This research also provides recommendations to conduct forecasts for the next summer season. Related to this objective the following research questions (RQs) are formulated and will be answered in this research:

RQ 1) How does the hydrological system around Somerlust behave? What are the most dominant sources of water?
RQ 2) What are the sources of faecal bacteria in this hydrological system?
RQ 3) What are the typical concentrations per source and net concentrations at Somerlust?
RQ 4) How do the faecal bacteria behave in the surface water?
RQ 5) How are the sources, typical concentrations and net concentrations at Somerlust related to weather conditions?

RQ 6) How do the model outputs compare to observations?
RQ 7) What is the sensitivity of the model to the variables?
RQ 8) How do the concentrations relate to human health risks?
RQ 9) What is required to make an actual forecast of the health risks of swim-events?

1.6 Reading guide

This paper continues with the research's methodology. In this methodology the reader will be follow the research steps. First of all it will explain why modelling and which model is used. Afterwards the importance of understanding the hydrological system around the location is discussed. The methodology follows with a literature study on faecal bacteria (RQ 2) (RQ 4) as input for the model setup. The sensitivity analysis and calibration and validation of the model are described and lastly a way to link the water quality to human health impacts (RQ 8). The next Chapter of this thesis is the results. The first findings are the biggest water sources for location Somerlust and their time to reach Somerlust (RQ 1). Afterwards the sensitivity of the model variables are reviewed (RQ 7). The Goodness of Fit analysis provides the initial and net concentrations per source (RQ 3), which leads to the final model outputs (RQ 6). After that the weather influences are analysed (RQ 5). Finally, human health risks of swimming at location Somerlust are assessed. Recommendations for Waternet to operationalize this model before the summer of 2017 are provided when answering the final research question 'What is required to make an actual forecast of the health risks of swim-events?' (RQ 9). This is described in Chapter 4. The discussion touches several aspects that could be improved in this model, however it also shows why the current model uses the best opportunities and provides thereby the best model result. The remaining part of the paper proceeds with a catchy conclusion, the reference list and eleven Annexes.

Figure 2 shows the structure of the study and of this report. The numbers matches with the research questions. When answers to the research questions are given in this report, the research question and its answer are summarized underneath that Chapter.

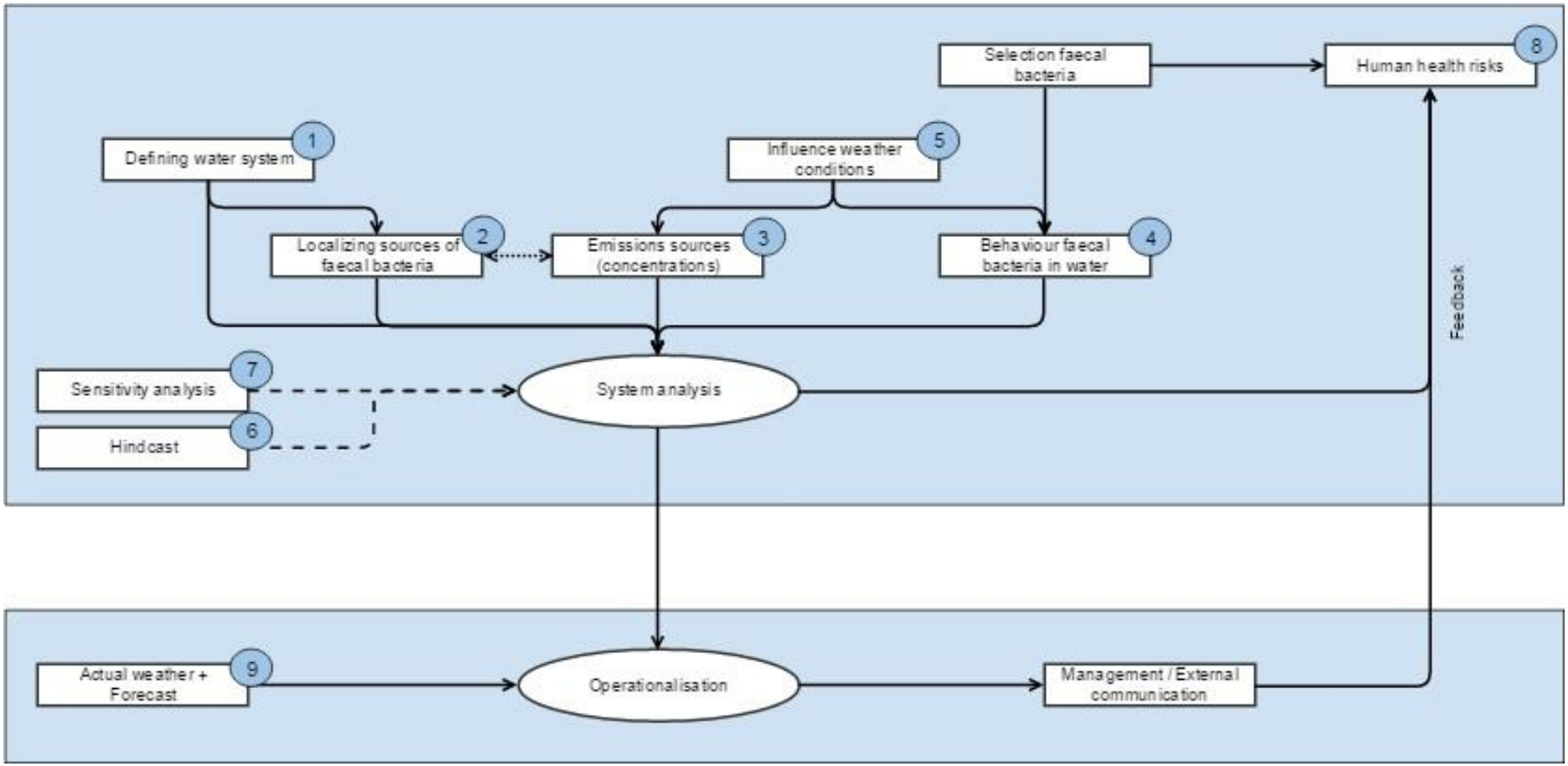

Figure 2 Process steps as a guideline for this research linked to the different research questions. The solid lines provide inputs for the other boxes, the dotted line shows that the boxes are linked and the dashed line shows that the system analysis is used to conduct a hindcast and sensitivity analysis but that the system analysis is grasped by the hindcast and sensitivity analysis.

2 Methods

The methodology for this research was divided into six Sections. Namely, the reason why modelling is applied, a description of the model used, the methodology how the hydrological system was analysed, a description about the water quality modelling, calibration, sensitivity analysis and validation and at last the basis for the risk assessment.

2.1 Why modelling

As described in the introduction, monitoring data of faecal bacteria is always behind the actual situation and samples are not taken on a daily basis; an accurate model would predict the water quality on a shorter time span. In addition, a model hindcast could not only give insight in the water quality at the days samples are taken but could give information about the water quality throughout the year. Moreover, modelling can give insight in the origin of water sources by conducting a fraction computation, the travel time of sources by conducting an age computation and the origin of the contamination of the water.

2.2 SOBEK2

The two dimensional hydrodynamic model SOBEK was used to model the water system around Somerlust as this model is already applied by Deltares and Waternet. Deltares has developed SOBEK together with the RIZA (National Dutch Institute of Inland Water Management and Wastewater Treatment) and other Dutch consulting companies (Deltares, 2016).

SOBEK perfectly suits to total water management as it can link rivers, canals and sewer systems (Deltares, 2016). Pumps, sluice gates, weirs and other structures can all be incorporated. SOBEK is a valuable model for integral water solutions on a big and small scale, for example flood forecasting (Moel *et al.,* 2012), sewer overflow design, river morphology regulation, but also for water quality control and simulating water quality processes (Deltares, 2016) (Table 1).

Product Line	Area of Interest
SOBEK River	Navigation
	Flood protection, flood-risk assessment
	Water pollution studies
	Estuaries with fresh and salt water
	Sand mining, sediment and morphology studies

Table 1 Areas of interest related to product line SOBEK River (Part of a table of Deltares, 2016)

The system includes boundary nodes, lateral flows, connection nodes, measurement points and stations, cross-sections, weirs, pump stations, bridges and many more. Besides the general nodes, other nodes can be added manually. This is done for this model by for example adding the Lek inlet, polders, sewer overflows and WWTPs. Results can be displayed in maps, charts, tables and animations.

The network of 'Boezemmodel 6,' designed by Waternet and last updated the 3th of November 2016, was used as the bases of this research. The 'Boezemmodel' covers all the water ways and their discharges from Utrecht to IJmuiden.

2.3 Hydrological system around Somerlust

First of all, the hydrological system around Somerlust had to be understood. Therefore the main sources of water and Somerlust's contaminants had to be known.

This Section of the reports gave insight in the water flow (Q) of this water system. Knowing where the water comes from and how long it took to reach Somerlust are two aspects needed to understand the hydrological system around Somerlust and thereby the Q. Afterwards the loads (C) could be added and those loads were dependent of the Q.

To model Somerlust's water quality, the relative contribution of the different sources to the total water quality at Somerlust was calculated with fraction calculations. In modelling, fraction calculations are model runs in which the original sources of the waters are tracked and finally the output of those runs are given in percentage of water at a certain location from another location. For example, a quarter of the water at location X (Somerlust) originates from location A, ten percent of the water comes from location B etcetera. All the fractions together should result in a total of 100 percent. An example of a fraction calculation and its output is shown in Figure 3. Besides fractions of water from different sources it is important to know how long the water took from flowing from location A (one of the sources) to location X. The latter is useful to understand later on in this research as the time influences the survival of faecal bacteria.

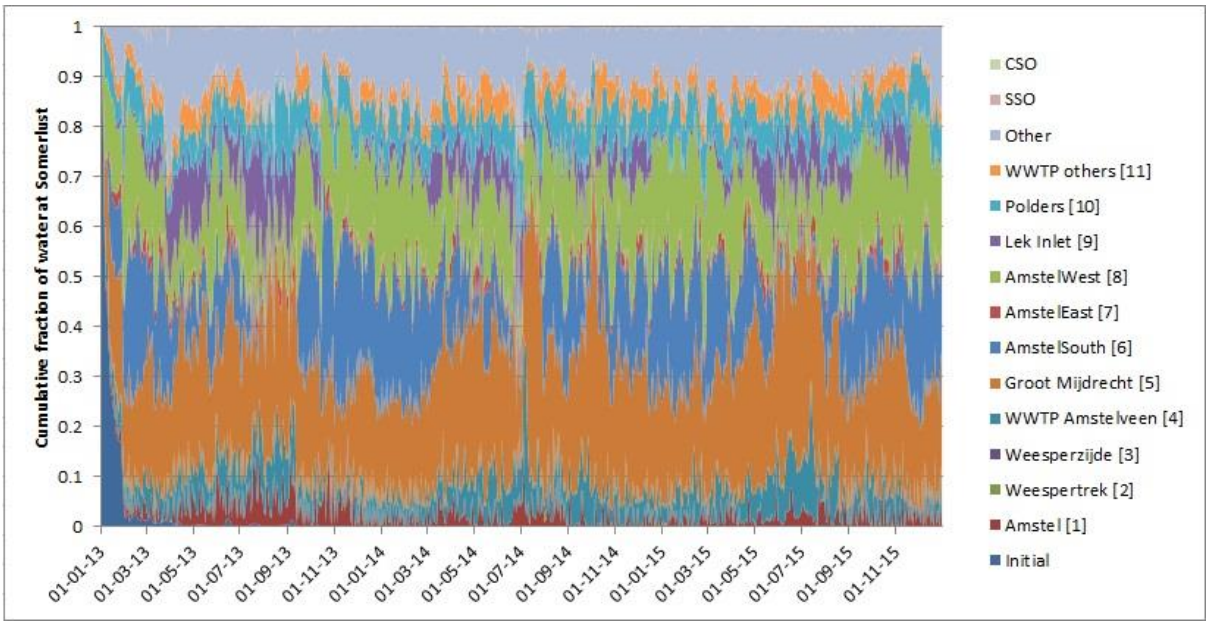

Figure 3 Example of a fraction calculation at location Somerlust

2.4 Water quality modelling

To model Somerlust's water quality not only the hydrological system (Q) had to be understood but also the sources of contamination (C) had to be included in the model.
Before this could be done, a literature study had to be conducted in order to find the sources which had to be included in the model, the sources' concentrations and their behaviour in the urban surface waters.

2.4.1 Sources and their concentration

Selection micro-organism

Different pathogens could be found in surface water, examples are *Campylobacter, Giardia, Cryptosporidium*, Norovirus and Enterovirus. Monitoring of the pathogens described above are expensive and labour intensive (STOWA and RIONED, 2016). "It is not practical or feasible to monitor the full spectrum of all pathogens that may occur in water" (US EPA, 2009). Besides, most of them come from faecal sources (US EPA, 2009), this part can be up to 99.9 percent (pers. comm. De Man, 2016). As a result, faecal coliforms are used as indicator organism for evaluating the microbiological suitability for recreational swimming (US EPA, 2009, Soller *et al.,* 2010). The European Bathing Water Directive focusses on two indicator bacteria for faecal contamination in specific, namely *Escherichia Coli* and intestinal enterococcus (IE) (EP, 2006), as both are efficient for monitoring water quality in fresh water related to swimming-associated gastroenteritis (US EPA, 1986). Waternet, the water management company in Amsterdam, sticks to the protocols of the European Bathing Water Directive and measures therefore only *E coli* and IE as indicators for the swim water quality (pers.

comm. Hersbach, 2016). As the model had to be validated with measured data, one of those faecal bacteria had to be used. From those, *E coli* concentrations show higher peaks than IE (pers. comm. Hersbach, 2016) and review of epidemiological studies on health effects from exposure to recreational water indicate that *E coli* correlates best with health outcomes for fresh water (Pruss, 1998). Therefore, *E coli* was used as the faecal bacteria indicator for contamination of the surface water with pathogens and the chance for human to get health complaints.

Inventory of possible sources

Micro-organism are naturally present in the surface waters and are also introduced by human activities. Only a small part of the total amount of bacteria, the pathogens, could result in health risks for human (van de Wal *et al.,* 2012). As faecal bacteria were used as an indicator for pathogens in this research, the sources of faecal bacteria were localized for the city of Amsterdam. Some micro-organisms originate from animals, like the dog and bird faeces. But also human faeces can get access to water -via overflows, WWTPs or houseboats- (STOWA and RIONED, 2014; de Man *et al.,* 2013).

Faecal bacteria of swimmers, houseboats and inland shipping, sewer overflows and manure runoff from polders can pollute the surface water (Mol *et al.,* 2005). WWTPs also take an important concentration of pollution into account (Blom *et al.,* 2003). And at last, runoff of dirt from the streets, including dog faeces and faecal droppings of (water) birds could also be sources of contamination (Schets *et al.,* 2008). The latter can also directly contaminate the water. All those different sources of faecal contamination are shown in Figure 4.

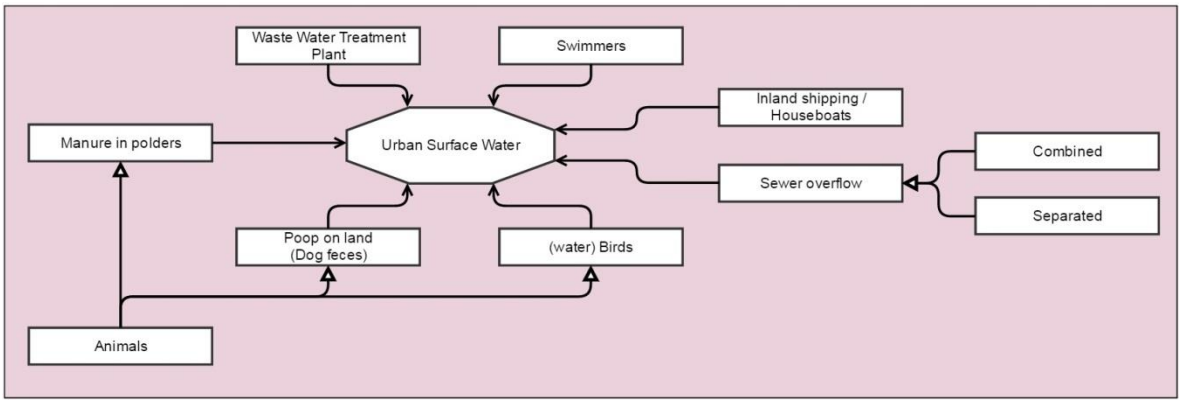

Figure 4 Schematisation showing the sources of faecal indicators (filled arrows) contaminating the urban surface water.

Cadavers could also contaminate the water, although the chance of occurrence is low (pers. comm. De Man, 2016). They were therefore ignored in this study.

Concentrations per source

Although Mol *et al.* (2005) and Helpdesk Water (2009) conclude that more swimmers on a certain location results in a higher amount of *E coli* in the water, pollution by swimmers was not taken into account in this model as a local point source. The reason for this was the unknown correlation between the additional *E coli* concentration and the swimmers and the unknown number of visitors of Somerlust per day. And, even though those numbers were not exactly known, it was assumed that pollution by swimmers is just a minor additional source.

During the last years, all the houseboats located around Somerlust were connected to the Amsterdam sewer system and were therefore also not included in the model as a contamination source. Pollution of boat trips could contaminate the water accidently, this could result in a difference in modelled and measured data, although this was hard to model and was also not assumed to be the biggest source of contamination. Boat trips passing by the location were therefore ignored.

Waternet conducted a q-PCR analysis of several samples taken in 2016 (Table 32 in Annex). The conclusion of those analyses was that the main source of faecal bacteria at Somerlust is human.

Traces of birds DNA was not found at all and traces of dog faeces from surface run-off were rare. Therefore both birds and dog faeces were not taken into account in this model. Nevertheless, to counter the exclusions, a continuous background load of 100 CFU/100mL was added to the model.

Table 2 The spectra of concentrations per source of faecal indicator bacteria in urban waters used in the model

Sources	Min Concentrations [CFU/100mL]	Max Concentrations [CFU/100mL]	Reference
WWTP	2.10^4	1.10^6	Reinthaler *et al.,* 2003; Waterschap de Dommel, 2016; Straathof *et al.,* 2012, Helpdeskwater, 2006
Combined sewer overflow	1.10^4	6.10^6	STOWA and RIONED 2014; de Man *et al.,* 2013; de Man *et al.,* 2014, Helpdeskwater, 2006
Separated sewer overflow	1.10^2	1.10^5	STOWA and RIONED 2014; de Man *et al.,* 2013; de Man *et al.,* 2014, Helpdeskwater, 2006
Manure in polders	$2.3.10^{10}$ /ha in swim-runoff-season		
Background		1.10^2	Waterschap de Dommel, 2016

In conclusion, only the *E coli* concentrations of the WWTP, sewer overflows, polders and the background pollution were included in the model. They were seen as the most direct and relevant sources. Overflow incidents of combined sewer systems as a result of heavy rainfall contaminates the water with a high amount of faecal bacteria (Table 2). This may then pose a potential health risk for people who are exposed to these waters. Ten Veldhuis *et al,* (2010) underpins this conclusion as presumed that there is a high chance that faecal bacteria are present in combined sewer overflows. Separated sewer overflows have a lower concentration of *E coli*/100mL, yet their occurrence of flow is higher than combined sewer overflows and they are located closer to Somerlust. Although effluents of WWTPs are filtered, still at least $2.2*10^2$ CFU *E coli*/mL enters the surface water (Reinthaler *et al.,* 2003). In literature the pollution from polders was not found in millilitres but in pollution per hectare during one swim-runoff-season, those data were converted into CFU/100mL and differs per polder per timestep. A full explanation of the latter can be found in the Annex.

This Section hereby provides the answer on research question 2:

'***What are the sources of faecal bacteria in this hydrological system?'***

Figure 5 displays the possible sources and answers thereby the research question. The sources which were not included in this research have a red sign in the upper right corner and the ones which were included have a green rectangle in the upper right corner. The numbers represent the minimum and maximum *E coli* concentrations in CFU/100mL found in literature. For the manure of polders this value is written as 'variable,' because the concentration was found in *E coli* per ha during one summer season and differs therefore per polder.

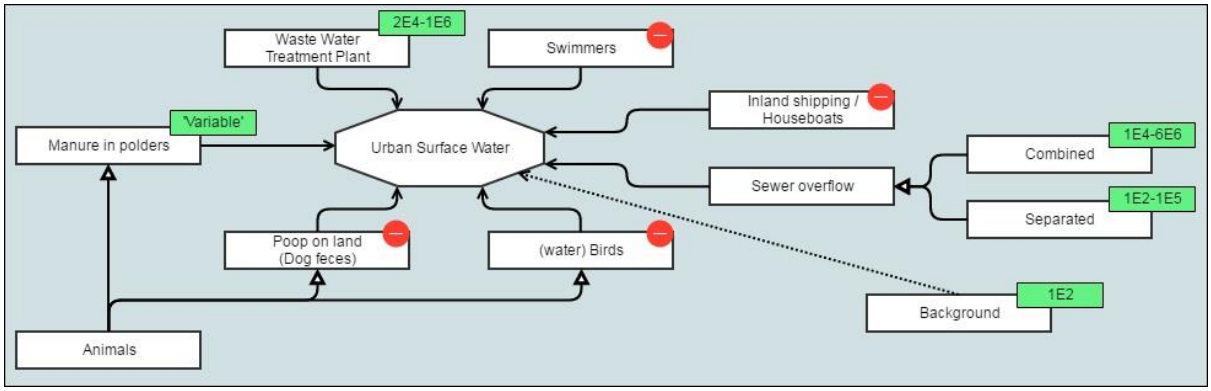

Figure 5 Overview of the sources included in this research with the minimum and maximum values in CFU/100mL in the upper right corners

2.4.2 Behaviour of micro-organisms in the surface water

Faecal bacteria, as an output of a warm body, survive some time in the surface water and will then slowly die. They are not able to grow in water (STOWA and RIONED, 2016, van den Wal *et al.,* 2012). The extent to which this happens varies between bacteria, viruses and pathogens and between the (water) conditions (temperature, turbidity, etc.).

Water temperature and sunlight incidence are major factors affecting viral stability. Other factors are predation, pH and salt concentration (Moresco *et al.,* 2016) and nutrient content and sedimentation (Lui *et al.,* 2006). Moreover, the effect of UV radiation is dependent of the depth of the water, mixing and turbidity (van Hengel, 2015; pers. comm. Vermeulen, 2016).

In this research was chosen to simulate the inactivation of the *E coli* bacteria with a function of temperature, salinity and solar radiation, following the formula described by Mancini (1978) and used in SOBEK:

$$\frac{dC}{dt} = \left((k0 + \theta S * \mathrm{Sal}) * \theta\, {}^{\mathrm{T}-20}_{T} + \mathrm{MrTRad}\right) * \mathrm{C} \qquad \textit{Eq. 1}$$

$$MrTRad = \Theta\mathrm{R} * Rad * FrUV * DayL * \frac{\left(1-e^{(-Ext*Depth)}\right)}{(Ext*Depth)} \qquad \textit{Eq. 2}$$

C	concentration of *E coli* bacteria (CFU/100mL);
k_0	decay rate (day^{-1}) at 20˚C, salinity of 0 ‰, in a dark condition; **0.725**
ϑ_S	salinity coefficient; **1.1.10^{-5}**
Sal	salinity (mg/L); **450**
ϑ_T	decay rate due to temperature deviation from 20^{0}C; **1.042**
Temp	water temperature (˚C); **'variable'**
MrTRad	Mortality rate by radiation (day^{-1});
Θ_R	Conversionfactor radiation to mortality (m2/W/d); **0.086**
Rad	Solar radiation at the surface (daily average) (W/m^2); **'variable'**
FrUV	Fraction UV radiation (-); **0.12**
DayL	Daylength (-); **'variable'**
Ext	Extinction of UV radiation (m^{-1}); **5**
Depth	Depth of the water (m); **'variable'**

In the Annex a comprehensive explanation can be found about the decay formula and the initial values used. The initial values are displayed in bold.

This leads to the answer on research question 4:

'How do the faecal bacteria behave in the surface water?'

Faecal bacteria cannot grow in water, they will only die. The mortality rate, in which this happens, differs due to weather and water conditions. The decay rate is most vulnerable for water temperature. The solar radiation is an additional factor which can add up to 0.2, in the situation of Amsterdam, on the decay rate per day. Figure 6 shows the final decay rates of *E coli* in the canals of Amsterdam over time as applied in SOBEK. This figure shows that the decay rate in summer is higher (due to the higher water temperatures) than the decay in winter.

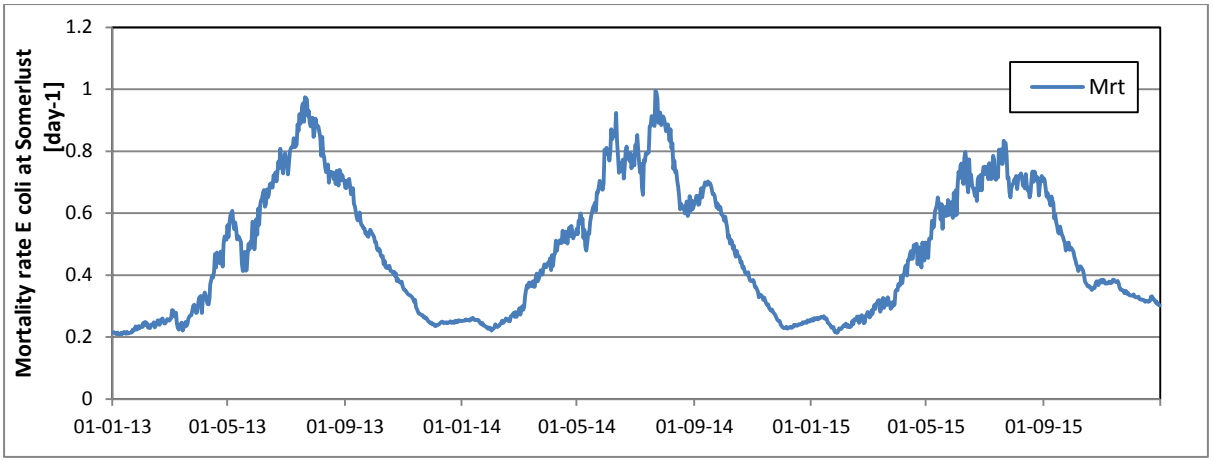

Figure 6 Mortality rate of *E coli* at location Somerlust plotted over the three years

2.4.3 Addition of CSOs and SSOs into the model

All the WWTPs in the surroundings of Amsterdam and their discharges were already included in the 'Boezemmodel.' However, the separated and combined sewer overflows were not. Therefore the overflows close to location Somerlust were added manually as point sources (Figure 7). The discharges of the separated sewer overflows were calculated by the model itself. This was done by simulating an area based discharge, related to the runoff areas, infiltration and rainfall as used in the model. All the input values are shown in Annex Table 29. The discharges of some of the combined sewer overflows in the upstream part of the Amstel River were measured by Waternet from August 2015 onwards. For the others and all overflows for the period before August 2015, the discharges were calculated manually. This was done by combining the overflow status, water level in the sewage, threshold levels of the overflows, overflow width's and discharge calculated with a rainfall-runoff model of Jan Willem Voort (Waternet). A comprehensive explanation of those calculations can be found in the Annex.

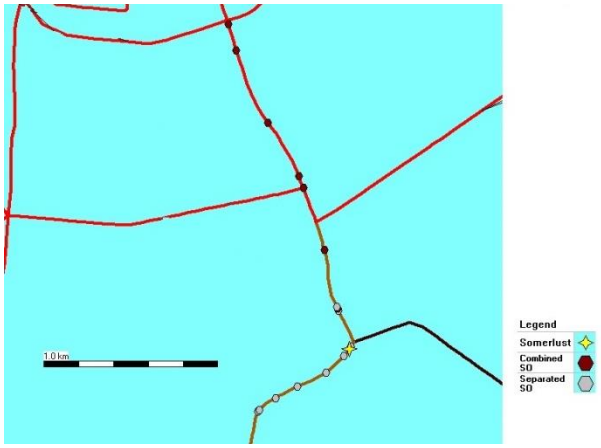

Figure 7 Added combined and separated sewer overflows close to location Somerlust

2.4.4 Model input and settings

After the CSOs, SSOs and their discharges were included in the model, the different loads had to be added to the sources. For the WWTPs, SSOs and CSOs the average concentrations following Table 2 were added to the sources in the model manually. The polders and their discharges were also already included in the model, however, the *E coli* concentration was not found in literature in CFU/100mL but in CFU per hectare and swim-runoff-season per soil type and land use. Those data had to be transferred into CFU/100mL and differed therefore per polder (due to the difference in hectares) and per day (due to different discharges per day per polder). A full explanation can be found in the Annex.

A constant background load of 100 CFU/100mL was added to all lateral flows.

The wind direction (degrees), wind velocity (m/s) and precipitation (mm/h) data as well as the input data for the boundary and lateral flows were abstracted out of the FEWS system of Waternet by Ben Staring. Solar radiation (W/m^2) was abstracted from the KNMI data of Schiphol. For the water temperature (°C), the daily averages of measurements within the city of Amsterdam were taken. For the days in which the water temperature was not measured, the data were gathered by interpolating the known data (see Table 23 in the Annex). All the meteorological data were homogeneous applied to the model.

The initial data in this model reached till 2015. Therefore a new run had to be made with FEWS to derive the data including year 2015. A comparison of the discharge at the Berlage-brug of 2013 between the old and new input file, tested the valuability of the new input file (Annex, Figure 53).

As the water of Somerlust was located at a bifurcation where the waters from all directions are assumed to mix with each other's, a dispersion coefficient of 1 (m^2/s) was applied on all the three branches directly connected to the bifurcation (Figure 8).

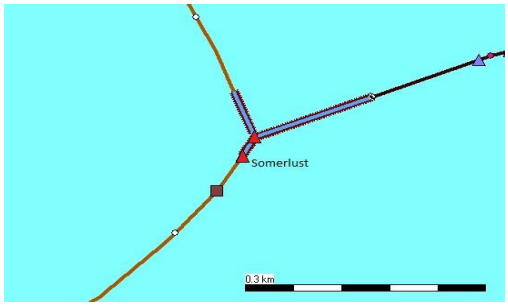

Figure 8 The selected branches to which the dispersion coefficient of 1 is applied

And at last, 'Somerlust' was added in the model as a measurement station. Its location was checked to be sure that the DELWAQ segment of Somerlust was connected to the bifurcation.

2.5 Calibration, sensitivity analysis and validation of the model

After all the needed input was included in the 'Boezemmodel' a sensitivity analysis was conducted to discover for which variables the model is sensitive. The variables tested in the sensitivity analysis were the loads of the contamination sources and the variables in the decay formula. The hypothesis was that the model is probably highly sensitive for all the concentrations of main sources, applying a decay rate and in specific the extinction of the water.

The water flow (Q) of the 'Boezemmodel' was already calibrated by Waternet using Chloride concentrations in the water and flow meters to check the water flow modelled. An example of the result of this calibration is shown in Figure 9 in which the Chloride concentrations in Amsterdam are modelled in comparison to the measured data.

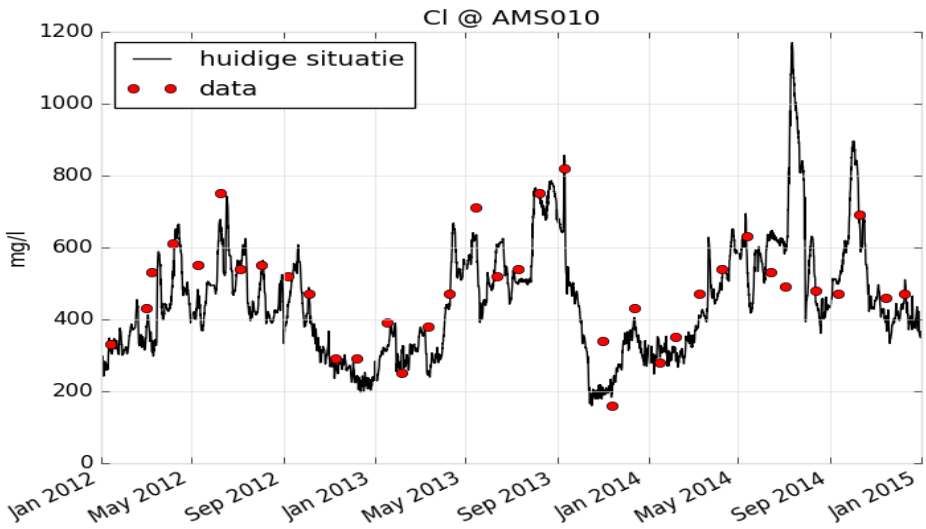

Figure 9 Calibration of the water flow in the 'Boezemmodel' with Chloride concentration as bench-mark (Erwin Meijers, 2016). With 'Huidige situation' the model output is aimed.

Besides the Q also the loads (C), which are added to the model and to which the model pointed out to be sensitive, needed to be calibrated. This was done by the estimated values as a result of the literature study described in Chapter 2.4. Moreover, constants in the decay rate were also taken into account. A Goodness of Fit validation to find the correct typical loads of the contamination sources in this water system and the best constants in the decay rate was applied afterwards. The validation process establishes the credibility of the model by demonstrating its ability to replicate the data of the water quality samples taken.

A final hindcast, as the output of the calibration-validation process, was conducted. This hindcast could give Waternet a better indication about Somerlust's water quality over the past years. It is important to conduct a proper hindcast before you are able to perform a proper forecast.

Waternet's field measurement data were used to validate the model. At the research area, measurements were taken during the last four years twice per month in the swim season (Mid April-end of September). However, in 2014, the samples were, due to construction work, not taken at location Somerlust itself but a bit more upstream of the Amstel at 'tHuis aan de Amstel' (pers. comm. Hersbach, 2016) (a graphic representation of both locations can be found in the Annex). Around 'tHuis aan de Amstel' more boats and some housing boats are located which might pose a potential threat of *E coli* contamination. Therefore only the data of 2013 and 2015 were taken into account.

The fine-tuning of the calibration (Goodness of Fit criteria) was done by target diagrams plotting the root-mean square difference of the model results with respect to the observations. Following Los and Blaas (2010), a normalized signed Root Mean Squared Difference (RMSD_s) of the model results in respect to the observations is compared to the normalized bias. Results drawn within the circle of 1 means "at least 'sufficient'" and an "RMSD_s=M_{R0}=0.74, compares 'good'." When the RMSD_s is negative, it means that the model standard deviation is smaller than the reference field's standard deviation (Los and Blaas, 2010). The bias is the models mean minus the mean of the reference.

2.6 Risk assessment

Finally a risk assessment was conducted in which the water quality, measured in E coli, was linked to human health risks of swimming in urban surface waters. This could be used by the management of Waternet when they are giving advice about the safety of swimming in the Amsterdam's canals.

In the Netherlands, a high number of health complaints after outdoor swimming reaches the authorities (Schets *et al.,* 2008). This could be clarified by the fact that "epidemiology studies of

recreational waters have demonstrated that swimmers exposed to faecal-contaminated waters are at risk of excess gastrointestinal illness (GI)" (Soller *et al.,* 2010).
GI symptoms are diarrhoea, indigestion, nausea, stomach-ache (Wade *et al.,* 2010; Stanley and Swierzewsk, 2008). But also eye infections, skin irritations and ear, nose and throat infections can be caused by GI (Soller *et al.,* 2010).

As described in the Chapter 2.4 the European Bathing Water Directive uses faecal bacteria *Escherichia coli* and Intestinal Enterococcus as the most important indicator for the contamination of water with pathogens. Table 3 shows the current water quality scales, which all the water companies have to use as their standard.

Table 3 Swim water quality scales as decided by the European Bathing Water Directive (EP, 2006).

Bacteria	Excellent	Good
IE (CFU/100ml)	200	400
***E coli* (CFU/100ml)**	500-999	1000-1800

2.6.1 Exposure

Pathogens can enter a human body by ingestion, inhalation or dermal contact (McKone and Daniels, 1991; STOWA and RIONED, 2014). Outdoor waters are visited on average 7 times per year and a visit lasts between 41 and 79 minutes (Schets *et al.,* 2011). The average volume ingested during recreation was studied by different authors and varied between 16 and 51 mL of water swallowed per swimming event (Schets *et al.,* 2011; Dufour *et al.,* 2006; Soller *et al.,* 2010). The average described by Schets *et al.* (2011), which is frequently used in other studies, assumes that a person ingests 37 millilitres of water per time. This means that if a person is swimming in water qualified as 'good,' he or she will then ingest 370 CFU of *E coli*. Note that children on average swallow more water, up to 51mL, during their recreational water visit than adults (Schets *et al.,* 2011; Dufour *et al.,* 2006). This means that, in water with the same quality, their chances of getting GI problems after their visit is higher compared to the average.

2.6.2 Epidemiologic studies

Some epidemiologic studies investigated the disease burden of swimming in outdoor waters. Yet, those studies are hard to compare. Van Asperen *et al.* (1998) tested the risk of gastroenteritis among triathletes and concluded that 5.2 percent of the triathletes got sick after swimming in water of 402 CFU/100mL. Wiedenmann *et al.* (2006) performed an epidemiologic study at five different public freshwater bathing sites with local citizens as participants and Fleisher *et al.* (1996) conducted about the same study ten years earlier. The information is shown in the Table 4.

Table 4 Results of previous epidemiologic studies in one table

Reference	Exposure	Participants	Age	Participants [nr.]	*E coli* concentrations in water (CFU/100mL)	% of getting GI problems (data)
Fleisher *et al.*, 1996	10 min, immersing their head at least 3x	Local citizens	18+	120	40*	6.7
Fleisher *et al.*, 1996	10 min, immersing their head at least 3x	Local citizens	18+	113	79*	6.2
Fleisher *et al.*, 1996	10 min, immersing their head at least 3x	Local citizens	18+	152	133*	5.9
Wiedenmann *et al.*, 2006	10 min, immersing their head at least 3x	Local citizens	4+	166	61	1.8
Wiedenmann *et al.*, 2006	10 min, immersing their head at least 3x	Local citizens	4+	207	72	1.9
Wiedenmann *et al.*, 2006	10 min, immersing their head at least 3x	Local citizens	4+	168	116	3.6
Wiedenmann *et al.*, 2006	10 min, immersing their head at least 3x	Local citizens	4+	212	181	5.2
van Asperen *et al.*, 1998	1-1.5km; 15-40min	Triathletes	21-48	802	204	5.2
Wiedenmann *et al.*, 2006	10 min, immersing their head at least 3x	Local citizens	4+	170	245	5.9
Wiedenmann *et al.*, 2006	10 min, immersing their head at least 3x	Local citizens	4+	211	379	6.6
Wiedenmann *et al.*, 2006	10 min, immersing their head at least 3x	Local citizens	4+	166	445	7.2
Fleisher *et al.*, 1996	10 min, immersing their head at least 3x	Local citizens	18+	134	661*	14.2
Wiedenmann *et al.*, 2006	10 min, immersing their head at least 3x	Local citizens	4+	208	4600	8.2
Wiedenmann *et al.*, 2006	10 min, immersing their head at least 3x	Local citizens	4+	168	4600	8.9

*Faecal coliforms, not specified into *E coli*

2.6.3 Conclusion

The different epidemiologic studies were reviewed by two studies in the Netherlands, Stuurgroep Water and STOWA respectively. Stuurgroep Water (2013) concludes that the risk of getting gastrointestinal health complaints after swimming once in approved water lies between seven and eight-and-an-half percent (500-999CFU/100mL). Following STOWA (2009) this chance increases up to eleven percent when swimming in water with a quality that is just sufficient (1000-1800CFU/100mL).

In 2015 another event happened in which people got sick after swimming in open surface water. Namely the Amsterdam City Swim of the 6th of September 2015. Due to the enormous rainfall, combined sewer overflows flood two days before the event and 31 percent of the swimmers, who answered the questionnaire of the GGD, became sick (GGD Amsterdam, 2016). The water quality was measured on the ACS-track on three different locations and varied between 4400 and 11000 CFU *E coli* /100mL, with an average of 7500 CFU/100mL (see Table 25, Annex).

However, even without swimming in urban surface waters, there is always a small chance that someone gets GI problems. From the data of Doorduyn *et al.* (2012) it is abstracted that the 'normal' chance of GI problems is 1.18 percent per week (see Annex). With 'normal' chance is referred to the average chance of an adult to get GI problems in their daily live, without swimming in open surface waters.

Combined, this results in Figure 10 in which the chance of getting GI problems is linked to the *E coli* concentrations in the urban surface water. The data are also shown in Table 26 in the Annex.

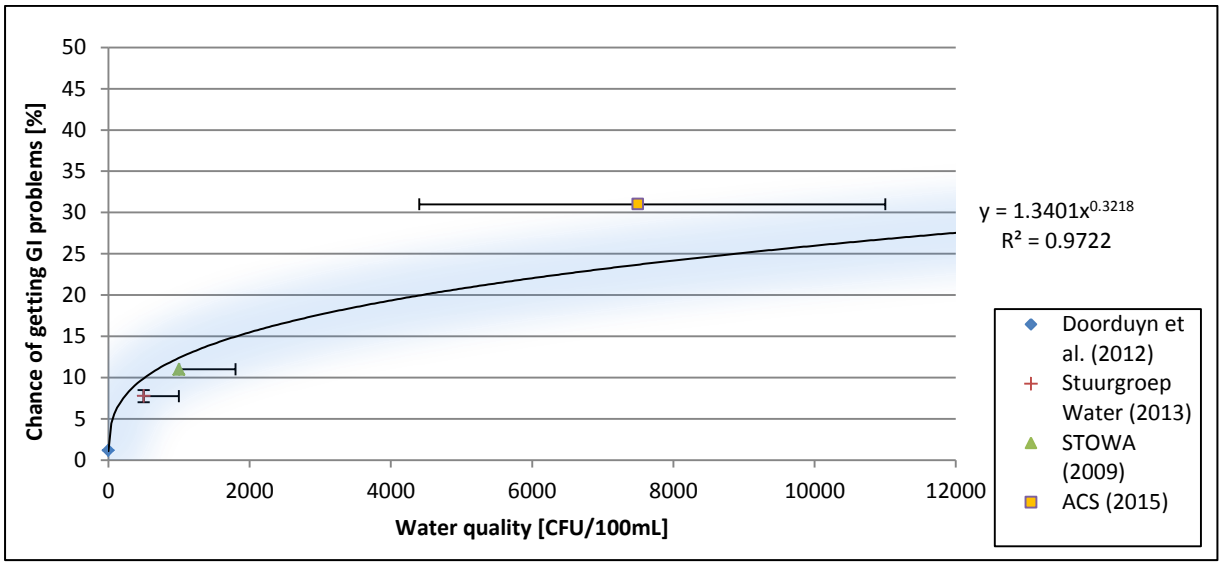

Figure 10 Curve which links the water quality to the chance of getting GI problems, as a conclusion of the concluding studies, ACS 2015 and the chance to get GI problems in general.

With producing Figure 10 an answer is also given on research question 8:

'How do the faecal bacteria concentrations relate to human health risks?'

Some epidemiologic studies investigated the disease burden of swimming in outdoor waters. Yet, those studies are hard to compare. However, when tried to do so, the chance of getting GI problems was related to the water quality in *E coli* CFU/100mL with the following formula:

$$Y = 1.3401x^{0.3218} \qquad \textit{Eq. 3}$$

With	Y	Chance of getting GI problems [%]
	x	Water quality in *E coli* [CFU/100mL]

This formula gives this research not only the possibility to produce a hindcast of the water quality at Somerlust from 2013 to 2015, but also the possibility to say something about the health implications of swimming in those waters.

3 Results

3.1 Hydrological analysis using fractions and age tracers

Somerlust is located at the point where the waters of the Amstel River and Weespertrekvaart converge and enter the canals of Amsterdam (Figure 11).

A fraction calculation for Somerlust was conducted in the 'Boezemmodel' of Waternet for year 2013, 2014 and 2015. Fraction calculations are useful to get insight in where the water at Somerlust originally comes from. Some of the smaller fractions were combined to give a better overview. Year 2015 is shown in this Chapter. 2013 and 2014 Figures can be found in the Annex, yet they have approximately the same shape.

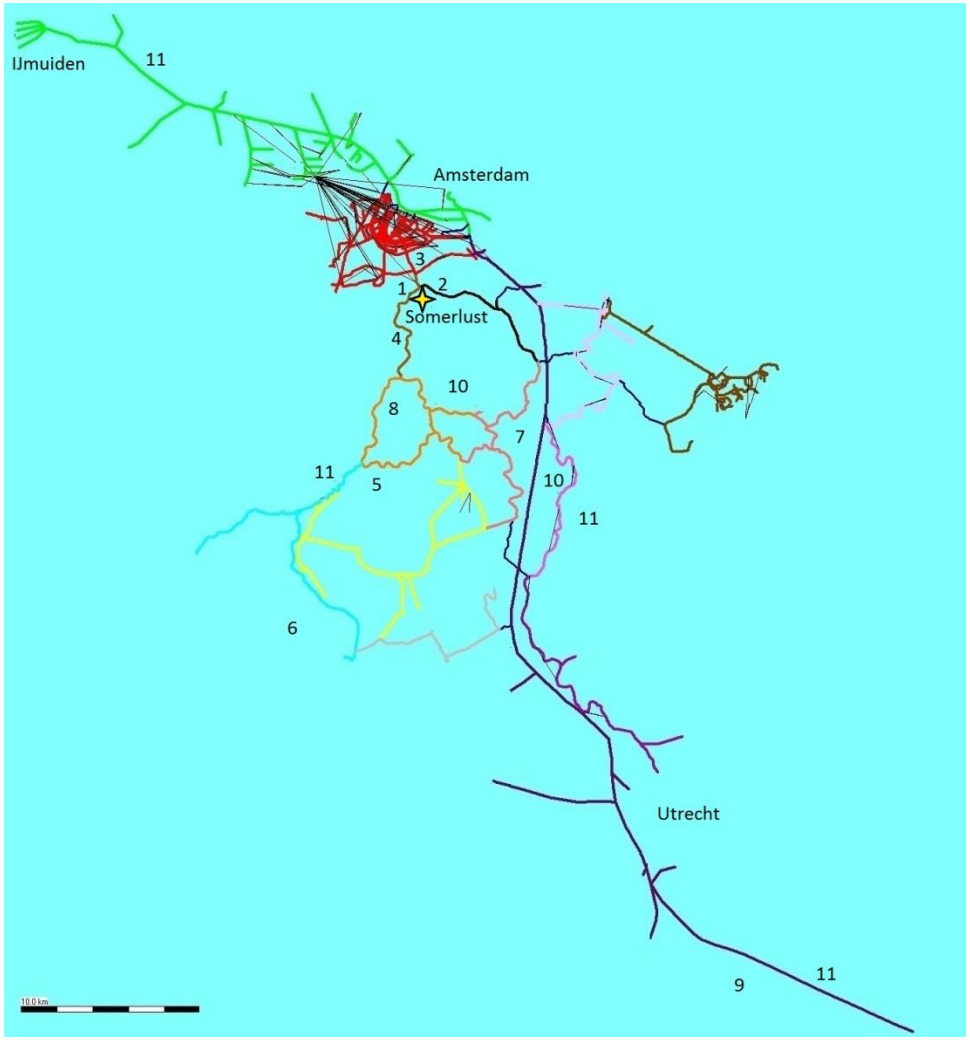

Figure 11 Simplified map of the water ways around Amsterdam (Boezemmodel), including numbers corresponding to the fractions

A simplified test was done to look in detail to the water around the location itself. Sources of water just upstream in the Amstel got a label 'Amstel,' water from the Weespertrekvaart close to Somerlust got the label 'Weespertrek' and at last waters just downstream the location, more towards the city centre, got the label 'Weesperzijde.' Figure 12 shows, first of all, that the water at Somerlust mainly comes from the direction of the Amstel [1]. Water from the Weespertrekvaart [2] and upstream 'Weesperzijde' [3] can barely be found.

The major sources of water at Somerlust are polder Groot Mijdrecht [5], the areas Amstel South [6] and West [8] and the Lek inlet [9]. The WWTP of Amstelveen [4] has around six to ten percent of the fraction on average and the other WWTPs combined [11] also cause a small fraction of the water. All the other polders [10] combined provide ten to twenty percent of the water of Somerlust. Figure 13 shows the fraction of WWTP Amstelveen in more detail in relation to the precipitation.

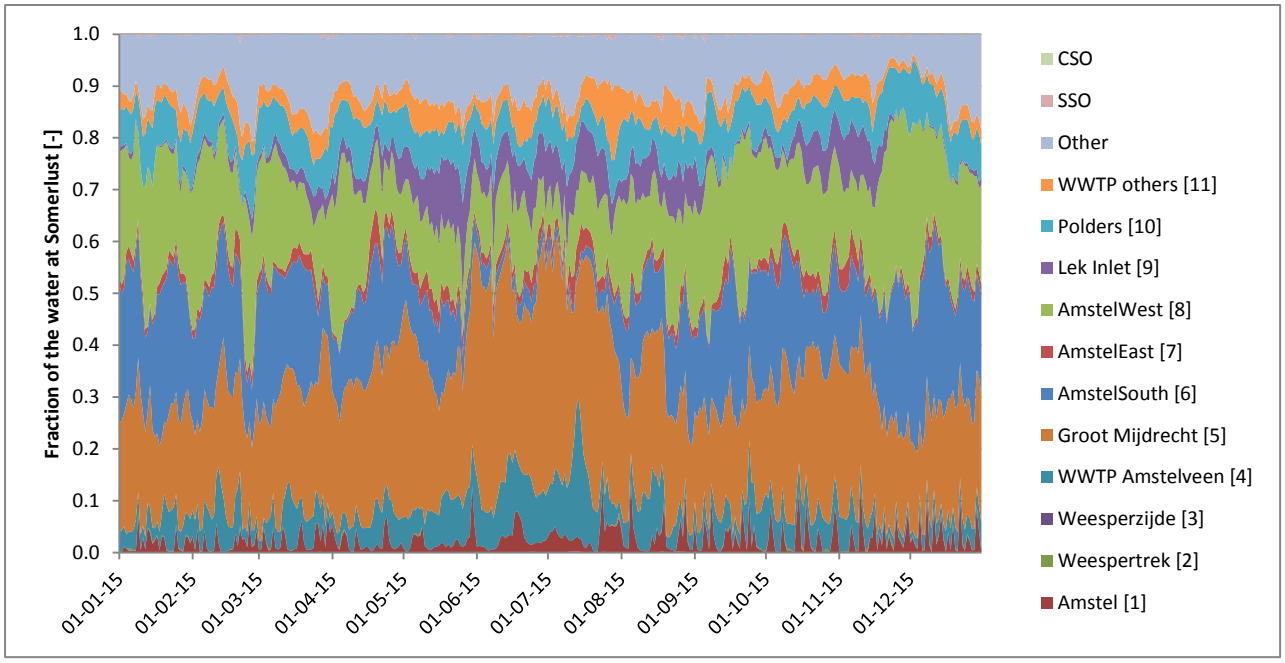

Figure 12 Fraction calculation of origin from the water at Somerlust (year 2015)

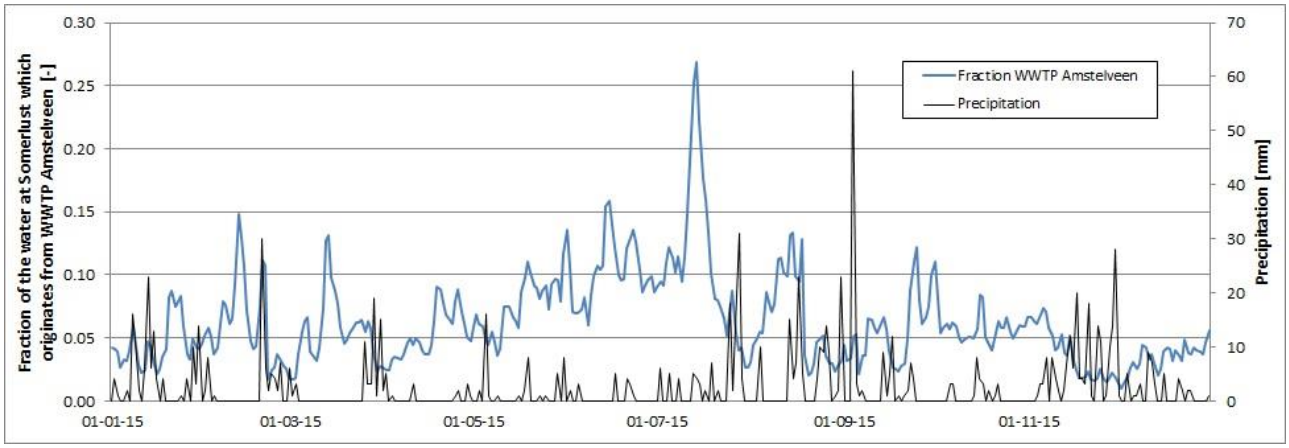

Figure 13 Line graph showing the fraction of WWTP Amstelveen and the precipitation

While looking at faecal bacteria indicators, not only the fraction of the water plays an important role, also the time till it reaches the location is important as those bacteria break down in the surface water (Chapter 2.4.2). For the most important fractions another analysis was done to look at the age of the water during summer season (half April till half September) (Table 5). Therefore two different tracers were connected in the model to the main sources of water. The first one was a continual tracer and the other one was a tracer with a constant decay per day. Based on the difference between the conservative and decayable tracer, the “age” of the water could be computed at any location in the model. Using this method, the travel time from source to the location Somerlust was determined.

Table 5 Fractions and age of the water during summer season for several bigger sources for location Somerlust (2015)

Source	Year	Fraction [min] [-]	Fraction [max] [-]	Fraction [average summer] [-]	Age [min] [days]	Age [max] [days]	Age [average summer] [days]
WWTP Amstelveen [4]	2015	0.02	0.27	0.08	0.4	7.8	4.0
Groot Mijdrecht [5]	2015	0.17	0.49	0.30	1.8	17.9	10.6
Amstel South [6]	2015	0.01	0.30	0.12	9.6	82.8	40.3
Amstel West [8]	2015	0.06	0.35	0.15	1.4	19.2	10.0
Lek Inlet [9]	2015	0.00	0.18	0.07	20.4	42.7	32.8

Table 5 shows Groot Mijdrecht having the highest fraction on average with an average age of about eleven days till the water reaches Somerlust. On the contrary, Amstel West and WWTP Amstelveen have lower fractions but the water reaches Somerlust sooner. The travel time between the original location and Somerlust will play an important role later onwards, as the shorter the timespan the shorter the time available for decay of the bacteria. In the Annex the fraction and age calculations of year 2013 can be found, the conclusions for this year are the same.

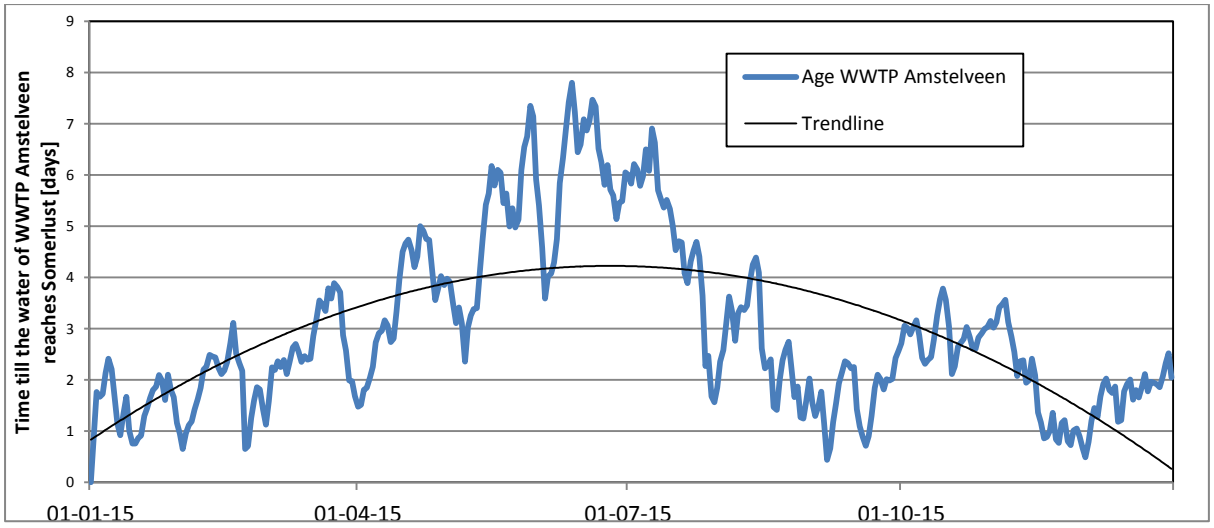

Figure 14 Graph showing the duration of the water of WWTP Amstelveen until it reaches Somerlust (2015)

Figure 14 illustrates the timespan for Amstelveen's WWTP in more detail, as this source of water is seen as important for location Somerlust. The travel time is longer in the summer period and shorter in the winter period. In the Annex the same graph can be found with the precipitation plotted in it as well (Figure 60).

Chapter 3.1 analyses the hydrological system around Somerlust as a first step of this research and thereby answers research question 1:

> ***'How does the hydrological system around Somerlust behave? What are the most dominant sources of water?'***

Overall it can be stated, that the highest amount of water comes from upstream the Amstel River. Downstream water and water from the Weespertrekvaart has minor fractions in the water of Somerlust or does not reach Somerlust at all. Groot Mijdrecht has the highest fraction in the water of Somerlust, although it has a travel time of 11 days before it reaches Somerlust. WWTP Amstelveen has a smaller fraction yet also a smaller travel period. This travel period varies within the year and is shorter in winter and longer in summer.

3.2 Sensitivity analysis

A sensitivity analysis was conducted to get an idea about the model's sensitivity to the different variables.

Table 6 Variables tested in the model and the values used in the sensitivity analyses

Variable	Option	Value
WWTP	A	2.10^4
	B	3.10^4
	C	4.10^4
	D	1.10^5
	E	2.10^5
	F	5.10^5
	G	1.10^6
Polders	A	Calculated
CSO	A	1.10^4
	B	1.10^5
	C	1.10^6
SSO	A	1.10^2
	B	1.10^3
	C	$4.5.10^3$
	D	1.10^4
	E	1.10^5
Decay?	A	yes
	B	no

Variable	Option	Value
cfRAD	A	0.0860
	B	0.0774
	C	0.0946
Chloride	A	450
	B	405
	C	495
frUV	A	0.120
	B	0.108
	C	0.132
RadSurf	A	Measured
MrtEC	A	*0.8000*
	B	0.7250
	C	0.6525
	D	0.7975
ChMrtEC	A	$1.10.10^{-5}$
	B	$9.90.10^{-6}$
	C	$1.21.10^{-5}$
TcEC	A	*1.0700*
	B	1.0420
	C	0.9378
	D	1.1462
Temp	A	Measured
Ext	A	5.0
	B	4.5
	C	5.5
	D	6.0

The variable concentration of the polders was assumed to be correct and was therefore not analyzed. The effect of radiation and water temperature is discussed in the weather analysis (Chapter 3.6). The other values tested are shown in Table 6. All the variables related to the decay rate are shown on the right column. For the decay rate the values of B and C varied ten percent from the originally found option A. MrtEC and TcEC constitute an exception in which option A the value of Mancini (1987) is and option B the value found in the literature review of Blaustein *et al*. (2013). As the extinction of UV radiation in Amsterdam's waters is measured by Waternet on several places and varies between 5 and 6, four values were tested.

3.2.1 Concentration of the waste water treatment plants

The effect of using different initial values for the waste water treatment plants, Figure 15, results in big differences of *E coli* concentrations during winter at location Somerlust. Especially when taken into account that the maximum difference in input values tested in Figure 15 is just one Log. Therefore it can be stated that, when there are plans for swimming in the water during winters, the WWTPs play an important factor. However, when zooming in to the summer season, Figure 16, the differences in input values are for a big part effaced by the higher decay rates. This concludes that the input of the WWTPs plays a major role in winters, but does not in summer.

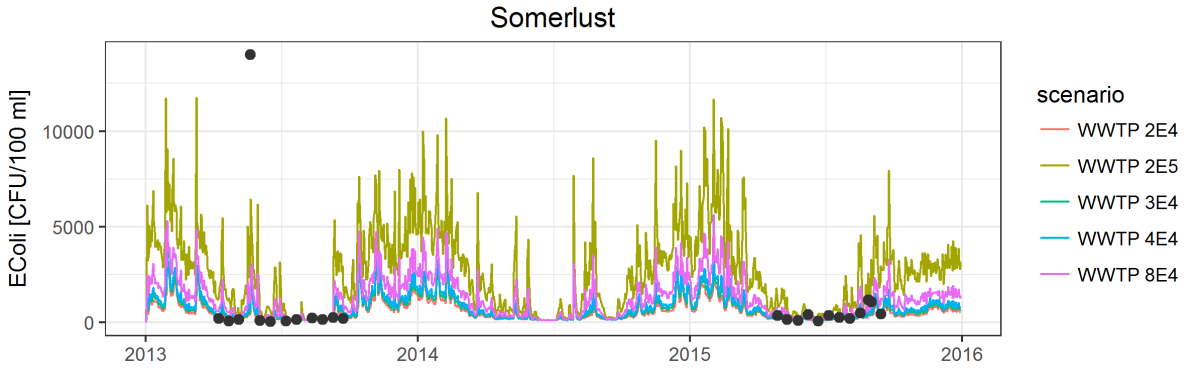

Figure 15 Testing different concentrations for the WWTPs and their effect on Somerlust over time

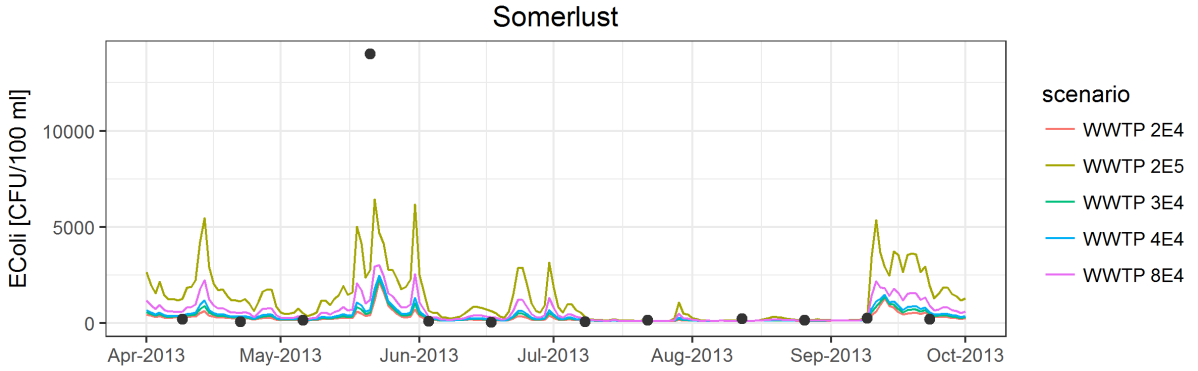

Figure 16 Testing different concentrations for the WWTPs and their effect on Somerlust for the summer of 2013 (zoomed into Figure 15)

3.2.2 Concentration of the combined sewer overflows

Also the model's sensitivity for different typical concentrations of the combined sewer overflows just downstream the Amstel on the water quality at location Somerlust was tested. The results are shown in Figure 17 and show that there is hardly any impact of the variable typical concentrations on Somerlust. The reason for this is discussed in Chapter 3.5.

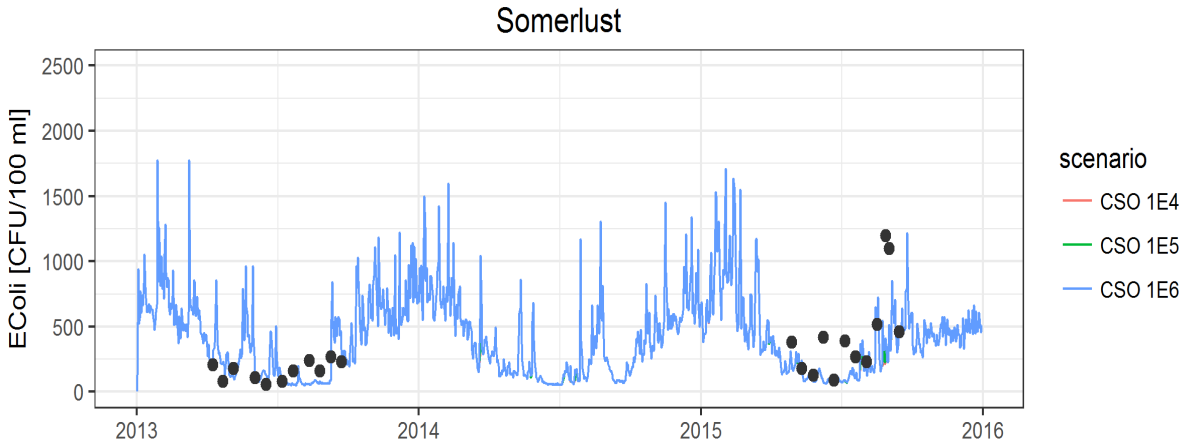

Figure 17 Effect of different input values for the combined sewer overflow on the *E coli* concentration at Somerlust

3.2.3 Concentration of the separated sewer overflows

The differences in impact of the separated sewer overflows on Somerlust were less extreme than applying different initial values for the WWTPs, however, clear differences can be found (Figure 18). In contrary to the influence of the WWTP, the differences in input values for the SSOs are visible in the swimming season. This can especially be seen in the summer of 2015 in which several rainfall events occurred. Therefore it is concluded that the model is sensitive for the concentration of the separated sewer overflows.

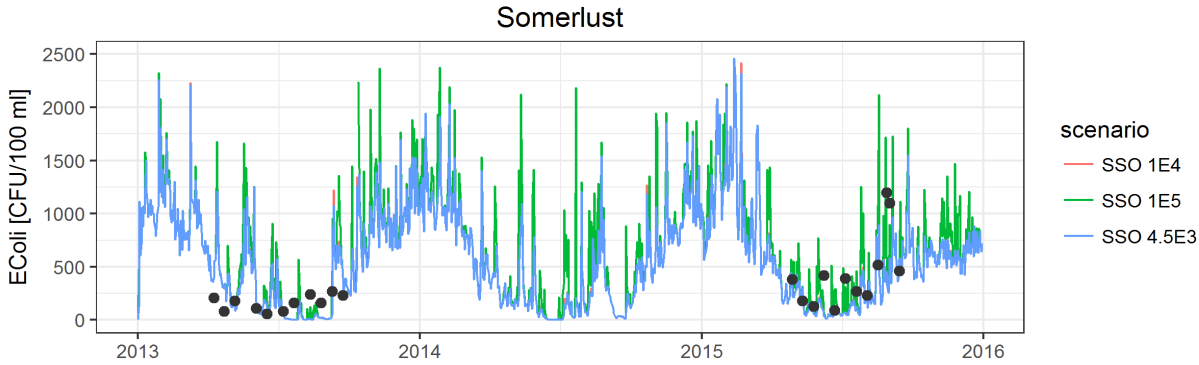

Figure 18 Impact of the different input values for the separated sewer overflows on Somerlust over time

3.2.4 Applying decay rates

That *E coli* do not multiply in surface water was already known and therefore it was assumed that the decay rate play an important role in the concentration of *E coli* at location Somerlust. However, the actual effect was highlighted when running a scenario without decay. The result can be found in Figure 19, yet can directly also be assumed as not realistic.

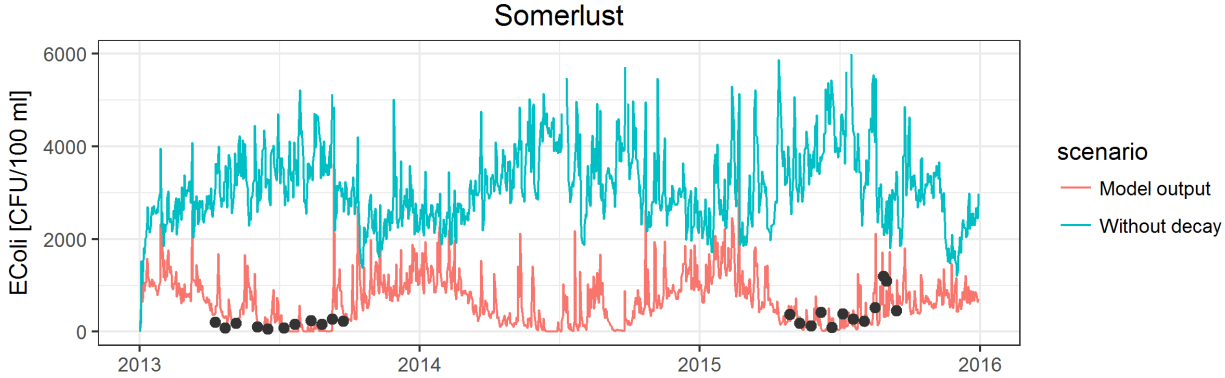

Figure 19 The impact of applying a decay rate on the *E coli* concentration at Somerlust or not applying a decay rate

Interesting is the fact that the initial concentration in summers would actually be higher, although, due to a higher decay in summer, the final concentrations at Somerlust are lower in the summer season.

Within the decay formula different variables can also be found, they are discussed in the next Sections.

3.2.5 Variable decay rate per day

The first variable is k_0; the decay rate (1/day) at 20 ˚C, for a salinity of 0 ‰ and in a dark condition. Mancini (1978) used a k_0 of 0.8 in his study but the more recent literature review of Blaustein *et al.* (2012) concluded that 0.725 is better. Therefore both values were tested. The lower value of 0.6525 is the minus ten percent of 0.725. An additional ten percent of 0.725 gave approximately 0.8 and is therefore not shown as an additional line here. Clear differences were found (Figure 20), although the differences are not that big as the differences that were seen when applying different typical concentrations to the WWTPs or SSOs.

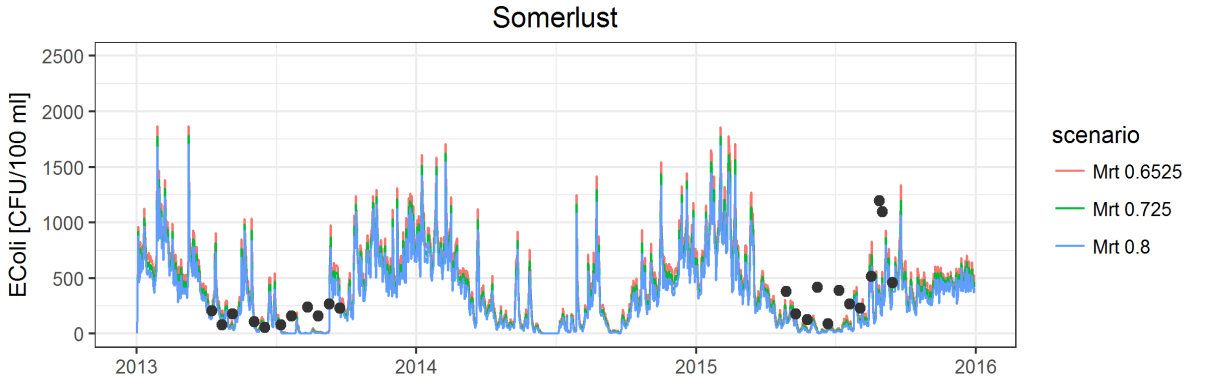

Figure 20 Different runs for k_0 values for the decay rate of *E coli* in Amsterdam

3.2.6 Variable fraction UV

Also for the fraction UV the initial value was checked as well as the values plus and minus ten percent. Those differences in fraction UV did not result in significant different model outputs (Figure 21).

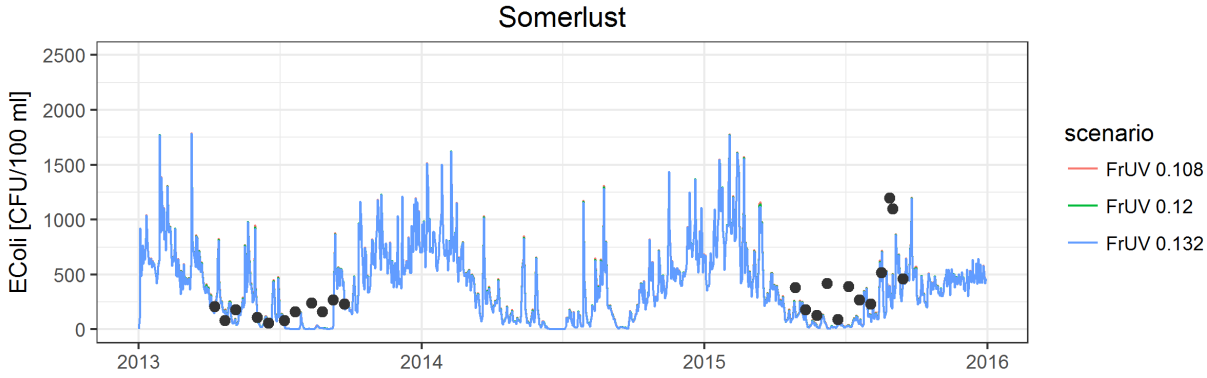

Figure 21 Different runs for fractionUV values for the decay rate of *E coli* in Amsterdam

3.2.7 Variable conversion factor for radiation

Differences in Θ_R, the conversion factor radiation to mortality (m^2/W/d), did also not result in significant differences for the module output (Figure 22).

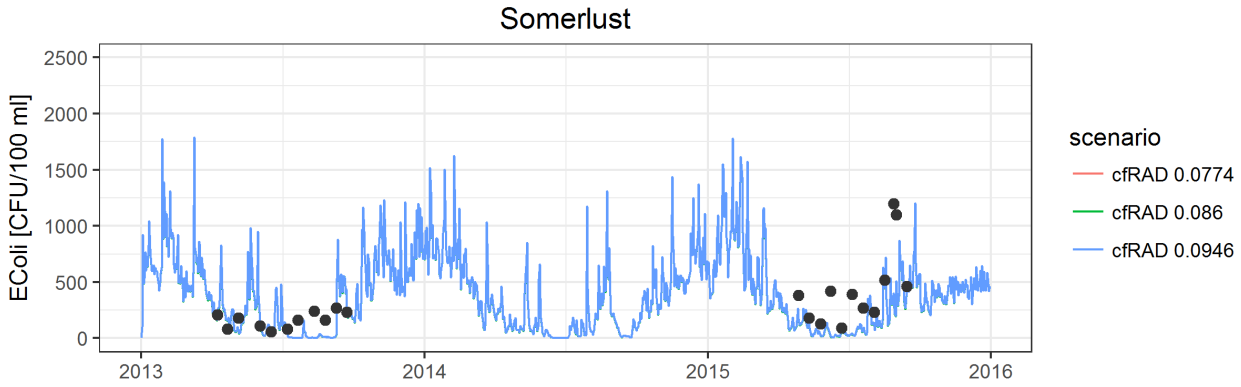

Figure 22 Different runs for conversion factor radiation to mortality (m2/W/d) for the decay rate of *E coli* in Amsterdam

3.2.8 Variable in extinction of UV radiation

Extinction of UV radiation (m^{-1}) was also tested with different runs. The extinction in the city of Amsterdam was measured on different places and the average lies between five and six. The average at location Somerlust bends towards six, however some experts by Waternet said that the water more upstream was more clear, therefore also an extinction coefficient of 4.5 was tested.

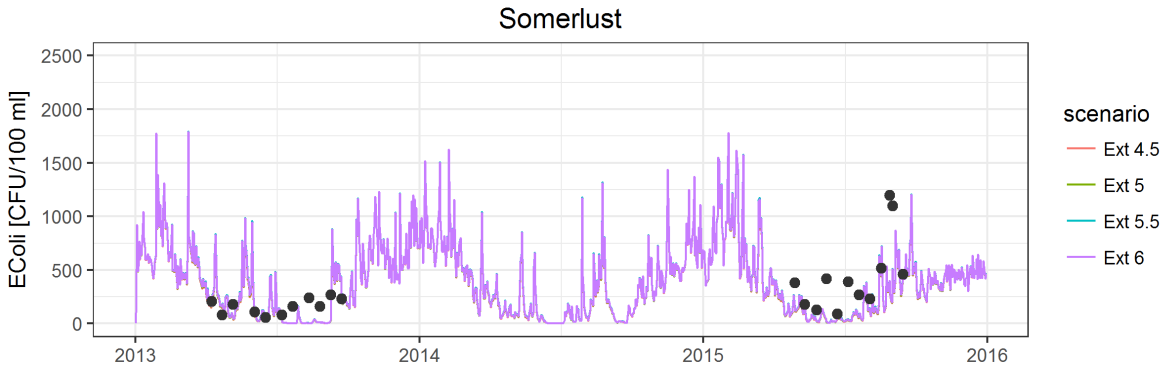

Figure 23 Four different runs for extinction of UV radiation (m-1) in the city of Amsterdam

The model result differs slightly per value of extinction. Yet, the differences are minor (Figure 23).

3.2.9 Variable salinity level in the water

The salinity in mg/L was also measured by Waternet and has a value of around 450 mg/L. This value was tested with the plus and minus ten percent values as well. Those runs gave no difference at all (Figure 24). In conclusion, the decay rate is not sensitive for those salinity levels in the water.

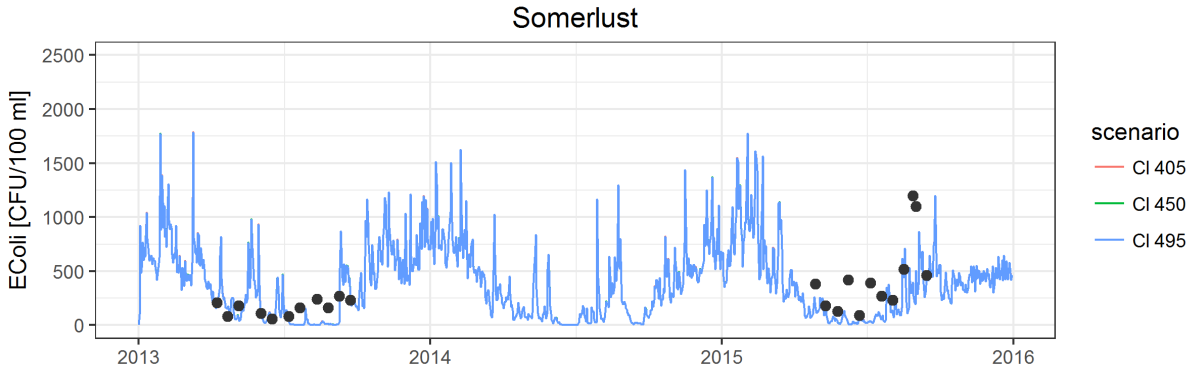

Figure 24 Different runs for the salinity (mg/L) in the water of Amsterdam

3.2.10 Variable salinity coefficient

The ϑ_S in the decay formula, the salinity coefficient, was found in literature and different runs where made (Figure 25). The value is very small and the ten percent difference gave minor differences that cannot be seen on Figure 25.

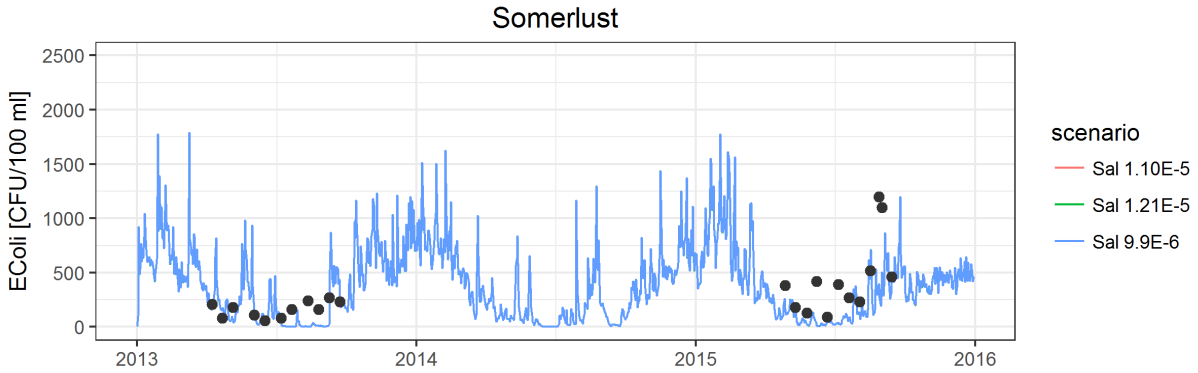

Figure 25 Different salinity coefficients for the decay rate of *E coli* in the city of Amsterdam

3.2.11 Variable temperature coefficient

The ϑ_T, decay rate due to temperature deviation from 20^0C is mostly used as 1.07, however the review of Blaustein *et al.* (2012) concluded that 1.042 is better. Those two values are tested together with one lower value and one higher value. The different runs show varying outputs especially in the colder months (Figure 26). It can be concluded that the model is sensitive for this ϑ_T value. Again the differences are effaced in summer, a sign that measurements in winter on the location itself would be welcome to calibrate the model.

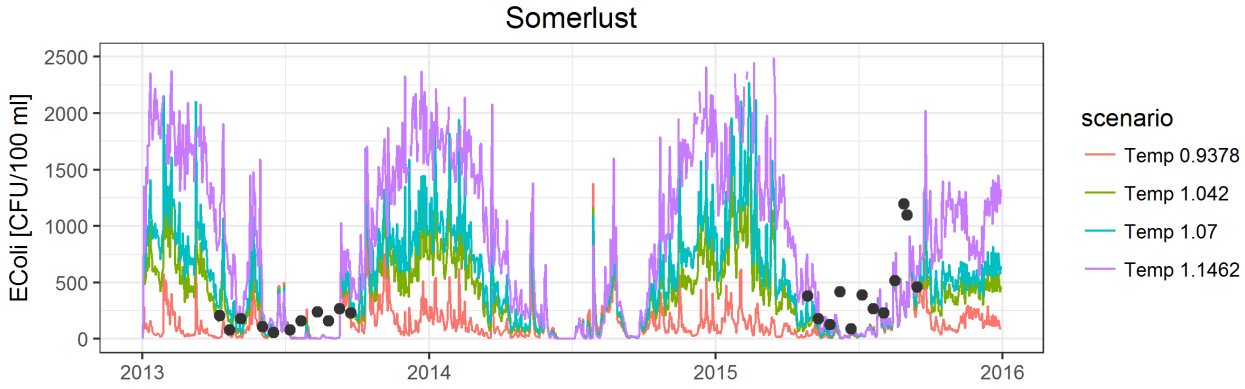

Figure 26 Four different runs with different decay rate due to temperature deviation from 20 degrees Celsius

This Chapter is summarized below and the answer on research question 7 is given as well:

'What is the sensitivity of the model to the variables?'

Different scenarios were run for both input values for contamination sources in the hydrological system and input values for the decay formula used. Different concentrations for the WWTPs gave high differences (up to 10log) between the fluctuations in winter season, yet the differences became smaller towards the summer period. For the separated sewer overflows the differences were less extreme (maximum 1000 CFU/100mL) but still gave different model results. The model is sensitive for this value especially as those SSOs are the main cause of *E coli* concentration at Somerlust in summer periods. CSOs were barely found back in the water fraction at Somerlust and also the model is not sensitive for its input value.

Besides the input values for the contamination sources, the constant values in the decay formula used in this model were also tested. A difference in salinity level and salinity coefficient (ϑ_S) gave no difference at all and fraction UV, the conversion factor for radiation (Θ_R) and extinction rate

gave just very slight differences (several CFU's/100mL). ϑ_T resulted in a 1log difference and the differences in k_0 resulted in a difference in model output up to 100 CFU/100mL.

In conclusion, the model is most sensitive for a different standard decay rate (k_0), and the decay rate for temperature deviation (ϑ_T) when looking to the constants in the decay formula of Mancini. Moreover, the model is also sensitive for the concentrations of the WWTP and SSO.

The hypothesis was that the model is highly sensitive for all the concentrations of main sources, applying a decay rate and in specific the extinction of the water.

The model results with or without applying of a decay rate varied up to 5.10^3 *E coli* CFU/100mL between each other. The model showed therefore to be sensitive for applying a decay rate, which also corresponds with the literature results concluding that faecal bacteria cannot survive outside a body. Besides the sensitivity for applying decay rate, the hypothesis had to be rejected as can be concluded that the model is most sensitive for only the different concentrations for the WWTPs and SSOs and is not that sensitive for the extinction rate. The model is namely more sensitive for the constants for the standard decay rate and the decay rate for temperature deviation than for the extinction rate.

3.3 Calibration and validation

The Q of this water system was already calibrated by Waternet, therefore only the Cs added to the model and the variables in the decay formula applied needed calibration.

Figure 27 is a simplified image of the water system around Somerlust. It shows clearly where the biggest sources of contamination are located in relation towards Somerlust. The spectra of concentrations per source of faecal bacteria were concluded from the literature study described in Chapter 2.4.1. One of the results of the sensitivity analyses was that the model is not sensitive for the CSOs input value. Therefore, the CSO concentration which was frequently used in literature (1.10^6) was assumed to be the typical concentration for the CSOs in this model. The concentration of the polders is variable as described in Chapter 2.4.4 and the background concentration was set at 1.10^2 CFU/100mL. For the WWTP and SSOs the initial concentration used for calibration was set at 1.10^5 and 1.10^3 respectively. For those sources the typical concentration which fits this water system and model best still had to be found. Table 7 concludes this paragraph.

Table 7 The spectra of concentrations per source of faecal indicator bacteria in urban waters used in the model (Chapter 2.4.1), including the initial concentrations used in the calibration and the typical concentration for this water system

Sources	Min Concentrations [CFU/100mL]	Max Concentrations [CFU/100mL]	Initial concentration [CFU/100mL]	Typical concentration [CFU/100mL]
WWTP	2.10^4	1.10^6	1.10^5	?
Combined sewer overflow	1.10^4	6.10^6	x	1.10^6
Separated sewer overflow	1.10^2	1.10^5	$4.5.10^3$	?
Manure in polders	$2.3.10^{10}$ /ha in swim-runoff-season		x	'variable'
Background		1.10^2	x	1.10^2

Table 8 Constants in the decay formula of Mancini with the initial values and the typical values for this model

Constants	Initial value	Typical value
k_0 [-]	0.725	?
ϑ_S [-]	x	$1.1.10^{-5}$
Sal [mg/L]	x	450
Θ_T [-]	1.042	?
Θ_R [m^2/W/d]	0.086	?
FrUV [-]	0.12	?
Ext [m^{-1}]	5	?

Besides the sources for contamination, also the decay formula used in this model involved constants. The data used for calibration was found in literature or measured. This was described in Chapter 2.4.1 in more detail. The sensitivity analyses showed no sensitivity of the model for the salinity level of the water and its coefficient. Therefore the value of 450 mg/L, which was the average of the samples taken in Amsterdam, is set as typical value for salinity in this model (Table 8). $1.1.10^5$ Was set as typical value for the salinity coefficient.

A Goodness of Fit validation to find the correct typical loads of the contamination sources in this water system and the best constants in the decay rate was applied afterwards.

3.3.1 Concentration of the waste water treatment plants

Waternet does not only take water quality samples at Somerlust. Another location at which they take samples is called 'AMS009.' AMS009 is located in the Amstel just downstream of the WWTP of Amstelveen (Figure 27).

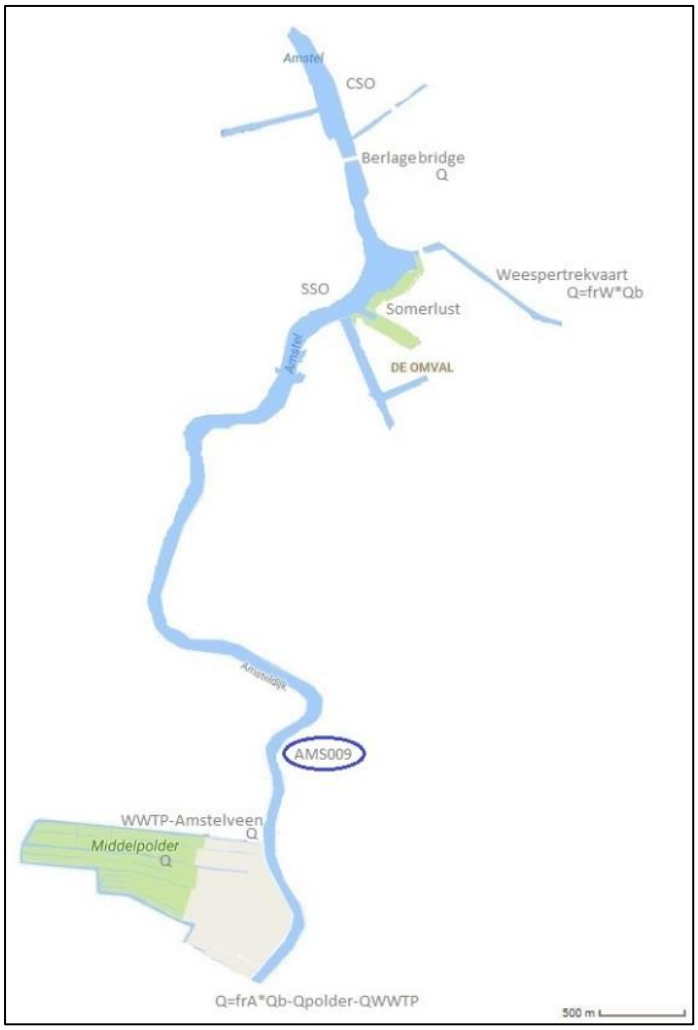

Figure 27 Simplification of the water system around Somerlust with measurement location AMS009 included

When looking at the effluent concentration of the WWTP of Amstelveen not only the water quality samples at Somerlust are important, but the results of AMS009 as well. AMS009 is located just downstream of the WWTP, this means that the time till the effluent concentrations of the WWTP reached this measurement location is shorter, thus less decay has occurred. Therefore AMS009 can give more accurate predictions of the actual WWTP effluent concentration than the data of Somerlust can. Furthermore, Waternet takes samples at AMS009 not only during the summer period but throughout the year. Therefore, first of all, the results of AMS009 are taken into account. The results of AMS009 (Figure 28 and Table 9) show that the means of an effluent with 8.10^4 and 2.10^5 CFU/100mL are higher than the reference mean. And the peaks of 2.10^5 CFU/100mL far outreaches the reference peaks. The distances to the centre of the diagram of the runs with an effluent of 2.10^4 and 3.10^4 CFU/100mL are about the same. The first one has a smaller RMSD_s and the second one has a smaller bias.

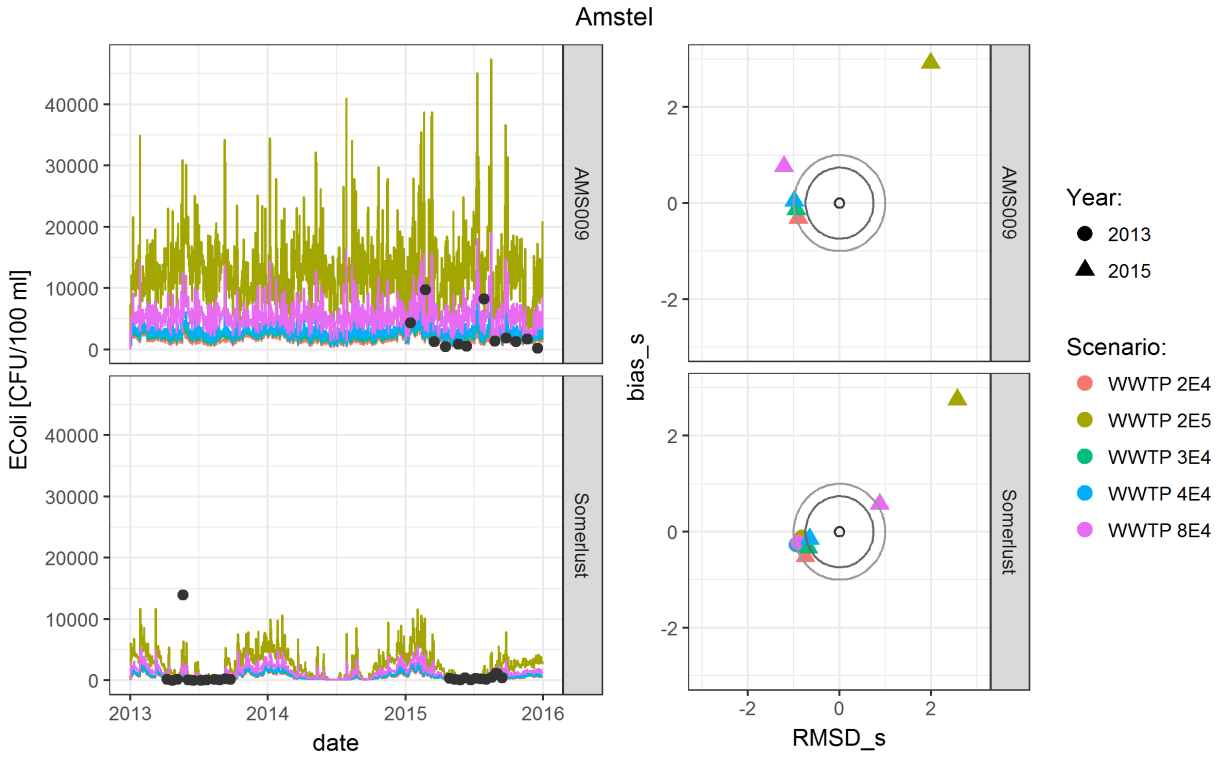

Figure 28 Target diagrams of both Somerlust and AMS009 in relation to different WWTP effluent concentrations

Table 9 Output of the target diagram of location AMS009 with the exact values for the biases, RMSD's and distances to the centre for the WWTP

Scenario	Year	Bias_s	RMSD_s	Distance
WWTP 2.10^4	2015	-0.313	-0.901	0.954
WWTP 2.10^5	2015	2.913	1.992	3.529
WWTP 3.10^4	2015	-0.133	-0.946	0.955
WWTP 4.10^4	2015	0.046	-0.994	0.995
WWTP 8.10^4	2015	0.763	-1.213	1.433

As a result, the runs of of 2.10^4 or 3.10^4 CFU/100mL were analysed for location Somerlust (Figure 29 and Table 10). From those two input values, the value of 3.10^4 CFU/100mL gave the best fit and was therefore used as typical input value for the WWTPs in this hydrological system.

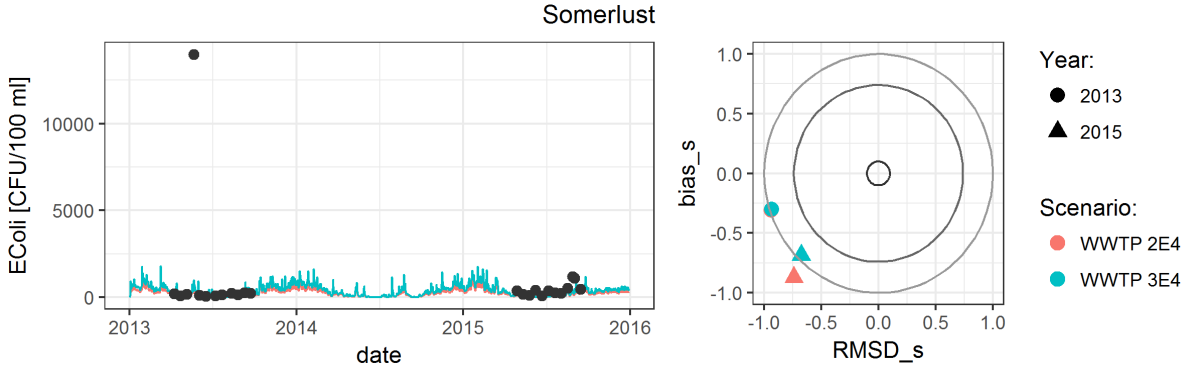

Figure 29 Target diagrams of two runs. One with an input value for the WWTPs of 2.10^4 CFU/100mL and one with 3.10^4 CFU/100ml.

Table 10 Output of the target diagram with the exact values for the biases, RMSD's and distances to the centre for the WWTP

Scenario	Year	Bias_s	RMSD_s	Distance
WWTP 2.10^4	2013	-0.310	-0.941	0.991
WWTP 3.10^4	2013	-0.301	-0.934	0.981
WWTP 2.10^4	2015	-0.870	-0.740	1.142
WWTP 3.10^4	2015	-0.685	-0.676	0.962

Please note that this diagram, the other diagrams below and the tables do not match the measurements like the final model output does. The reason for this is that the variables were first of all viewed separately and afterwards all the typical values for this model where combined in order to get the final model result.

3.3.2 Concentration of the separated sewer overflows

The separated sewer overflows are located closely to Somerlust and the sensitivity showed that the model results are sensitive for different concentrations for the SSOs. Therefore, several concentrations were submitted into the Goodness of Fit validation (Figure 30). The different locations of $4.5.10^3$ and 1.10^5, as input value for the concentration of SSOs, on the target diagram confirmed the sensitivity of the model for the different concentrations.

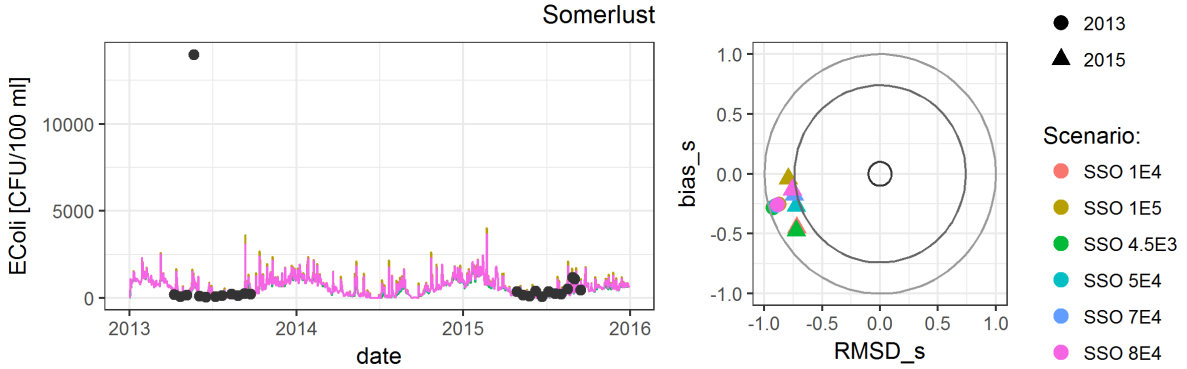

Figure 30 Target diagram with different *E coli* concentrations in the effluent of the SSOs and their effect on Somerlust

Two runs needed an additional review, namely the runs with 1.10^5 *E coli* in CFU/100mL as input value for SSO and 7.10^4. When looking at 2013 the scenario with an SSO concentration of 1.10^5 gave the best output. However, when looking at 2015, different values can be found (Table 11). Namely a more accurate bias was obtained with 1.10^5 *E coli*, yet the RMSD and distance of 7.10^4 *E coli* were smaller. Finally, the *E coli* concentration of 1.10^5 CFU/100mL was used as the typical concentration of the separated sewer overflows on the other side of the water at Somerlust. The reason for this is the bigger difference in bias than RMSD difference and the output for 2013 is slightly better for 1.10^5 as well. This value is on the upper limit of the concentrations found in literature, but it gives the best match though, therefore it is recommended to search for mis-connections in the sewer system which might have caused the high concentration.

Table 11 Output of the target diagram with the exact values for the biases and RMSD's of a SSO with an effluent of 1.10^5 or 7.10^4 *E coli* (CFU/100mL)

Scenario	Year	Bias_s	RMSD_s	Distance
SSO 1.10^5	2013	-0.252	-0.873	0.909
SSO 7.10^4	2013	-0.262	-0.889	0.927
SSO 1.10^5	2015	-0.042	-0.793	0.794
SSO 7.10^4	2015	-0.178	-0.743	0.764

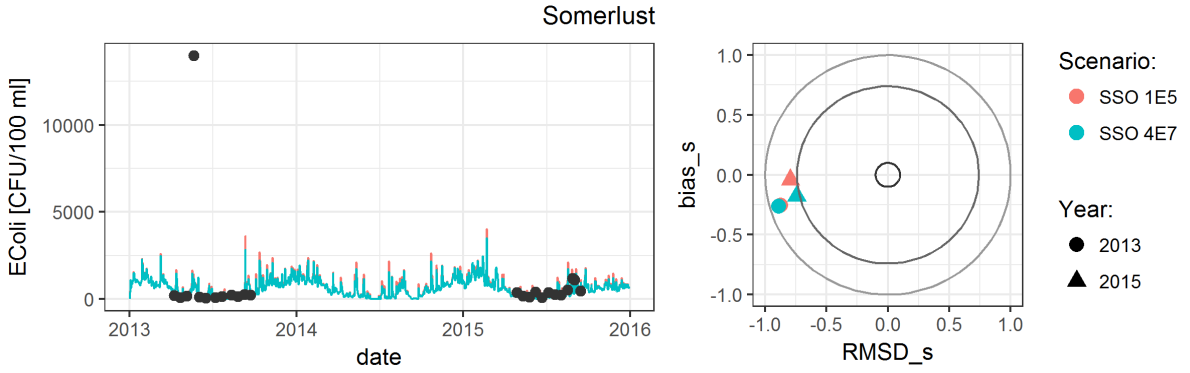

Figure 31 Target diagram with only the plots of SSO loads of 1.10^5 and 4.10^7 *E coli* [CFU/100mL]

3.3.3 Variable decay rate per day

K_0, the decay rate (1/day) at 20 ˚C, for salinity of 0 ‰ and in a dark condition, was also validated with a target diagram. K_0 of 0.6525 gave the closest fit for both 2013 and 2015 (Figure 32 and Table 12), the lowest biases for 2013 and 2015 and lowest RMSD_s for 2013. The RMSD_s for 2015 was slightly higher than the other values, although the difference is minor. Besides, the distance to the centre of the diagram was still smaller with a K_0 of 0.6525. Therefore is K_0 of 0.6525 used as the final value for the general decay rate.

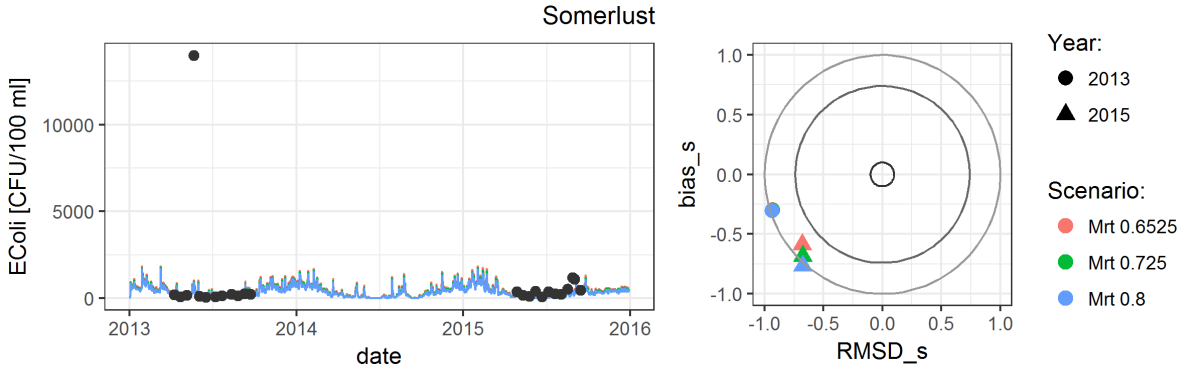

Figure 32 Target diagram for different k_0 values for the decay rate of *E coli* in Amsterdam

Table 12 Output of the target diagram with the exact values for the biases, RMSD's and distances to the centre for Mrt/ K_0

Scenario	Year	Bias_s	RMSD_s	Distance
Mrt 0.6525	2013	-0.296	-0.932	0.977
Mrt 0.725	2013	-0.301	-0.934	0.981
Mrt 0.8	2013	-0.305	-0.935	0.984
Mrt 0.6525	2015	-0.587	-0.682	0.900
Mrt 0.725	2015	-0.685	-0.676	0.962
Mrt 0.8	2015	-0.768	-0.677	1.024

3.3.4 Variable fraction UV

The sensitivity analyses showed already that the model is just slightly sensitive for a different fraction UV. This is underpinned by the target diagram and table with biases, RMSD_s and distance to the centre (Figure 33 and Table 13). However a very slight preference for a fraction UV of 0.108 is found and therefore was this value used in the further modelling.

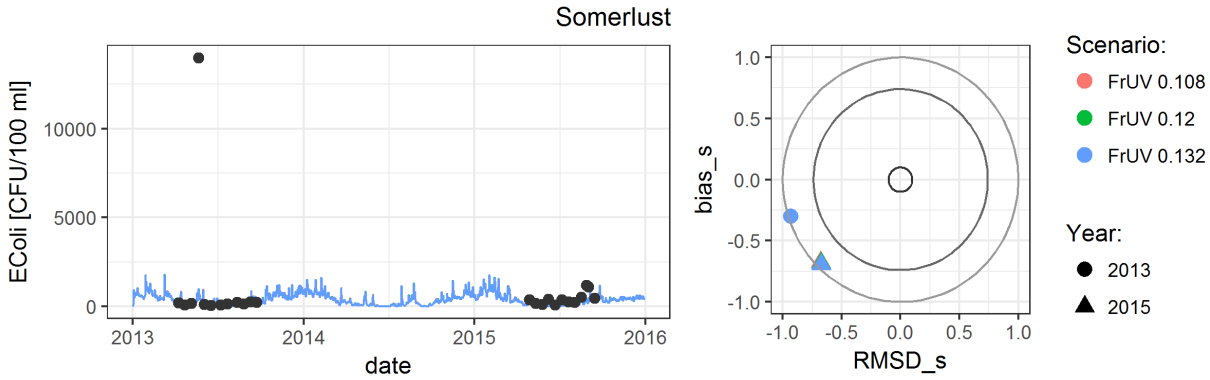

Figure 33 Target diagram for fractionUV values for the decay rate of *E coli* in Amsterdam

Table 13 Output of the target diagram with the exact values for the biases, RMSD's and distances to the centre for FrUV

Scenario	Year	Bias_s	RMSD_s	Distance
FrUV 0.108	2013	-0.300	-0.933	0.981
FrUV 0.12	2013	-0.301	-0.934	0.981
FrUV 0.132	2013	-0.302	-0.934	0.981
FrUV 0.108	2015	-0.673	-0.678	0.955
FrUV 0.12	2015	-0.685	-0.676	0.962
FrUV 0.132	2015	-0.696	-0.674	0.968

3.3.5 Variable conversion factor for radiation

As with the sensitivity for fraction UV, the model also did not seem to be sensitive for the conversion factor for radiation. The Goodness and Fit analysis showed a slight preference for the lower conversion factor of 0.0774 (Figure 34 and Table 14) and therefore this value is used as the conversion factor for radiation.

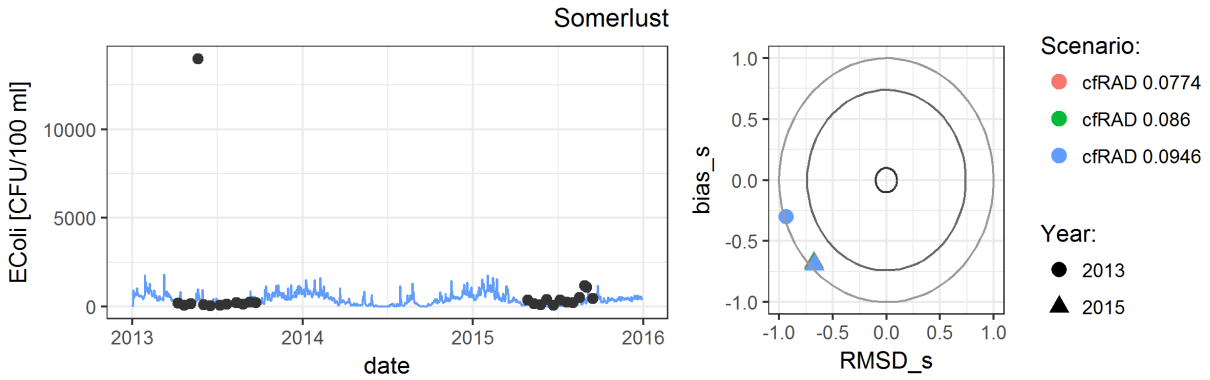

Figure 34 Target diagram for conversion factor radiation to mortality (m2/W/d) for the decay rate of *E coli* in Amsterdam

Table 14 Output of the target diagram with the exact values for the biases, RMSD's and distances to the centre for cfRAD

Scenario	Year	Bias_s	RMSD_s	Distance
cfRAD 0.0774	2013	-0.300	-0.933	0.981
cfRAD 0.086	2013	-0.301	-0.934	0.981
cfRAD 0.0946	2013	-0.302	-0.934	0.981
cfRAD 0.0774	2015	-0.673	-0.678	0.955
cfRAD 0.086	2015	-0.685	-0.676	0.962
cfRAD 0.0946	2015	-0.696	-0.674	0.968

3.3.6 Variable in extinction of UV radiation

The four different runs with a different extinction of UV radiation resulted in minor differences (Figure 35), although the distance to the centre of the run with the extinction of UV radiation of 5.5 was the smallest (Table 15). Therefore this value is chosen. This result matches the samples taken around Somerlust with extinction rates of about 5.5 up to 6.

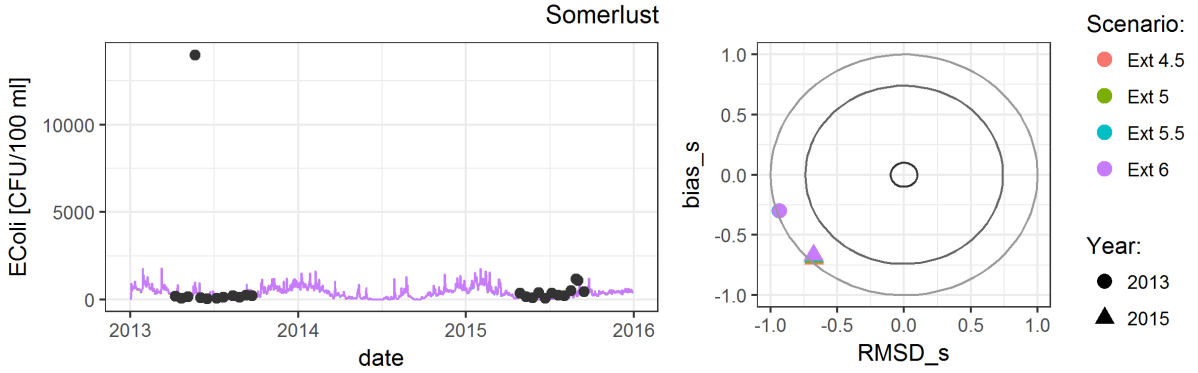

Figure 35 Four different runs for extinction of UV radiation (m-1) in the city of Amsterdam

Table 15 Output of the target diagram with the exact values for the biases, RMSD's and distances to the centre for extinction

Scenario	Year	Bias_s	RMSD_s	Distance
Ext 4.5	2013	-0.302	-0.934	0.981
Ext 5	2013	-0.301	-0.934	0.981
Ext 5.5	2013	-0.300	-0.933	0.980
Ext 6	2013	-0.300	-0.933	0.981
Ext 4.5	2015	-0.697	-0.673	0.969
Ext 5	2015	-0.685	-0.676	0.962
Ext 5.5	2015	-0.665	-0.679	0.951
Ext 6	2015	-0.674	-0.678	0.956

3.3.7 Variable temperature coefficient

In the sensitivity analyses it was seen that the effect of ϑ_T effaced in summer, yet significant differences were found in the Goodness of Fit analyses. The different runs were entered in the target diagrams and the initial value of 1.1462 showed the best fit for 2013 (Figure 36 and Table 16). The distances to the centre of the runs with a temperature coefficient of 1.042 or 1.07 were about 0.015 smaller than the distance of the run with a temperature coefficient of 1.1462, however the bias of the run with ϑ_T 1.1462 was about 0.2 closer to the to the reference bias. Therefore, in combination with the better result in 2013, the value for ϑ_T was set at 1.1462.

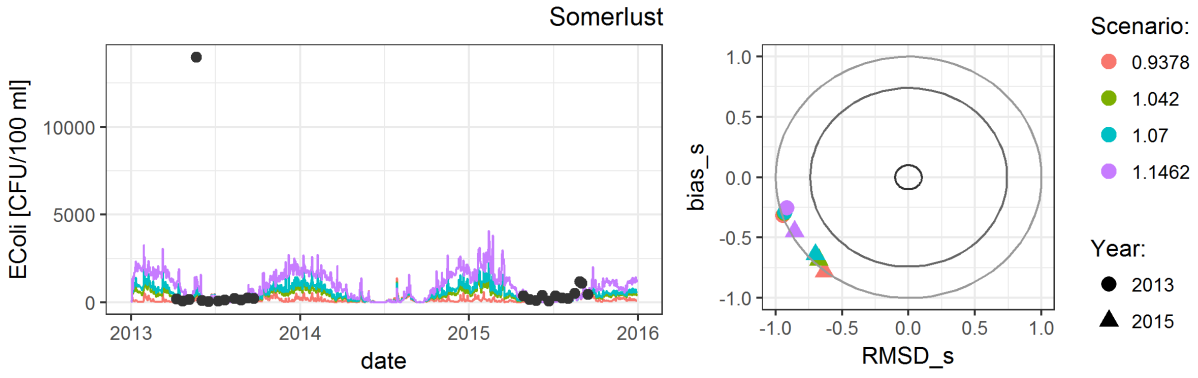

Figure 36 Target diagram with four different runs with different decay rate due to temperature deviation from 20 degrees Celsius

Table 16 Output of the target diagram with the exact values for the biases, RMSD's and distances to the centre for temperature coefficient

Scenario	Year	Bias_s	RMSD_s	Distance
Temp 0.9378	2013	-0.316	-0.946	0.998
Temp 1.042	2013	-0.301	-0.934	0.981
Temp 1.07	2013	-0.293	-0.929	0.974
Temp 1.1462	2013	-0.256	-0.916	0.951
Temp 0.9378	2015	-0.785	-0.633	1.008
Temp 1.042	2015	-0.685	-0.676	0.962
Temp 1.07	2015	-0.641	-0.701	0.950
Temp 1.1462	2015	-0.449	-0.856	0.966

3.3.8 Conclusion for the decay rate

The results of the Goodness of Fit analyses for the constants of the decay formula in this model are concluded in Table 17. Those typical values are used in the final model settings.

Table 17 Concluding table with the constants in the decay formula and the typical values used in this model

Constants	Typical value
k_0 [-]	0.6525
ϑ_S [-]	$1.1.10^{-5}$
Sal [mg/L]	450
Θ_T [-]	1.1462
Θ_R [m^2/W/d]	0.0774
FrUV [-]	0.108
Ext [m^{-1}]	5.5

3.4 Model results

Including all the typical values, found with the sensitivity and Goodness and Fit analyses, in the model, results in a final model hindcast in total *E coli* in CFU/100mL at Somerlust. The following graph (Figure 37) is obtained when comparing this model result with the measured data by Waternet.

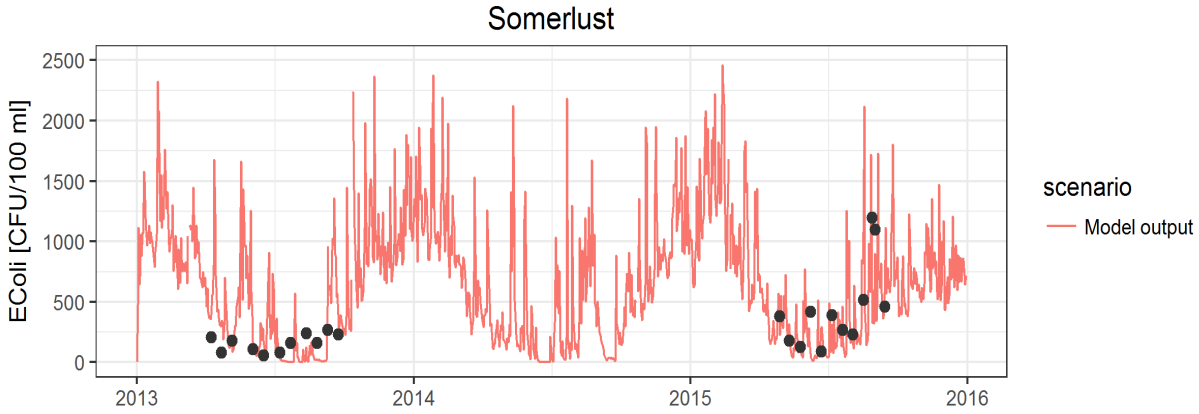

Figure 37 Final model output of *E coli* concentration CFU/100mL over time at location Somerlust compared to the measurements

The final model output gave an RMSD_s of -0.87 in 2013 and -0.79 in 2015 (Table 18), so the model is at least reasonable. The bias_s for 2013 is -.25, whereas the bias_s of 2015 is -0.04 (Figure 38). This means that the bias of around -0.25, in 2013, concludes that the model slightly under predicts the mean of the observations. The means of the model and measurements of 2015 were approximately the same.

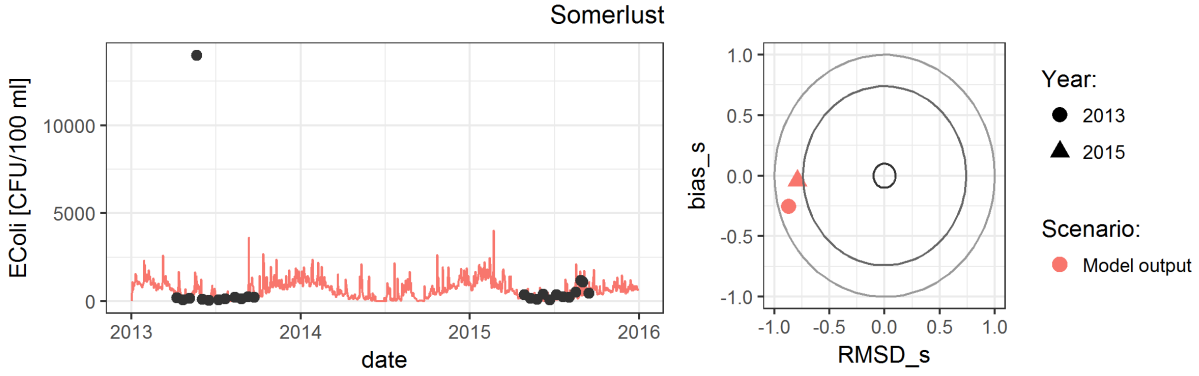

Figure 38 Representation of the root-mean square difference of the model results with respect to the observations

Table 18 Output of the target diagram with the exact values for the biases, RMSD's and distances to the centre for the final model result

Scenario	Year	bias_s	RMSD_s	Distance
Model output	2013	-0.253	-0.873	0.909
Model output	2015	-0.042	-0.793	0.794

The next paragraphs summarize research question 6 and this Chapter:

'How do the model outputs compare to observations?'

The simulation of our model compares 'sufficiently' for year 2013 to the observations and for year 2015 approaches 'good'. 2014 Was not taken into account in this assessment. The target diagram shows that the peaks of the measurements are not all caught by the model, but that its mean in 2015 lies just below the mean of the measurements. Although the results of both 2013 and 2015 are located within the circle, which means that they are both reasonable, the results also show negative RMSD_s'. A negative RMSD_s means that the peaks of the model results are lower in comparison to the reference peaks. The peaks in the model are underestimated. This should be taken into account when looking back with the hindcast or producing a forecast with this model.
The mean, on the contrary, almost reaches the reference mean in 2015 (bias_s=-0.04).

3.5 Typical concentrations of faecal bacteria per source

Diving into literature of previous studies showed the boundaries of concentrations per source in which the typical concentrations should be located (Chapter 2.4.1). By producing the sensitivity and Goodness and Fit analyses the typical concentrations that reproduced the best model output were found. The typical concentrations per source used as the final inputs for the model are shown in Table 19.

Table 19 Minimum and maximum concentration per source as was found in literature (Table 2) together with the final typical concentrations used in the model

Sources	Min Concentrations [CFU/100mL] *literature*	Max Concentrations [CFU/100mL] *literature*	Typical concentrations model [CFU/100mL]
WWTP	2.10^4	1.10^6	***3.10^4***
Combined sewer overflow	1.10^4	6.10^6	***1.10^6***
Separated sewer overflow	1.10^2	1.10^5	***1.10^5***
Manure in polders	$2.3.10^{10}$ /ha in swim-runoff-season		***variable***
Background		1.10^2	***1.10^2***

The net concentrations at location Somerlust was found by releasing decayable tracers to the four biggest fractions. Due to the variable concentrations of the polders, it was hard to give them also a decayable tracer in the model. It was therefore assumed that the net concentration of polders is the difference between the final concentrations at Somerlust minus the WWTPs and overflows (Table 20).

Table 20 The numbered tracers with the associated sources

Tracer	Source
1	Separated sewer overflows
2	Combined sewer overflows
3	WWTP Amstelveen
4	WWTP others
Left-over	Polders

The black line in Figure 39 represents the total *E coli* concentration at Somerlust over the years 2013, 2014 and 2015. In pink the measurements by Waternet are shown, yet it has to be said that the data in year 2014 is taken on another location close to Somerlust. The nicest thing about modelling and putting tracers on the contamination sources is that not only the total *E coli* concentrations are known but also the shares of each of those sources throughout the period.

Figure 39 shows that the *E coli* concentration of the WWTP Amstelveen causes most of the contamination. Although in summer period this concentration and fraction is less, due to a higher decay rate and longer timespan till the water reaches Somerlust (Chapters 3.1 and 2.4.2). The peaks of concentration of *E coli* at Somerlust are mainly caused by the separated sewer overflows on the other side of the water (Figure 40, for more detail). Contamination from polders around Amsterdam play a minor role in the *E coli* concentration at Somerlust over the whole period, this can especially be seen in Figure 41. The other WWTPs in the 'Boezemmodel' are taken together as one fraction and peak in winter seasons (Figure 41). During winters, the water is colder, there is less radiation and more rainfall. The latter causes faster discharges, which results in a shorter period till the water reaches Somerlust and therefore also less decay of the bacteria.

The CSOs are located just downstream of the research area, yet they can only be found back in some very narrow peaks. The reason for this is that the daily discharges of the water there are

mostly positive (Figure 64, Annex), resulting in water flowing towards the city instead of towards Somerlust. However, on hourly timescales negative discharges are found (Figure 63, Annex). Those negative discharges have resulted in a very few peaks of CSO influence at Somerlust.

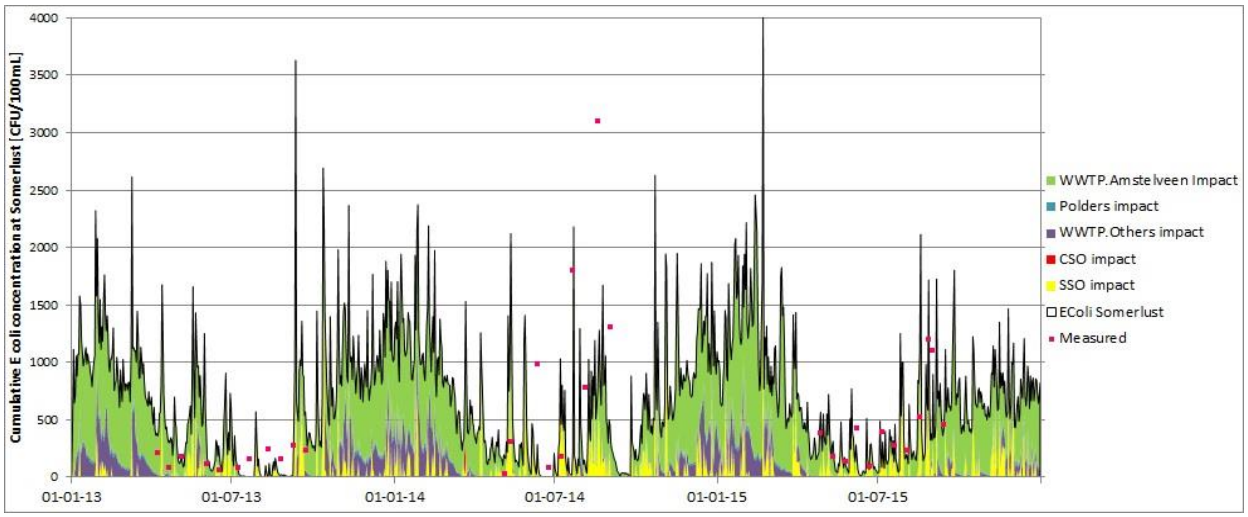

Figure 39 *E coli* concentration at Somerlust in the period 2013-2015 with the shares of each source of pollution shown and the measurements

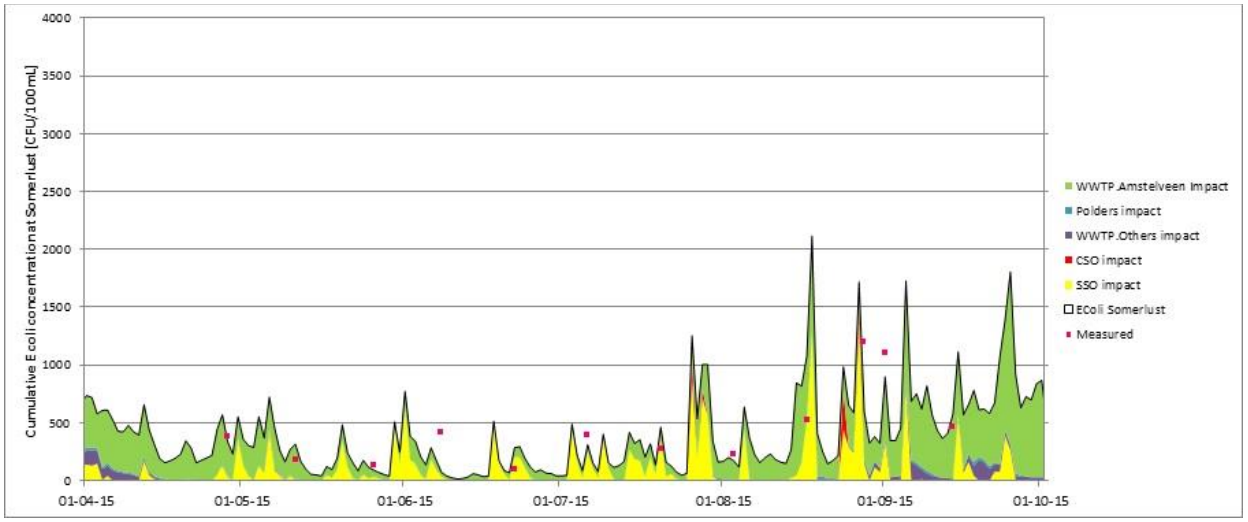

Figure 40 *E coli* concentration at Somerlust in the summer of 2015 with the shares of each source of pollution shown and the measurements (zoomed into Figure 39)

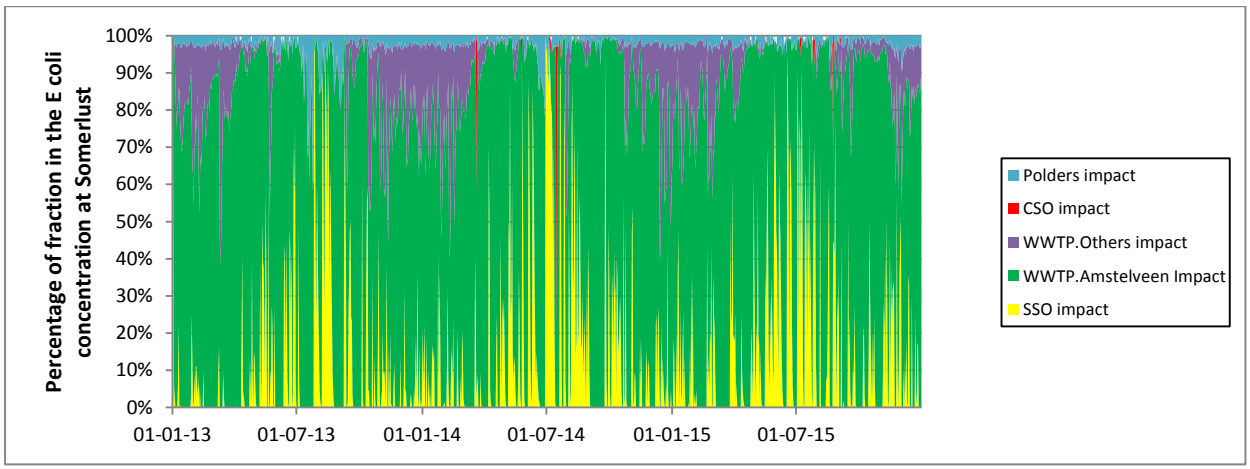

Figure 41 Figure with percent of each of the defined fractions in the *E coli* concentration at Somerlust

This part of the research thereby answers research question 3:

'What are the typical concentrations per source and net concentrations at Somerlust?'

The inflow of faecal bacteria into Somerlust's water system differs per source. The contamination from polders differs per day and per polder but is in general not that high. Although WWTPs are filtered 3.10^4 CFU/100mL flows out of their effluent. The separated sewer overflows give the best match with a flow of 1.10^5 CFU/100mL, which is within the boundaries found in literature. Although, as this value is on the upper limit and the model fit seems to increase with an increasing load for the SSOs, it is recommended to search for mis-connections to the sewer system. The combined sewer overflows have a typical concentration of 1.10^6 CFU/100mL, yet they flow less and have less influence on Somerlust. Next to the point sources a background load of 1.10^2 CFU/100mL is added to all lateral flows.

The net concentrations at Somerlust differ per source per day, but overall can be stated that the WWTP of Amstelveen has the highest fraction and loads on average. Yet the peaks in summer season are mainly caused by the SSOs. The influence of other WWTPs can mainly found back in winter periods (not swim season) and the CSOs do not play a major role for Somerlust's water quality.

3.6 Influence of weather conditions

Different pathogens or faecal indicators react different on weather conditions. Weather conditions affecting pathogens and faecal bacteria and their concentration are temperature of the water, precipitation (van de Wal *et al.,* 2012) and UV radiation (Moresco *et al.,* 2016; Liu *et al.,* 2006).

E coli bacteria survive longest in lowest water temperatures (Wang and Doyle, 1998; van Bruggen, 2010). This can also be seen in the decay rate over the year. UV intensity and exposure time both decrease the bacterial survival (van Hengel, 2015), therefore are the UV index and day length also of importance.

Precipitation might dilute the faecal bacteria concentrations in urban waters. The impact of the concentrations of for example the WWTP decrease due to the dilution of the rain (pers. comm. De Man, 2016; pers. comm. Meijers, 2016). On the other hand, precipitation shortens the travel time till the water reaches Somerlust, might lower the water temperature and might also increase the inflow of faecal bacteria in the water. Heavy rainfall events increase namely the number of faecal indicators in surface water as a result of the input of the sources 'sewer overflows' and 'surface runoff' (Rechenburg *et al.,* 2006 and Goyal *et al.,* 1977, ten Veldhuis *et al.,* 2010). Resulting in "heavy rainfall events contributing to surface water contamination in Amsterdam" (Schets *et al.,* 2008) and therefore it may also pose a potential health risks to citizens exposed to this contaminated water (ten Veldhuis *et al.,* 2010). Not only is the amount of precipitation of importance but also the duration of the rain event. Lower rainfall intensity results in lower or less discharges of sewer overflows and therefore less pollution from runoff (Schets *et al.,* 2007).

All those studies show and clarify the effects of weather conditions on E coli concentrations in urban surface waters. But are those effects also seen in the model in- and output?

In reality the *E coli* concentration per source would most likely differ due to rainfall events. If it is the first rainfall event since a long period or is it the third day in a row, would give other concentrations flowing out of the separated sewer overflows, but also matter for the loads of the WWTPs and polders. However, this model is a simplification of the truth and therefore did not take this into account. The typical concentrations of the WWTPs and both sewer overflows had a constant value. Yet, the discharges of both sewer overflows were obviously linked to the rainfall events. The discharges of the WWTPs also fluctuate over time and are really measured. The discharges of the polders are also measured but thereby fluctuating concentrations of *E coli* bacteria were manually calculated. In these calculations high precipitation was combined with slightly higher *E coli* concentrations.

When comparing the model output with water temperature, radiation and precipitation (Figure 42 and Figure 43), immediately the patterns of the peaks of the model output and precipitation are noticed. They are both displayed on another scale, although the pattern is relatively similar. Although, there is a slight delay of the *E coli* concentration reacting on the rainfall, it can be stated that the peaks in summer season are a response of the rainfall events.

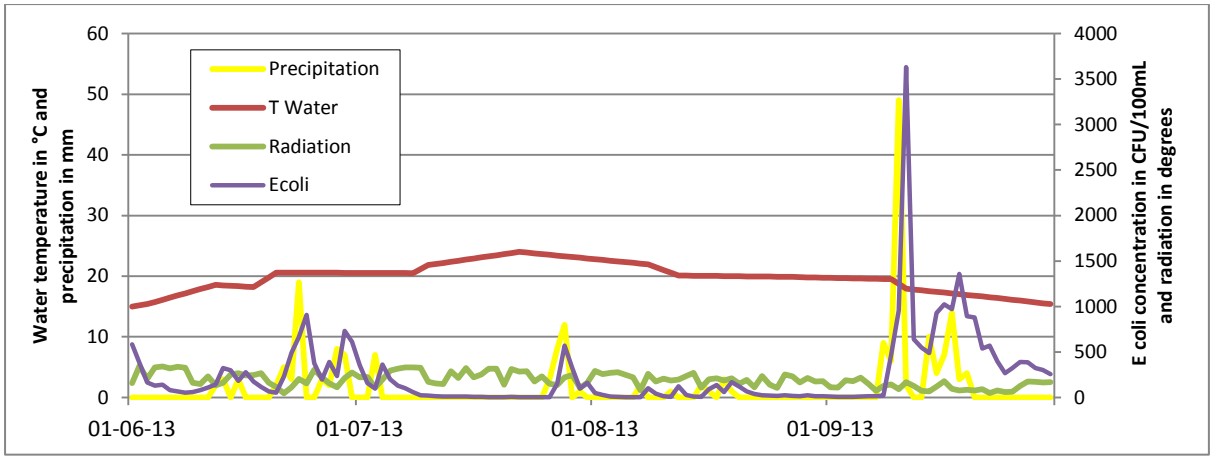

Figure 42 Precipitation, water temperature, radiation and the *E coli* concentration at Somerlust of 2013 plotted in one diagram

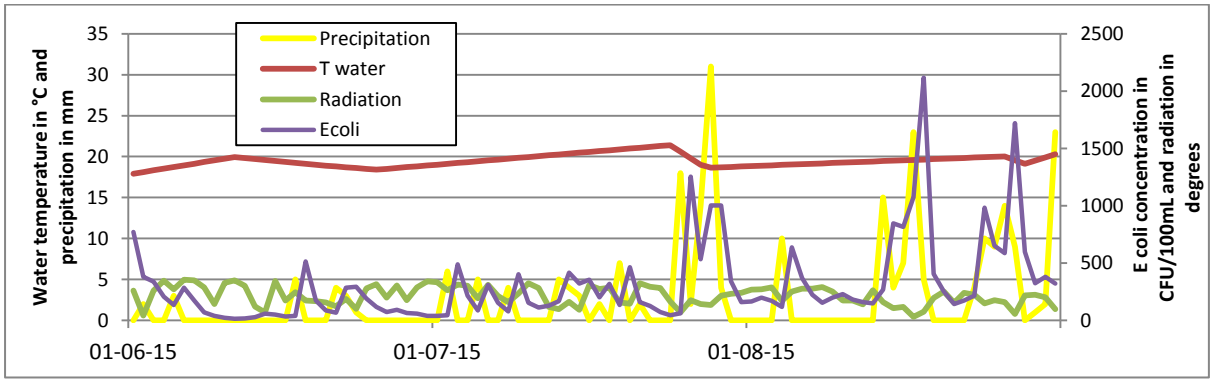

Figure 43 Precipitation, water temperature, radiation and the *E coli* concentration at Somerlust of 2015 plotted in one diagram

When looking at the sources of the *E coli* concentration at Somerlust and comparing those with the rainfall, it are indeed the SSOs which are flowing and an higher input of the WWTPs due to a higher discharge (Figure 44). The figure for the summer of 2013 can be found in the Annex.

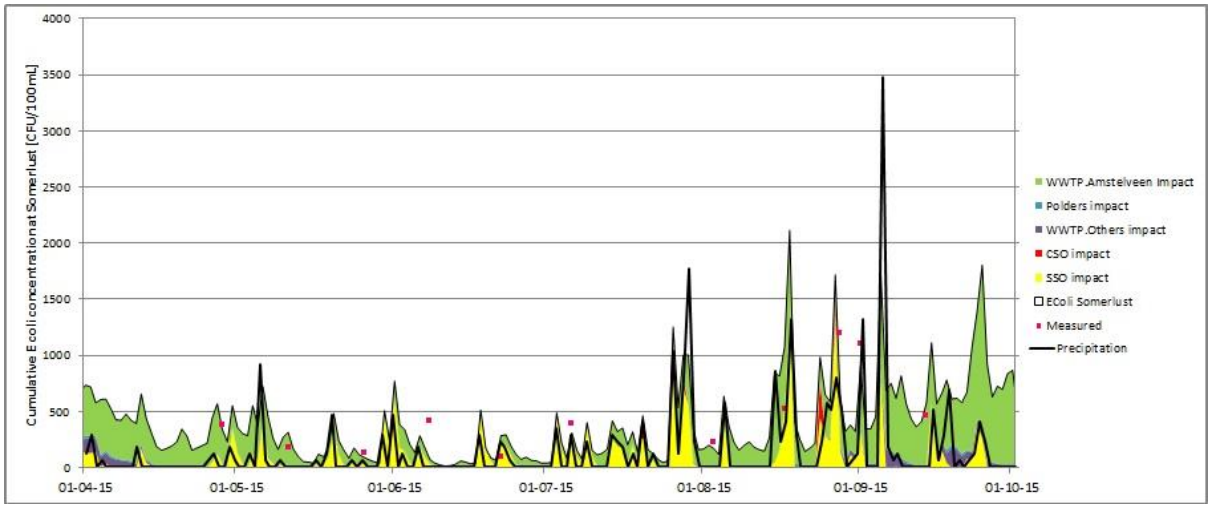

Figure 44 *E coli* concentration at Somerlust in the summer of 2015 with fractions and precipitation

Another conclusion which can be drawn is about the difference in reaction time of the SSO and WWTPs on a rainfall event. The effect of precipitation on the SSOs is seen immediately and in the day afterwards. The effect of the rainfall event on the WWTP influence at Somerlust is mostly seen in 2 days after the rainfall event.

Moreover, the temperature of the water is of importance for Somerlust's water quality, as due to higher water temperatures the decay rate increases (Figure 51, in Annex). In 2013 slightly higher water temperatures are measured and the *E coli* concentration was as low as zero during the period that the temperature reached the 22°C (Figure 45). Only a short peak in *E coli* concentration during one bigger rainfall event was noticed.

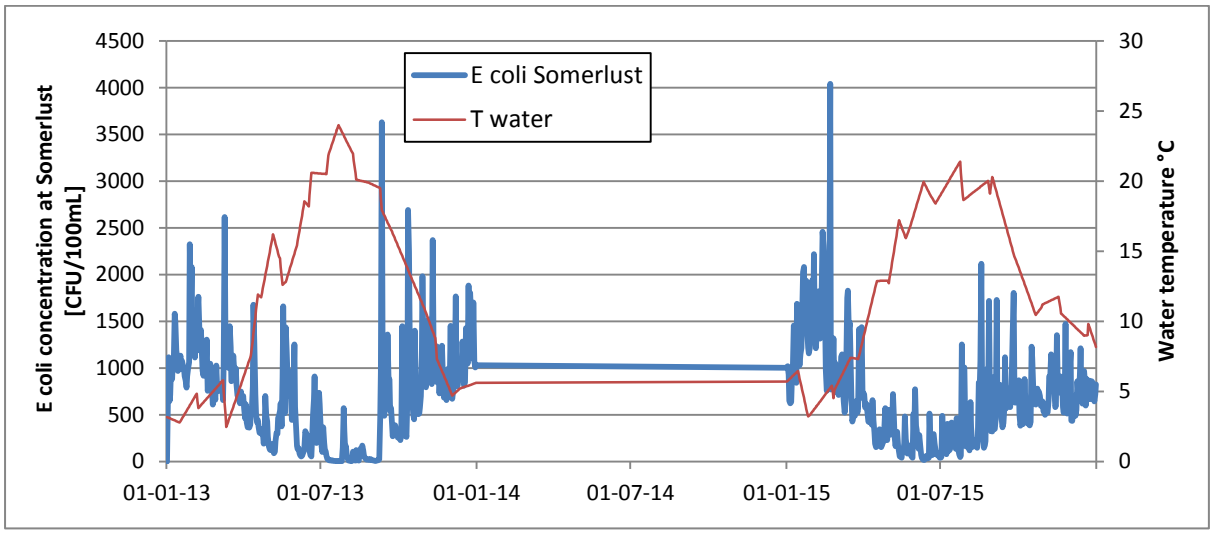

Figure 45 Line chart with the *E coli* concentration and water temperature at Somerlust for years 2013 and 2015

The solar radiation is not limiting but can give an additional decay of *E coli*. This can also be seen in the Annex in which the decay formula is explained. To show the effect of decay, an example is shown below. The precipitation during that week was zero, the temperature of the water was almost constant, but a big decrease in radiation was found in the middle of the week. During those two days, the *E coli* concentration increased due to an increase in influence of the WWTP of Amstelveen. The decay during those days was lower and more *E coli* survived. Yet, as radiation just adds up for an additional part, the differences are not as big as it could be due to a rainfall event for example.

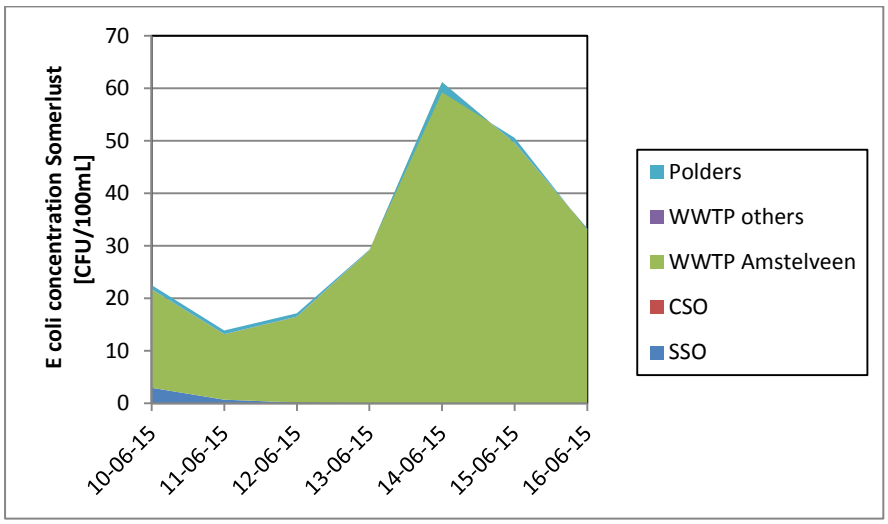

Figure 46 *E coli* concentration and its fractions at Somerlust over one week in the summer of 2015

Table 21 Precipitation, water temperature and radiation over the same week as Figure 46

Date	Precipitation [mm]	T water [°C]	Radiation [W/m2]
10-06-15	0	19.7	327
11-06-15	0	19.9	351
12-06-15	0	19.8	301
13-06-15	0	19.7	120
14-06-15	0	19.6	69
15-06-15	0	19.5	344
16-06-15	0	19.3	173

To run some additional weather scenarios on top of the three years modelling was unfortunately not possible with this 'Boezemmodel'. The meteorological data are easily to adjust and thus simulate, yet as the designers of the 'Boezemmodel' did not make a full hydrological model but used the measured discharges as their input for the laterals, those data are not changing with changing weather conditions.

This part of the research ought to answer research question 4:

'How are the sources, typical concentrations and net concentrations at Somerlust related to weather conditions?'

The WWTPs and polders are included in the model with measured discharges, which have been influenced by the weather. The SSOs in this model are directly connected to a rainfall-runoff model in SOBEK and the discharges of the CSOs are also based on the rainfall events. Runoff from streets was not taken into account in this model. The model is simplified by having constant values for the WWTPs, SSOs and CSOs. The *E coli* concentrations for the polders were manually calculated and were hereby accounted for the bigger rainfall events. Yet, the polders do not play an important role in the water quality at Somerlust.

Precipitation causes the *E coli* concentration peaks in the summer seasons and the sources which are mainly responsible for those peaks are first of all the SSOs and secondly the WWTP of Amstelveen. Higher water temperatures results in high decay rates, less survival of *E coli* and thus better water quality. The radiation is responsible for an additional decay with a maximum of 0.2 to the decay rate which is mainly caused by high water temperatures.

3.7 Assessment of human health risks

By using the curve and formula of Figure 10 (Chapter 2.6), the results of the model could be related to human health risk. Previously, with samples, three days after the sampling Waternet got an indication about the water quality some days ago. There was not yet a clear link towards the chance of getting GI problems. The European Bathing Water Directive was mainly taken into account. But with about twelve samples per summer season, it was still hard to say something about the water quality throughout the whole period. Peaks namely could be missed or the other way around in which peaks are captured but the better water quality are missed. Due to modelling the water quality at location Somerlust and being able to link the water quality to human health effects, the health effect of recreation at Somerlust can better be estimated.

Table 22 Summary of the summers of 2013 and 2015 and its water quality linked to the chance of getting GI problems

Summer season	Days	Water quality [CFU/100mL]	Chance of getting GI problems [%]	Days	Water quality [CFU/100mL]	Chance of getting GI problems [%]
2013	9	1000-3630	12-19%	66	<100	< 5.9%
2014	16	1000-2182	12-16%	54	<100	< 5.9%
2015	11	1000-2115	12-16%	34	<100	< 5.9%

Table 22 shows a summary of the model outputs of the summers of 2013, 2014 and 2015 in which the days with certain water qualities and its chance of getting GI problems are all captured, making use of the curve shown in Figure 10.

Waternet used the daily norm of 1800 CFU/100mL last year as the level above which warnings were send. Following the formula a norm of 1800 CFU/100mL would mean a fifteen percent chance of getting GI problems. In the summer of 2013 there was one day in which the level of 1800 CFU/100mL was reached and this value immediately rose to 3630 CFU/100mL. In the summer of 2014 there were two days at which the level of 1800 CFU/100mL was exceeded, namely with values of 2122 and 2182 CFU/100mL. From mid April until the end of September 2015 there were also two days in which the level of 1800 CFU/100mL was exceeded.

4 Recommendations for making an actual forecast

During this research changes in water quality in *E coli* CFU/100mL at Somerlust during the years 2013, 2014 and 2015 were modelled. The model results for 2013 compare 'sufficiently' and for 2015 'good' to observations. The results of 2015 had a bias of just -0.04. The measured data of year 2014 was seen as not valid due to a different measurement location. The typical concentrations of the contamination sources were found, the separated and combined sewer overflows included in the model and a link was made towards human health risks. This framework offers a good basis for an actual forecast.

The first step will be to cut the 'Boezemmodel', which flows from Utrecht onwards, into a smaller area that is of most importance for the *E coli* concentration in the swimming season at Somerlust itself. The area includes all the SSOs and CSOs, the WWTP of Amstelveen and the Middelpolder and is shown in Figure 48. Cutting the 'Boezemmodel' in a smaller part results also in a shorter time needed to run this model, which is practical if this model is operationalized.

The discharge at the Berlagebrug (Q_b) is measured already. The discharges of the Amstel and Weespertrekvaart can be calculated with $Q_a=frA*Q_b-Q_{WWTPAmstelveen}-Q_{polder}$ and $Q_w=frW*Q_b$ respectively (Figure 48). In order to conduct a forecast a rainfall-runoff model should be fitted with the previous discharges. Jan Wilem Voort (Waternet) made already a format for this in late January 2017.

Currently the model is designed in 1D. Therefore the process of mixing within the water was ignored. Contamination that enters the water on the other side of the canal, is immediately also on this side of the water. The mixing of the water of the Amstel, Weespertrekvaart and the water downstream at the location of Somerlust itself is probably not fully understood in this model. Reproducing this part of the water system in a D-Flow Flexible Mesh (2D or 3D) would in this case provide a solution to see whether mixing gives a significant difference. If this is the case, the whole water system within the boundaries of Figure 48 could be reproduced in 2D. Reproducing this model in 3D can even be considered, as experts of Waternet also noticed two different water flows in the vertical direction. When the D-Flow Flexible Mesh does not give any difference in longitudinal and lateral mixing, modelling in the original SOBEK file can be continued.

Forecasting the model for three days in advance will be sufficient. This is also a time period for which the KNMI is able to give decent forecast about the weather. There is also no need to look too long back in time, however the exact days needed for this are still debatable. Figure 14 shows an average age of the water from WWTP Amstelveen in the summer period of four days, yet the maximum lies at eight days. This would vote for eight or nine days hindcasting and three days forecasting. On the contrary, the weather analyses shows an effect of the WWTP of Amstelveen on changing weather conditions of about two days, this might point towards a hindcast of three or four days being sufficient (Figure 47).

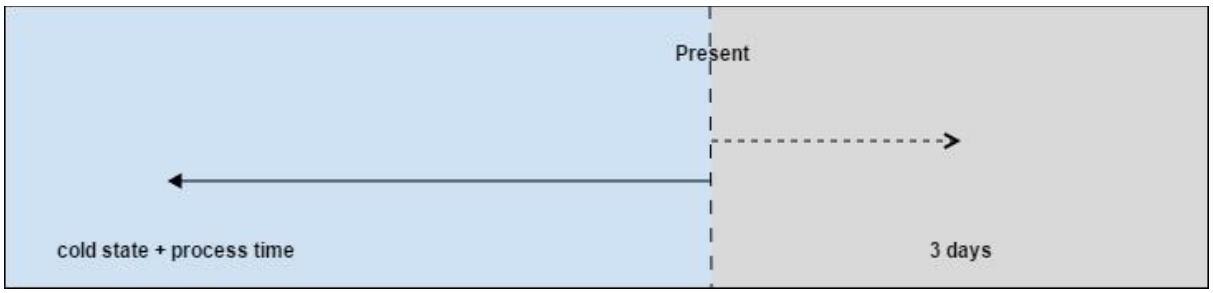

Figure 47 Simplified graph of the process time needed for a forecast

Two final recommendations for an accurate forecast are the following:

1) As the SSOs on the other side of the water have shown to be of such an importance and the typical concentration that gave the best fit with the measurements was on the upper side of the literature results, it would be useful to search for faulty connections on the sewer system in the Rivierenbuurt; and
2) Amstelveen's WWTP is also a major source affecting the water quality at Somerlust. However, no decent effluent concentrations for this WWTP are yet known. Taking some additional samples here would also increase the reliability of the model. Nonetheless, dry matter samples are taken there.

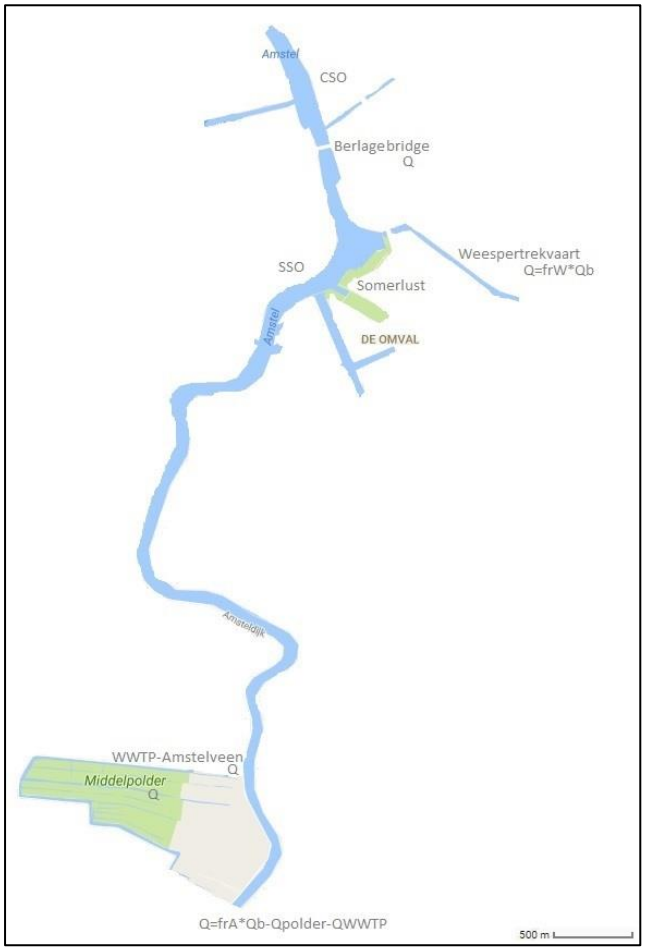

Figure 48 Schematisation of the water system around Somerlust

This Section serves to answer research question 9 and to provide Waternet the steps towards an operationalized model for the summer of 2017:

'What is required to make an actual forecast of the health risks of swim-events?'

The first step towards operationalization is to cut the 'Boezemmodel' into a smaller area. This is most important for the water quality at Somerlust during the summer season (Figure 48). A rainfall-runoff model should be designed to forecast the discharges of the Amstel and Weespertrekvaart. As there is the impression that longitudinal and lateral mixing of the water is of importance around Somerlust, the model should be developed into D-Flow Flexible Mesh to see whether mixing gives another model result.

5 Discussion

This study has demonstrated the potential use of modelling to simulate and forecast the water quality in the city of Amsterdam. Currently, the model result in comparison to the reference is classified as sufficient, however there is still place for improvement and discussion.

Right now, twelve samples of 2013 and twelve samples of 2015 were used to validate these three years of data. The data of 2014 were invalid. As a conclusion, the model was validated with 24 samples water quality samples. The model improves with the availability of more water quality monitoring data in the future and *E coli* concentration measurements at the discharges of the biggest sources. However, the 24 water quality samples were taken during interesting periods for this research, namely over two swimming seasons. Besides, the typical values used in the decay formula do not differ much from the initial values found in literature. Moreover, the model is not sensitive for the loads of the CSOs, the background concentration was set at a constant value of 1.102 CFU/100mL, the concentrations of the polders were calculated manually and not tested with the 24 samples and the effluent concentration of the WWTP of Amstelveen was also tested with the data of AMS009. This means that only the concentrations of the SSOs are solely dependent on the water quality samples taken by Waternet. However, as these SSOs are located closely to Somerlust, the water quality samples at Somerlust give proper indications about the concentration of the SSOs. Besides, the validated concentration is still within the literature spectra. The model results also compares sufficiently with the reference. As a conclusion, the 24 water quality samples were a good basis for validation.

New monitoring activities should take the samples at the same moment of the day. The sampling moment could introduce differences in the dataset. For future monitoring campaign, excluding this variation and investigating the effect of sampling moment at the day is interesting. However, currently no direct indications were found for big differences in *E coli* concentrations as a result of the period of the day. Besides, all the samples are now taken between 8 o'clock in the morning and 1 o'clock in the afternoon and most of them between 9 and 11 o'clock. Therefore, this effect will be minor for this research.

In this model set-up mostly constant *E coli* values were used for the sources. Linking the *E coli* concentrations to rainfall events would even be better. However, such detailed information was not found in literature and the effluents of the contamination sources were not measured. Precipitation was taken into account with the discharges though. Namely, the discharges of the WWTPs and polders were actually measured and discharges of CSOs and SSOs were linked to the rainfall events. Therefore provides this model still the best model results. Another aspect related to weather conditions is the homogeneous weather pattern that is applied. For the meteorological data, the data of the two most nearby measuring stations (De Bilt (Utrecht) and Schiphol (Amsterdam)) are interpolated. As the 'Boezemmodel' extends from Utrecht to Ijmuiden, these meteorological data will give a proper average. However, heavy rainfalls could be local, especially in the summer. Also radiation can differ from place to place. On the contrary, this model only extends over sixty kilometres and is covered by two weather measurement stations. For modelling this is accurate. When applying the model for a smaller area, as proposed for the forecast, only applying the KNMI data of Schiphol would likely be enough.

It was not possible to conduct a weather analyses with made up weather scenarios, because the sources and their discharges are added as point sources into the model and not directly linked to the meteorological input. This did not influence the model nor its results, but would have been an interesting additional analyses for this study. If the proposed model for forecasting would be fully weather related, then such weather analyses could be conducted. A regression method could be used to check the weather patterns with the model output and measurements.

In Chapter 2.6 a link have been made between the water quality in *E coli* (CFU/100mL) and the chance of getting GI problems during the next week. Although this method was discussed with expert Heleen de Man, uncertainties exist and assumptions have to be made to link *E coli* concentrations directly to human health risk. It should, for example, be kept in mind that *E coli* is an

bacterial indicator and no other faecal bacteria or real pathogens are included. Furthermore, the model is based on different literature studies in which different methods were used to obtain the data. On the contrary, *E coli* is used in this model because epidemiological studies on health effects from exposure to recreational water indicate that *E coli* correlates best with health outcomes for fresh water (Pruss, 1998). Moreover, the majority of the days during the swimming season have a water quality lower than 2000 *E coli* CFU/100mL. For this spectrum of water quality the shape of the curve relating the water quality to the human health impacts is justified with references that reviewed several other studies. As a result, this study developed a method for Waternet that indicates not only the water quality around Somerlust, but also the health impacts of swimming in waters with certain qualities.

A general result for the water quality of Amsterdam's canals is that high water temperatures cause more decay of the *E coli* bacteria. On the contrary, high water temperatures could also activate growth of viruses or bacteria, like blue algae. However, *E coli* are known as the best indicator for human health risks of swimming in fresh waters. This model is therefore purely tested on *E coli*. The majority of the days with water temperatures above 22°C resulted in water with *E coli* concentrations lower than 12 CFU/100mL. When the water temperature in the city of Amsterdam is measured before a swim event, like the Amsterdam City Swim, takes place, this could already indicate risks and the need for more detailed analyses.

Somerlust is a very interesting location to model the water quality, as it is a frequently used un-official swim location in the city of Amsterdam. However, the location is not yet fully located within the canals of Amsterdam where the City Swim event takes place. Another location that is located on the trajectory of the City Swim, would of course be very needed as follow-up study to forecast the water quality for such big event. Especially as in this case the CSOs do not play an important role for the water quality at Somerlust, but at another location within the canals it will definitely influence the water quality. Data of water quality samples must be available for that location.

This study showed that the WWTP of Amstelveen causes the highest fraction of *E coli* load at Somerlust throughout the year, however the peaks in summer season are linked to rainfall events and flooding of the SSOs on the other side of the water. Polders and the CSOs downstream Somerlust play a minor role in the water quality concentration at Somerlust. These results are useful for the management of Waternet as these results indicate, for example, that monitoring the separated sewer overflows is more important than monitoring the combined sewer overflows when Somerlust is the location of interest.

6 Conclusion

The aim of this research was to model the water quality in the urban surface water at Somerlust in Amsterdam to forecast the health risk of participants of a swim-event. Nine research questions were used as a guideline through this research and report. On all nine questions answers are given, which can be found within this report.

The studies first part analysed the hydrological system around Somerlust. The major waters come from upstream the Amstel River. Groot Mijdrecht is the biggest water source. However its water has an age of about eleven days before it reaches Somerlust and the bacteria are likely to die in this period. Therefore is no health impact of this source expected. On the other hand, Amstelveen's WWTP has a fraction of about seven percent of the water, but has an age of only four days till it reaches Somerlust. In this period potential pathogens can still form a serious health risk, mainly in periods with lower water temperatures. The shorter the time until the water from different sources reaches Somerlust, the less decay of *E coli* has occurred and therefore more *E coli* are likely to reach Somerlust.

WWTPs, separated and combined sewer overflows and polders are seen as the main sources of microbial contamination in the surface water in Amsterdam. For those sources typical concentrations of *E coli* have been found. Also the decay of *E coli* have been investigated and showed higher decay rates in summer than in winters. The higher decay rate in summer is caused by higher water temperatures and more chance of higher radiation. This is optimal for people who want to swim in the canals, as they are probably more enthusiastic of swimming in the water in summer periods with warmer water temperatures.

The most interesting aspect of modelling and being able to identify the relative contribution of the different contamination sources is that not only the total *E coli* concentrations are known but also the shares of each of those sources. As a result, the model results show high fractions over the whole period of Amstelveen's WWTP. However, this fraction lowers during summer periods. In the summer periods, the peaks are mostly caused by separated sewer overflows on the other side of the water. The combined sewer overflows downstream the Amstel barely reach Somerlust. The other WWTPs in the 'Boezemmodel' provide a bigger fraction of contamination during the winter, compared to summer, but are also then not significant. The polders have a quite constant share of only three percent of the pollution.

To better understand the model, its outcome and the water system in Amsterdam a sensitivity analyses was conducted. The model has shown to be sensitive for the typical values for the WWTPs and SSOs and for the values of k_0 (general decay rate) and ϑ_T (decay rate due temperature deviation) in the decay formula. The model is not sensitive for the salinity level of the water.

Precipitation is highly important in this model as it causes the concentration peaks in summer. The water temperature is positively related with the decay rate. This means that higher water temperatures result in higher *E coli* decay rates in this water system. Radiation can increase this decay rate with up to 0.2.

In this research not only the *E coli* concentration at Somerlust is modelled but also a link towards human health effects is made by literature analysis. In this analysis a formula is produced with the water quality on the x-as and chance of getting GI problems on the y-as. Combining the model output and the link to human health effects concludes in 66 days in the summer of 2013 with a chance of getting GI problems in the upcoming week lower than six percent and in 2015 there were 34 days with a chance lower than six percent.

This model better indicates the water quality at Somerlust over the past years and functions thereby as a basis for a proper forecast. In conclusion, the current model provides a sufficient correlation between the model output and measurements, although more sampling and producing in 2D or 3D instead of 1D could increase the reliability of the model. However, with this model and accompanied research, a decent framework has been produced for Waternet to operationalize this model before next summer.

References

Amsterdam Marketing, 2015. *Feature: Water in Amsterdam*. The Netherlands, Amsterdam, Amsterdam Marketing.

Asperen, I. van, Medema, G., Borgdorff, M., Sprenger, M., Havelaar, A., 1998. *Risk of gastroenteritis among triathletes in relation to faecal pollution of fresh waters.* Published in: International Journal of Epidemiology, 27, 1, 309-315.

Blaustein, R., Pachepsky, Y., Hill, R., Shelton, D., Whelan, G., 2012. *Escherichia coli survival in waters: Temperature dependence*. Published in: Elsevier, Water Research, 47, 1, 569-578.

Blom, J., Vos, T., Krooneman, J. Ham, A. van de, 2003. *Bereiding van industriewater uit RWZI effluent*. Published in: H2O, 23, 1, 19-21.

Bruggen, N. van, 2010. *Zwemwateronderzoek*: de Viersprong. The Netherlands, Ridderker, Waterschap Hollandse Delta.

Byappanahalli, M., Nevers, M., Korajkic, A., Staley, Z., Harwood, V., 2012. *Enterococci in the Environment*. Published in: Microbiology and Molecular Biology Reviews, 76, 4, 685-706.

Deltares, 2016. *SOBEK Hydrodynamics, Rainfall runoff and Real Time Control:* User Manual. The Netherlands, Delft, Deltares.

Doorduyn, Y., Pelt, W. van, Havelaar, A., 2012. *The burden of infectious intestinal disease (IID) in the community:* A survey of self-reported IID in the Netherlands. Published in: Epidemiology and infection, 140, 7, 1185-1192.

Dufour, A., Evans, O., Behymer, T., Cantu, R., 2006. *Water ingestion during swimming activities in a pool: a pilot study*. Published in: Water Health, 4, 4, 423-430.

European Parlement, 2006. *Richtlijn 2006/7/EG*. Published in: Publicatieblad van de Europese Unie, L64, 37-51.

Fleisher, J., Kay, D., Salmon, R., Jones, F., Wyer, M., Godfree, A., 1996. *Marine waters contaminated with domestic sewage:* nonenteric illnesses associated with bather exposure in the United Kingdom. Published in: Public Health, 86, 9, 1228-1234.

Goyal, S., Gerba, P., Melnick., L., 1977. *Occurrence and distribution of bacterial indicators and pathogens in canal communities along the Texas coast*. Published in: Applied Environmental Microbiology, 34, 2, 139-149.

Hengel, M. van, 2015. *Climate effects on pathogen delivery and survival in rivers*: a global modelling approach. The Netherlands, Wageningen, Wageningen University and Research, Environmental Systems Analysis Group, MSc Thesis Climate Studies.

Leenen, I., Rijs, G., Ruiter, H., 2004. *Richtgetallen voor emissiebronnen voor zwemwaterprofielen*. Grontmij-Riza-rapportage.

Los, F., Blaas, M., 2010. *Complexity, accuracy and practical applicability of different biogeochemical model versions.* Published in: Journal of Marine Systems, 81, 1, 44–74.

Lui, L., Phanikumar, M., Molloy, S., Whitman, R., Shively, D., Nevers, M., Schwab, D., Rose, J., 2006. *Modelling the Transport and Inactivation of E. coli and Enterococci in the Near-Shore Region of Lake Michigan*. Published in: Environmental science and Technology, 40, 16, 5022-5028.

Lenderink, G., Meijgaard, E. van, 2008. *Increase in hourly precipitation extremes beyond expectations from temperature changes*. Published in: Natrure Geoscience, 1, 1, 511-514.

Man, H. de, Leenen, I., Knapen, F. van, Roda Husman, A. de, 2013. *Potential health risk associated with exposure to microorganisms in urban floods.* NOVATECH 2013.

Man, H. de, 2014. *Best urban water management practices to prevent waterborne infectious diseases under current and future scenarios*. The Netherlands, Utrecht, Utrecht University, Proefschrift.

McKone, T., Daniels, J., 1991. *Estimating human exposure through multiple pathways from air, water, and soil.* Published in: Regulatory Toxicology and Pharmacology, Volume 13, Issue 1Table 12 Swim water quality scales, as decided by the European Bathing Water Directive (EP, 2006).

Moel, H. de, Asselman, N., Aerts, J., 2012. *Uncertainty and sensitivity analysis of coastal flood damage estimates in the west of the Netherlands.* Published in: Natural Hazards and Earth System Sciences, 12, 1, 1045-1058.

Mol, G., Naeff, H., Bonten, L., Beek, C. van, 2005. *Fecale belasting van oppervlaktewater door af- en uitspoeling van mest* (tweede, herziene versie). The Netherlands, Wageningen, Alterra rapport 1215.

Moresco, V., Damazo, N., Barardi, C., 2016. *Thermal and temporal stability on the enteric viruses infectivity in surface freshwater*. Published in: Water Science and Technology, 16, 3, 620-627.

OIS, 2015. *Waterrecreatie in Amsterdam*. The Netherlands, Amsterdam, Gemeente Amsterdam, Onderzoek, Informatiek en Statistiek.

Pruss, A., 1998. *Review of epidemiological studies on health effects from exposure to recreational water.* Published in: International Journal of Epidemiology, 27, 1, 1-9.

Rechenburg, A., Koch, C., Classen, T., Kistemann, T., 2006. *Impact of sewage treatment plants and combined sewer overflow basins on the microbiological quality of surface water*. Published in: Water Science Technology, 54, 1, 95-99.

Reddy, K., Khaleel, R., Overcash, R., 1981. *Behavior and Transport of Microbial Pathogens and Indicator Organisms in Soils Treated with Organic Wastes.* Published in: Journal of Environmental Quality, 10, 10, 255-266.

Reinthaler, F., Feierl, G., Posch, J., Wust, G., Haas, D., Ruckenbauer, G., Mascher, F., Marth, E., 2003. *Antibiotic resistance of E. coli in sewage and sludge*. Published in: Water Research, 37, 8, 1685-1690.

Sanders, E., Yuan, Y., Pitchford, A., 2013. *Fecal Coliform and E. coli Concentrations in Effluent-Dominated Streams of the Upper Santa Cruz Watershed*. Published in : Water, 5, 1, 243-261.

Schets, F., Wijnen, J. van, Schoon, H., Italiaander, R., Berg, H. van den, de Rosa Husman, A., 2007. *De microbiologische kwaliteit van het grachtenwater in Amsterdam.* RIVM rapport 330000011/2007.

Schets, F., Wijnen, J. van, Schijven, J., Schoon, H., Roda Husman, A. de, 2008. *Monitoring of Waterborne Pathogens in Surace Waters in Amsterdam, The Netherlands, and the Potential Health Risk Associated with Exposure to Crypotosporidium and Giardia in These Waters.* Published in: Applied Environmental Microbiology, 74, 7, 2069-2078.

Schets, F., Schijven, J. , de Roda Husman, A., 2011. *Exposure assessment for swimmers in bathing waters and swimming pools*. Published in: Water research, 45, 7, 2392-2400.

Soller, J., Bartrand, T.,Ashbolt, N., Ravenscroft, J., Wade, T., 2010. *Estimating the primary etiologic agents in recreational freshwaters impacted by human sources of faecal contamination.* Published in: Water Research. 44, 16, 4736-4747.

Straathof, N., Wiewel, B., Zoetelief, S., 2012. *Aan de Amsterdamse grachten: Een interdisciplinair onderzoek naar de kwaliteit van en invloeden op het Amsterdamse oppervlaktewater*. Beta-gamma bachelor, Thema III Interdisciplinair Onderzoek.

STOWA, 2009. *Volksgezondheid en water in het stedelijk gebied*: Gezondheidsrisicoanalyse. The Netherlands: Amersfoort, July 2009.

STOWA, 2013. *De invloed van watervogels op de bacteriologische zwemwaterkwaliteit*. The Netherlands: Amersfoort, Rapport 12, 2013.

STOWA and RIONED, 2014. *Water in de openbare ruimte heeft risico's voor de gezondheid*: Een gezondheidsrisicoanalyse voor fonteinen, bedriegertjes, water op straat en water in wadi's. The Netherlands: Amersfoort, July 2014.

STOWA and RIONED, 2016. *Gezondheidsrisico's van fonteinen in overstortvijvers beoordelen met RainTools*. The Netherlands: Amersfoort, June 2016.

US EPA, 1986. *Ambient Water Quality Criteria for Bacteria*. United States of America: U.S. Environmental Protection Agency, Office of Research and Development Microbiology and Toxicology Division, Cincinnati, Ohio.

US EPA, 2009. *Review of published studies to characterize relative risks from different sources of fecal contamination in recreation water*. United States of America: U.S. Environmental Protection Agency, Office of Water, Health and Ecological Criteria Division.

Veldhuis, J. ten, Clemens, F., Sterk. G., Berends. B., 2010. *Microbial risks associated with exposure to pathogens in contaminated urban flood water*. Published in: Elsevier, Water Research, 44, 9, 2910-2918.

Wade, T., Sams, E., Brenner, K., Haugland, R., Chern, E., Beach, M., Wymer, L., Rankin, C., Love, D., Li, Q., Noble, R., Dufour, A.,, 2010. *Rapidly measured indicators of recreational water quality and swimming-associated illness at marine beaches: a prospective cohort study.* Published in: Environmental Health, 114, 1, 24-28.

Wal, A. van de, Velzen, E. van, Kardinaal, E., 2012. *Effect van veranderingen in klimaat en ruimtedruk op de micorbiologische zwemwaterkwaliteit.* Published in: H2O, 16, 1, 25 - 27.

Wang, G., Doyle, M., 1998. *Survival of Enterohemorrhagic Escherichia coli O157:H7 in Water*. Published in: Journal of Food Protection, 6, 1, 657-775.

Waterschap de Dommel, 2016. *Waterkwaliteitsmodellering van de bacterie Escherichia coli in de Dommel*; De effecten van 3 RWZI's en 40 overstorten op de waterkwaliteit van de Dommel. Maart 2016.

Wiedenmann, A., Kruger, P., Dietz, K., Lopez-Pila, J., Szewzyk, R., Botzenhart, K., 2006. *A Randomized Controlled Trial Assessing Infectious Disease Risks from Bathing in Fresh Recreational Waters in Relation to the Concentration of Escherichia coli, Intestinal Enterococci, Clostridium perfringens, and Somatic Coliphages.* Published in: Environmental Health Perspect., 114, 2, 228-236.

Personal Conversation

Dr. ir. N Hofstra, 2016. Assisstant Professor, Environmental System Analysis group, Wageningen University and Research
L. Hersbach, 2016. Project leader 'Watersysteembesturing,' Waternet, Amsterdam
Dr. ir. H. de Man, 2016. Freelancer / Advisor Sanitas Water
E. Meijers, 2016. Senior Researcher, Deltares
L. Vermeulen, 2016. pHd candidate Environmental Systems Analysis Group, Wageningen University

Online

Actueel Hoogtebestand Nederland, n.d. *Postcodetool.* [online] Available at: http://www.ahn.nl/pagina/postcodetool.html [Accessed on 06/09/2016]

GGD Amsterdam, 2016. *Onderzoek gezondheidsrisico's deelnemers Amsterdam City Swim.* [online] Available at: http://www.ggd.amsterdam.nl/nieuwsoverzicht/onderzoek-acs/ [Accessed on 05/09/16]

Helpdesk Water, 2009. Zwemprof verie 2.6 [xls] April 2009. Available at: http://www.helpdeskwater.nl/publish/pages/18264/zwemprof_versie_2_6_nl_def.xlsx

Stanley, J., Swierzewski, M., 2008. *Overview of Gastrointestinal Symptoms*. [online] Available at: http://www.healthcommunities.com/general-gi-symptoms/overview-of-gi-symptoms.shtml [Accessed on 21/10/2016]

Stuurgroep Water, 2013. *Beslisnotitie werkwijze individuele metingen en meetfrequentie microbiologische parameters zwemwaterrichtlijn*. [online] Available at: http://www.helpdeskwater.nl/onderwerpen/gebruiksfuncties/zwemwater/zwemwater-index/zwemwaterdocumenten/@36649/beslisnotitie/

Annexes

1. Explanation of the decay rate and values

Chapter 2.4.2 includes *Eq.1* and *Eq.2*. The values in these decay formulas are explained in the next Section.

Mancini uses in 1978 0.8 and 1.07 for k_0 and ϑ_T respectively. In 2012, his values were re-evaluated by Blaustein *et al.* A database of 450 *E coli* survival datasets was assembled and from those datasets new k_0 and ϑ_T values were conducted for river waters, namely 0.725 and 1.042. Those values are used in this model. The values for salinity coefficient ($1.1.10^{-5}$), conversation factor radiation to mortality (0.086) and fraction UV (0.12) are all standard and wordwide used values.

For salinity a constant value of 450 mg/L is used. This value is the average of the measured data in the city of Amsterdam. For the water temperature (°C), the daily averages of measurements within the city of Amsterdam are taken. For the days in which the water temperature was not measured, the data were gathered by interpolating the known data. This results in Table 23. Solar radiation (W/m^2) is abstracted from the KNMI data of Schiphol (Table 23). The day length is calculated by the model itself by using the latitude of the study area (52.2 degrees). The results are shown in Figure 49. And at last, the water depth is also calculated by the model itself (Figure 50).

Table 23 Daily values of water temperature and radiation, used as model and decay input

Date	T water	Radiation [w/m2]	Date	T water	Radiation [w/m2]	Date	T water	Radiation [w/m2]
01-01-13	3.2	23.6	12-02-13	4.1	63.2	26-03-13	4.9	207.1
02-01-13	3.1	30.7	13-02-13	4.2	94.8	27-03-13	5.1	213.3
03-01-13	3.1	24.0	14-02-13	4.3	18.6	28-03-13	5.3	158.7
04-01-13	3.1	9.8	15-02-13	4.4	63.9	29-03-13	5.5	104.2
05-01-13	3.1	5.0	16-02-13	4.4	42.5	30-03-13	5.6	101.3
06-01-13	3.0	33.9	17-02-13	4.5	97.5	31-03-13	5.8	165.4
07-01-13	3.0	4.9	18-02-13	4.6	91.6	01-04-13	6.0	225.6
08-01-13	3.0	10.5	19-02-13	4.6	31.3	02-04-13	6.2	230.8
09-01-13	3.0	8.9	20-02-13	4.7	78.4	03-04-13	6.3	224.5
10-01-13	2.9	32.5	21-02-13	4.8	88.7	04-04-13	6.5	43.3
11-01-13	2.9	17.2	22-02-13	4.8	98.8	05-04-13	6.7	172.7
12-01-13	2.9	39.7	23-02-13	4.9	47.3	06-04-13	6.9	191.9
13-01-13	2.8	56.0	24-02-13	5.0	24.7	07-04-13	7.0	217.7
14-01-13	2.8	42.4	25-02-13	5.0	21.9	08-04-13	7.2	176.5
15-01-13	2.8	27.8	26-02-13	5.1	45.6	09-04-13	7.4	116.2
16-01-13	2.8	62.6	27-02-13	5.2	65.9	10-04-13	7.6	70.6
17-01-13	2.9	26.4	28-02-13	5.2	54.1	11-04-13	8.1	36.7
18-01-13	3.0	26.5	01-03-13	5.3	36.0	12-04-13	8.7	66.4
19-01-13	3.1	21.2	02-03-13	5.4	51.4	13-04-13	9.2	160.0
20-01-13	3.2	19.9	03-03-13	5.5	55.4	14-04-13	9.7	164.1
21-01-13	3.3	15.3	04-03-13	5.5	149.0	15-04-13	10.3	169.2
22-01-13	3.4	51.0	05-03-13	5.6	140.5	16-04-13	10.8	116.3
23-01-13	3.5	28.9	06-03-13	5.7	76.9	17-04-13	11.4	134.0
24-01-13	3.6	52.7	07-03-13	5.7	59.3	18-04-13	11.9	257.4
25-01-13	3.7	77.3	08-03-13	5.8	98.0	19-04-13	11.9	134.5
26-01-13	3.8	20.6	09-03-13	5.0	21.9	20-04-13	11.8	279.3
27-01-13	3.9	22.5	10-03-13	4.1	18.5	21-04-13	11.8	259.6
28-01-13	4.0	60.9	11-03-13	3.3	43.8	22-04-13	11.7	219.6
29-01-13	4.1	18.8	12-03-13	2.5	139.1	23-04-13	12.0	157.4
30-01-13	4.2	41.7	13-03-13	2.6	135.0	24-04-13	12.3	241.1
31-01-13	4.3	38.8	14-03-13	2.8	145.7	25-04-13	12.7	193.8
01-02-13	4.4	14.2	15-03-13	3.0	46.1	26-04-13	13.0	53.6
02-02-13	4.5	67.2	16-03-13	3.2	77.2	27-04-13	13.3	241.9
03-02-13	4.6	26.0	17-03-13	3.3	70.5	28-04-13	13.6	273.4
04-02-13	4.7	68.9	18-03-13	3.5	113.0	29-04-13	14.0	232.9
05-02-13	4.8	50.5	19-03-13	3.7	61.8	30-04-13	14.3	190.5
06-02-13	4.3	72.9	20-03-13	3.9	78.0	01-05-13	14.6	291.6
07-02-13	3.8	48.0	21-03-13	4.0	124.0	02-05-13	14.9	156.6
08-02-13	3.9	71.5	22-03-13	4.2	136.0	03-05-13	15.2	243.1
09-02-13	3.9	35.4	23-03-13	4.4	136.1	04-05-13	15.6	289.4
10-02-13	4.0	79.2	24-03-13	4.6	128.2	05-05-13	15.9	281.5
11-02-13	4.1	57.9	25-03-13	4.8	163.1	06-05-13	16.2	267.9

Date	T water	Radiation [w/m2]	Date	T water	Radiation [w/m2]	Date	T water	Radiation [w/m2]
07-05-13	16.0	194.9	18-06-13	19.0	265.7	30-07-13	23.0	104.3
08-05-13	15.7	150.0	19-06-13	19.8	163.0	31-07-13	22.9	163.2
09-05-13	15.5	229.1	20-06-13	20.6	116.2	01-08-13	22.8	293.1
10-05-13	15.3	193.4	21-06-13	20.6	46.5	02-08-13	22.7	255.3
11-05-13	15.1	121.6	22-06-13	20.6	113.8	03-08-13	22.6	269.8
12-05-13	14.8	165.6	23-06-13	20.6	204.3	04-08-13	22.4	278.8
13-05-13	14.6	177.1	24-06-13	20.6	153.9	05-08-13	22.3	248.4
14-05-13	14.5	163.2	25-06-13	20.6	305.8	06-08-13	22.2	221.6
15-05-13	13.9	191.3	26-06-13	20.6	222.8	07-08-13	22.1	80.8
16-05-13	13.2	56.4	27-06-13	20.6	155.6	08-08-13	22.0	260.2
17-05-13	12.6	40.2	28-06-13	20.6	114.1	09-08-13	21.5	176.5
18-05-13	12.7	79.6	29-06-13	20.6	213.8	10-08-13	21.0	206.1
19-05-13	12.7	192.1	30-06-13	20.5	275.0	11-08-13	20.6	184.8
20-05-13	12.8	32.3	01-07-13	20.5	223.3	12-08-13	20.1	196.9
21-05-13	12.8	32.2	02-07-13	20.5	224.4	13-08-13	20.1	234.3
22-05-13	13.0	160.2	03-07-13	20.5	110.8	14-08-13	20.1	269.3
23-05-13	13.2	222.5	04-07-13	20.5	197.6	15-08-13	20.1	108.6
24-05-13	13.4	162.3	05-07-13	20.5	294.3	16-08-13	20.0	201.6
25-05-13	13.6	205.6	06-07-13	20.5	318.1	17-08-13	20.0	211.1
26-05-13	13.8	175.7	07-07-13	20.5	331.8	18-08-13	20.0	187.3
27-05-13	14.0	341.0	08-07-13	20.5	330.9	19-08-13	20.0	212.3
28-05-13	14.2	319.6	09-07-13	21.2	326.7	20-08-13	20.0	151.0
29-05-13	14.4	86.2	10-07-13	21.8	173.4	21-08-13	20.0	194.4
30-05-13	14.6	170.0	11-07-13	22.0	156.0	22-08-13	20.0	113.4
31-05-13	14.8	296.8	12-07-13	22.2	148.0	23-08-13	19.9	235.0
01-06-13	15.0	156.9	13-07-13	22.4	289.1	24-08-13	19.9	141.0
02-06-13	15.2	349.2	14-07-13	22.6	214.1	25-08-13	19.9	105.9
03-06-13	15.4	203.8	15-07-13	22.7	324.4	26-08-13	19.9	252.8
04-06-13	15.8	329.4	16-07-13	22.9	222.6	27-08-13	19.9	233.7
05-06-13	16.1	340.6	17-07-13	23.1	254.4	28-08-13	19.8	163.9
06-06-13	16.5	321.5	18-07-13	23.3	317.8	29-08-13	19.8	216.0
07-06-13	16.8	338.7	19-07-13	23.5	316.8	30-08-13	19.8	175.9
08-06-13	17.2	327.0	20-07-13	23.6	142.2	31-08-13	19.8	178.9
09-06-13	17.5	163.1	21-07-13	23.8	313.5	01-09-13	19.7	111.9
10-06-13	17.9	149.3	22-07-13	24.0	283.9	02-09-13	19.7	110.8
11-06-13	18.2	232.8	23-07-13	23.9	289.6	03-09-13	19.7	189.7
12-06-13	18.6	133.8	24-07-13	23.8	174.3	04-09-13	19.6	178.6
13-06-13	18.5	162.3	25-07-13	23.6	232.2	05-09-13	19.6	217.0
14-06-13	18.4	251.7	26-07-13	23.5	152.4	06-09-13	19.6	151.3
15-06-13	18.3	266.8	27-07-13	23.4	138.7	07-09-13	19.6	74.0
16-06-13	18.3	242.7	28-07-13	23.3	222.7	08-09-13	19.5	126.9
17-06-13	18.2	247.2	29-07-13	23.2	246.5	09-09-13	19.5	143.8

Date	T water	Radiation [w/m2]	Date	T water	Radiation [w/m2]	Date	T water	Radiation [w/m2]
10-09-13	18.7	89.7	22-10-13	12.2	90.3	03-12-13	4.7	37.4
11-09-13	17.9	169.7	23-10-13	12.1	51.7	04-12-13	4.8	7.4
12-09-13	17.8	126.0	24-10-13	11.9	102.8	05-12-13	4.8	5.1
13-09-13	17.7	74.5	25-10-13	11.8	19.1	06-12-13	4.9	21.5
14-09-13	17.5	66.4	26-10-13	11.6	55.7	07-12-13	4.9	15.2
15-09-13	17.4	120.1	27-10-13	11.5	52.8	08-12-13	5.0	21.9
16-09-13	17.3	179.3	28-10-13	11.4	45.3	09-12-13	5.0	34.0
17-09-13	17.2	95.6	29-10-13	11.2	54.4	10-12-13	5.1	44.7
18-09-13	17.0	78.9	30-10-13	11.1	85.6	11-12-13	5.1	49.4
19-09-13	16.9	84.7	31-10-13	10.9	37.6	12-12-13	5.2	41.4
20-09-13	16.8	75.7	01-11-13	10.8	18.5	13-12-13	5.2	18.5
21-09-13	16.7	90.9	02-11-13	10.6	15.4	14-12-13	5.2	26.9
22-09-13	16.5	50.0	03-11-13	10.4	32.5	15-12-13	5.3	21.2
23-09-13	16.4	77.2	04-11-13	10.3	27.7	16-12-13	5.3	27.2
24-09-13	16.3	58.8	05-11-13	10.1	19.2	17-12-13	5.3	9.7
25-09-13	16.1	62.7	06-11-13	9.9	24.1	18-12-13	5.3	19.9
26-09-13	16.0	126.7	07-11-13	9.8	33.3	19-12-13	5.3	29.6
27-09-13	15.8	174.9	08-11-13	9.6	43.3	20-12-13	5.4	37.0
28-09-13	15.7	171.3	09-11-13	9.5	46.1	21-12-13	5.4	5.4
29-09-13	15.5	166.7	10-11-13	9.3	47.2	22-12-13	5.4	8.6
30-09-13	15.4	168.8	11-11-13	9.1	41.8	23-12-13	5.4	25.0
01-10-13	15.2	161.5	12-11-13	9.0	10.1	24-12-13	5.5	3.0
02-10-13	15.1	122.5	13-11-13	8.8	56.7	25-12-13	5.5	35.9
03-10-13	15.0	138.3	14-11-13	8.1	18.9	26-12-13	5.5	19.8
04-10-13	14.8	83.6	15-11-13	7.3	56.7	27-12-13	5.5	6.4
05-10-13	14.7	76.9	16-11-13	7.2	31.8	28-12-13	5.5	38.7
06-10-13	14.5	114.4	17-11-13	7.0	15.7	29-12-13	5.6	38.1
07-10-13	14.4	112.7	18-11-13	6.9	23.7	30-12-13	5.6	24.2
08-10-13	14.2	67.8	19-11-13	6.7	23.4	31-12-13	5.6	20.7
09-10-13	14.1	66.9	20-11-13	6.6	27.8	01-01-14	5.6	21.1
10-10-13	14.0	94.0	21-11-13	6.4	38.2	02-01-14	5.6	22.3
11-10-13	13.8	9.6	22-11-13	6.3	19.1	03-01-14	5.7	19.3
12-10-13	13.7	72.0	23-11-13	6.1	39.9	04-01-14	5.7	21.1
13-10-13	13.5	9.6	24-11-13	6.0	29.1	05-01-14	5.7	39.8
14-10-13	13.4	18.2	25-11-13	5.9	42.4	06-01-14	5.7	28.9
15-10-13	13.2	28.9	26-11-13	5.7	27.3	07-01-14	5.7	21.3
16-10-13	13.1	71.3	27-11-13	5.6	13.3	08-01-14	5.8	26.3
17-10-13	12.9	86.5	28-11-13	5.4	19.2	09-01-14	5.8	10.0
18-10-13	12.8	42.0	29-11-13	5.3	8.9	10-01-14	5.8	36.2
19-10-13	12.7	54.1	30-11-13	5.1	33.6	11-01-14	5.8	25.5
20-10-13	12.5	62.8	01-12-13	5.0	16.3	12-01-14	5.9	49.0
21-10-13	12.4	50.3	02-12-13	4.8	37.6	13-01-14	5.9	32.5

Date	T water	Radiation [w/m2]	Date	T water	Radiation [w/m2]	Date	T water	Radiation [w/m2]
14-01-14	5.9	12.2	25-02-14	5.9	46.4	08-04-14	13.6	135.0
15-01-14	5.9	8.8	26-02-14	6.0	99.9	09-04-14	14.1	220.6
16-01-14	5.9	10.9	27-02-14	6.1	34.7	10-04-14	14.1	108.7
17-01-14	5.8	16.8	28-02-14	6.2	71.8	11-04-14	14.2	164.2
18-01-14	5.6	34.6	01-03-14	6.2	60.5	12-04-14	14.3	180.0
19-01-14	5.5	20.7	02-03-14	6.3	123.8	13-04-14	14.4	190.3
20-01-14	5.3	8.7	03-03-14	6.4	39.9	14-04-14	14.4	154.5
21-01-14	5.2	6.1	04-03-14	6.5	101.6	15-04-14	14.5	150.6
22-01-14	5.0	36.3	05-03-14	6.6	129.5	16-04-14	14.6	258.8
23-01-14	4.8	10.1	06-03-14	6.7	79.1	17-04-14	14.7	183.0
24-01-14	4.7	24.1	07-03-14	7.4	68.9	18-04-14	14.7	137.3
25-01-14	4.5	21.8	08-03-14	8.1	145.6	19-04-14	14.8	227.0
26-01-14	4.4	24.5	09-03-14	8.9	159.6	20-04-14	14.9	220.3
27-01-14	4.2	32.5	10-03-14	9.6	152.8	21-04-14	15.0	100.3
28-01-14	4.0	20.0	11-03-14	9.7	114.5	22-04-14	15.0	198.3
29-01-14	3.9	46.4	12-03-14	9.8	163.0	23-04-14	15.1	233.9
30-01-14	3.7	35.0	13-03-14	9.9	153.8	24-04-14	15.2	149.4
31-01-14	3.6	61.9	14-03-14	10.1	104.3	25-04-14	15.2	233.1
01-02-14	3.4	30.8	15-03-14	10.2	101.5	26-04-14	15.3	183.9
02-02-14	3.3	59.1	16-03-14	10.3	136.6	27-04-14	15.4	104.6
03-02-14	3.1	79.9	17-03-14	10.4	67.0	28-04-14	15.5	123.3
04-02-14	3.7	58.8	18-03-14	10.5	59.6	29-04-14	15.5	126.5
05-02-14	4.3	61.6	19-03-14	10.6	148.3	30-04-14	15.6	130.9
06-02-14	4.4	42.2	20-03-14	10.7	183.9	01-05-14	15.7	161.8
07-02-14	4.5	10.4	21-03-14	10.9	90.0	02-05-14	15.8	107.3
08-02-14	4.5	21.8	22-03-14	11.0	102.2	03-05-14	15.8	219.7
09-02-14	4.6	19.7	23-03-14	11.1	126.2	04-05-14	15.9	202.0
10-02-14	4.7	39.8	24-03-14	11.2	177.7	05-05-14	16.0	268.6
11-02-14	4.8	48.4	25-03-14	11.3	164.2	06-05-14	16.1	169.3
12-02-14	4.9	72.5	26-03-14	11.4	113.3	07-05-14	16.1	207.5
13-02-14	4.9	37.2	27-03-14	11.5	169.2	08-05-14	15.7	79.5
14-02-14	5.0	41.4	28-03-14	11.6	198.7	09-05-14	15.2	191.4
15-02-14	5.1	55.6	29-03-14	11.8	184.4	10-05-14	14.8	80.2
16-02-14	5.2	77.5	30-03-14	11.9	150.7	11-05-14	14.3	84.5
17-02-14	5.3	66.4	31-03-14	12.0	160.0	12-05-14	13.9	185.5
18-02-14	5.4	36.2	01-04-14	12.1	178.1	13-05-14	13.9	272.1
19-02-14	5.4	49.7	02-04-14	12.3	160.2	14-05-14	14.2	234.8
20-02-14	5.5	17.1	03-04-14	12.5	182.6	15-05-14	14.6	299.0
21-02-14	5.6	74.0	04-04-14	12.7	44.3	16-05-14	15.1	311.2
22-02-14	5.7	82.3	05-04-14	13.0	176.2	17-05-14	15.5	311.0
23-02-14	5.8	86.7	06-04-14	13.2	49.7	18-05-14	16.0	309.0
24-02-14	5.8	102.5	07-04-14	13.4	131.7	19-05-14	16.4	282.4

Date	T water	Radiation [w/m2]	Date	T water	Radiation [w/m2]	Date	T water	Radiation [w/m2]
20-05-14	16.8	265.9	01-07-14	20.5	341.0	12-08-14	20.0	210.2
21-05-14	17.3	157.6	02-07-14	20.9	279.2	13-08-14	19.6	262.4
22-05-14	17.7	267.5	03-07-14	21.3	327.7	14-08-14	19.3	211.7
23-05-14	18.1	223.1	04-07-14	21.1	244.9	15-08-14	19.0	195.5
24-05-14	18.6	222.7	05-07-14	20.8	167.2	16-08-14	18.7	148.5
25-05-14	19.0	228.2	06-07-14	20.6	117.1	17-08-14	18.4	63.0
26-05-14	19.5	117.0	07-07-14	20.3	215.2	18-08-14	18.1	147.3
27-05-14	19.9	82.4	08-07-14	20.1	50.0	19-08-14	17.8	152.5
28-05-14	20.1	38.5	09-07-14	19.7	39.2	20-08-14	17.8	139.9
29-05-14	20.3	69.9	10-07-14	20.0	281.9	21-08-14	17.8	155.8
30-05-14	20.4	322.2	11-07-14	20.4	230.4	22-08-14	17.8	89.8
31-05-14	20.6	280.4	12-07-14	20.7	256.8	23-08-14	17.9	170.5
01-06-14	20.8	293.9	13-07-14	21.1	208.7	24-08-14	17.9	201.6
02-06-14	21.0	219.3	14-07-14	21.4	184.8	25-08-14	17.9	63.9
03-06-14	21.2	232.2	15-07-14	21.8	137.6	26-08-14	17.9	103.7
04-06-14	21.3	127.1	16-07-14	22.1	308.0	27-08-14	17.9	249.2
05-06-14	21.5	176.9	17-07-14	22.5	268.5	28-08-14	17.9	108.2
06-06-14	21.7	333.2	18-07-14	22.8	299.9	29-08-14	17.9	208.0
07-06-14	21.9	229.4	19-07-14	23.2	246.5	30-08-14	18.0	122.0
08-06-14	22.1	247.6	20-07-14	23.5	145.8	31-08-14	18.0	145.1
09-06-14	22.2	207.4	21-07-14	23.9	74.4	01-09-14	18.0	182.2
10-06-14	22.4	197.7	22-07-14	24.2	315.0	02-09-14	18.0	204.5
11-06-14	22.6	344.7	23-07-14	24.1	318.4	03-09-14	18.2	228.8
12-06-14	21.2	292.8	24-07-14	23.9	291.1	04-09-14	18.4	205.2
13-06-14	19.8	338.3	25-07-14	23.8	106.0	05-09-14	18.5	100.3
14-06-14	20.0	180.8	26-07-14	23.7	181.9	06-09-14	18.7	85.8
15-06-14	20.2	235.0	27-07-14	23.6	230.6	07-09-14	18.9	157.1
16-06-14	20.4	151.0	28-07-14	23.4	145.4	08-09-14	19.1	201.6
17-06-14	20.4	187.6	29-07-14	23.3	189.4	09-09-14	19.2	85.5
18-06-14	20.5	231.3	30-07-14	23.2	261.7	10-09-14	19.4	133.8
19-06-14	20.5	78.9	31-07-14	23.0	256.0	11-09-14	19.5	161.8
20-06-14	20.6	167.4	01-08-14	22.9	230.9	12-09-14	19.6	195.5
21-06-14	20.6	290.0	02-08-14	22.8	188.5	13-09-14	19.6	169.3
22-06-14	20.6	317.7	03-08-14	22.7	265.2	14-09-14	19.7	158.1
23-06-14	20.7	238.7	04-08-14	22.5	285.8	15-09-14	19.7	190.0
24-06-14	20.7	240.2	05-08-14	22.4	248.0	16-09-14	19.8	158.3
25-06-14	20.6	206.9	06-08-14	23.0	77.4	17-09-14	19.6	184.6
26-06-14	20.5	280.9	07-08-14	22.8	207.4	18-09-14	19.5	180.6
27-06-14	20.4	170.6	08-08-14	22.2	125.9	19-09-14	19.4	155.2
28-06-14	20.3	225.1	09-08-14	21.7	246.3	20-09-14	19.2	122.9
29-06-14	20.2	291.4	10-08-14	21.1	96.8	21-09-14	19.1	147.6
30-06-14	20.1	228.8	11-08-14	20.5	244.4	22-09-14	19.0	141.8

Date	T water	Radiation [w/m2]	Date	T water	Radiation [w/m2]	Date	T water	Radiation [w/m2]
23-09-14	18.8	94.2	04-11-14	10.8	45.6	16-12-14	4.8	25.6
24-09-14	18.7	56.8	05-11-14	10.6	31.7	17-12-14	4.8	9.5
25-09-14	18.6	116.1	06-11-14	10.4	17.0	18-12-14	4.9	15.7
26-09-14	18.5	70.7	07-11-14	9.5	23.6	19-12-14	4.9	23.6
27-09-14	18.3	122.6	08-11-14	9.4	74.8	20-12-14	5.0	16.7
28-09-14	18.2	129.7	09-11-14	9.4	60.9	21-12-14	5.1	12.3
29-09-14	18.1	68.8	10-11-14	9.3	73.1	22-12-14	5.1	10.3
30-09-14	17.9	83.8	11-11-14	9.2	60.8	23-12-14	5.2	36.8
01-10-14	17.8	81.5	12-11-14	9.1	27.2	24-12-14	5.2	14.1
02-10-14	17.6	66.8	13-11-14	9.1	63.2	25-12-14	5.3	27.0
03-10-14	17.3	148.8	14-11-14	9.0	27.4	26-12-14	5.3	28.7
04-10-14	17.0	123.6	15-11-14	8.7	10.5	27-12-14	5.4	5.6
05-10-14	16.7	105.1	16-11-14	8.5	12.5	28-12-14	5.5	45.9
06-10-14	16.4	26.3	17-11-14	8.2	43.2	29-12-14	5.5	30.0
07-10-14	16.1	91.2	18-11-14	8.0	12.4	30-12-14	5.6	15.3
08-10-14	15.7	36.5	19-11-14	7.7	9.7	31-12-14	5.6	40.3
09-10-14	15.4	113.9	20-11-14	7.5	13.8	01-01-15	5.7	17.8
10-10-14	15.2	118.2	21-11-14	7.3	57.8	02-01-15	5.8	39.5
11-10-14	15.1	56.4	22-11-14	7.0	46.6	03-01-15	5.8	8.7
12-10-14	14.9	111.8	23-11-14	6.8	41.8	04-01-15	5.9	44.9
13-10-14	14.7	43.4	24-11-14	6.5	46.4	05-01-15	5.9	18.2
14-10-14	14.5	22.0	25-11-14	6.3	35.9	06-01-15	6.0	30.7
15-10-14	14.3	115.7	26-11-14	6.0	26.2	07-01-15	6.0	37.5
16-10-14	14.2	78.0	27-11-14	5.8	14.8	08-01-15	6.1	4.5
17-10-14	14.0	90.6	28-11-14	5.5	25.0	09-01-15	6.2	13.0
18-10-14	13.8	97.0	29-11-14	5.3	45.0	10-01-15	6.2	13.4
19-10-14	13.6	52.1	30-11-14	5.0	7.1	11-01-15	6.3	32.5
20-10-14	13.5	86.5	01-12-14	4.8	6.4	12-01-15	6.3	12.7
21-10-14	13.3	28.9	02-12-14	4.5	8.2	13-01-15	6.4	11.2
22-10-14	13.1	64.4	03-12-14	4.3	8.8	14-01-15	6.5	27.0
23-10-14	12.9	33.6	04-12-14	4.3	11.6	15-01-15	6.2	7.5
24-10-14	12.7	17.0	05-12-14	4.2	19.3	16-01-15	5.9	40.6
25-10-14	12.6	46.3	06-12-14	4.2	40.6	17-01-15	5.6	55.3
26-10-14	12.4	36.8	07-12-14	4.2	8.9	18-01-15	5.4	12.6
27-10-14	12.2	88.2	08-12-14	4.1	23.7	19-01-15	5.1	24.5
28-10-14	12.0	32.4	09-12-14	4.1	32.4	20-01-15	4.8	25.6
29-10-14	11.8	19.0	10-12-14	4.2	40.0	21-01-15	4.6	33.9
30-10-14	11.7	30.6	11-12-14	4.3	17.2	22-01-15	4.3	15.9
31-10-14	11.5	51.9	12-12-14	4.4	6.3	23-01-15	4.0	34.5
01-11-14	11.3	82.1	13-12-14	4.5	19.3	24-01-15	3.7	66.4
02-11-14	11.1	73.5	14-12-14	4.6	41.0	25-01-15	3.5	23.1
03-11-14	10.9	25.5	15-12-14	4.7	22.8	26-01-15	3.2	18.8

Date	T water	Radiation [w/m2]	Date	T water	Radiation [w/m2]	Date	T water	Radiation [w/m2]
27-01-15	3.3	37.3	10-03-15	6.6	160.2	21-04-15	12.9	274.1
28-01-15	3.3	6.5	11-03-15	6.7	157.5	22-04-15	12.9	83.0
29-01-15	3.4	28.5	12-03-15	6.8	173.8	23-04-15	12.9	229.7
30-01-15	3.5	61.6	13-03-15	6.9	170.6	24-04-15	12.9	238.4
31-01-15	3.5	53.8	14-03-15	7.0	29.6	25-04-15	12.9	104.9
01-02-15	3.6	44.3	15-03-15	7.2	50.7	26-04-15	12.9	53.0
02-02-15	3.7	56.0	16-03-15	7.3	131.9	27-04-15	12.9	277.8
03-02-15	3.8	71.3	17-03-15	7.4	158.6	28-04-15	12.9	226.6
04-02-15	3.9	80.1	18-03-15	7.4	49.8	29-04-15	12.9	115.7
05-02-15	3.9	60.6	19-03-15	7.4	145.9	30-04-15	12.9	275.6
06-02-15	4.0	90.2	20-03-15	7.4	100.3	01-05-15	12.7	215.5
07-02-15	4.1	41.6	21-03-15	7.4	81.1	02-05-15	13.1	255.4
08-02-15	4.2	61.2	22-03-15	7.3	165.3	03-05-15	13.5	91.4
09-02-15	4.3	25.2	23-03-15	7.3	115.9	04-05-15	13.8	233.6
10-02-15	4.4	17.7	24-03-15	7.3	99.5	05-05-15	14.2	200.9
11-02-15	4.4	18.1	25-03-15	7.3	43.3	06-05-15	14.6	171.6
12-02-15	4.5	24.9	26-03-15	7.3	60.8	07-05-15	15.0	292.8
13-02-15	4.6	87.2	27-03-15	7.6	98.3	08-05-15	15.3	197.3
14-02-15	4.7	35.4	28-03-15	7.8	43.5	09-05-15	15.7	172.6
15-02-15	4.8	97.2	29-03-15	8.1	37.3	10-05-15	16.1	269.9
16-02-15	4.8	94.3	30-03-15	8.3	168.1	11-05-15	16.5	260.4
17-02-15	4.9	74.2	31-03-15	8.6	160.2	12-05-15	16.8	252.4
18-02-15	5.0	115.0	01-04-15	8.8	143.8	13-05-15	17.2	283.3
19-02-15	5.1	110.8	02-04-15	9.1	182.4	14-05-15	17.0	244.9
20-02-15	5.2	21.3	03-04-15	9.3	148.1	15-05-15	16.9	247.8
21-02-15	5.2	37.2	04-04-15	9.6	138.0	16-05-15	16.7	140.6
22-02-15	5.3	103.5	05-04-15	9.8	209.7	17-05-15	16.6	284.3
23-02-15	5.4	104.6	06-04-15	10.1	119.3	18-05-15	16.4	89.1
24-02-15	5.0	83.1	07-04-15	10.3	183.3	19-05-15	16.2	258.6
25-02-15	4.5	56.8	08-04-15	10.6	166.3	20-05-15	16.1	264.4
26-02-15	5.1	28.5	09-04-15	10.8	221.5	21-05-15	15.9	311.1
27-02-15	5.2	107.4	10-04-15	11.1	219.3	22-05-15	16.1	224.2
28-02-15	5.3	107.8	11-04-15	11.4	98.4	23-05-15	16.2	218.3
01-03-15	5.5	133.7	12-04-15	11.6	228.0	24-05-15	16.4	326.0
02-03-15	5.6	89.7	13-04-15	11.9	212.0	25-05-15	16.5	188.9
03-03-15	5.7	51.5	14-04-15	12.1	241.6	26-05-15	16.7	274.5
04-03-15	5.8	59.3	15-04-15	12.4	252.7	27-05-15	16.9	261.0
05-03-15	5.9	120.1	16-04-15	12.6	159.4	28-05-15	17.1	200.3
06-03-15	6.1	68.6	17-04-15	12.9	139.4	29-05-15	17.3	93.8
07-03-15	6.2	122.7	18-04-15	12.9	266.9	30-05-15	17.5	277.1
08-03-15	6.3	156.1	19-04-15	12.9	208.9	31-05-15	17.7	73.6
09-03-15	6.4	104.3	20-04-15	12.9	270.8	01-06-15	17.9	258.8

Date	T water	Radiation [w/m2]	Date	T water	Radiation [w/m2]	Date	T water	Radiation [w/m2]
02-06-15	18.1	42.2	14-07-15	20.4	163.7	25-08-15	20.0	176.5
03-06-15	18.3	260.6	15-07-15	20.5	93.4	26-08-15	20.0	158.4
04-06-15	18.5	345.6	16-07-15	20.6	306.7	27-08-15	19.6	57.2
05-06-15	18.7	271.3	17-07-15	20.7	273.0	28-08-15	19.1	219.2
06-06-15	18.9	355.1	18-07-15	20.8	286.2	29-08-15	19.5	223.0
07-06-15	19.1	348.7	19-07-15	20.9	157.9	30-08-15	19.9	202.0
08-06-15	19.3	289.2	20-07-15	21.0	145.1	31-08-15	20.3	99.5
09-06-15	19.5	142.1	21-07-15	21.1	323.8	01-09-15	20.1	162.7
10-06-15	19.7	327.0	22-07-15	21.2	293.1	02-09-15	19.9	169.3
11-06-15	20.0	350.8	23-07-15	21.3	281.3	03-09-15	19.6	120.3
12-06-15	19.8	300.7	24-07-15	21.4	163.9	04-09-15	19.4	69.4
13-06-15	19.7	120.0	25-07-15	20.6	70.9	05-09-15	19.2	139.0
14-06-15	19.6	69.4	26-07-15	19.8	177.0	06-09-15	19.0	106.7
15-06-15	19.5	344.3	27-07-15	19.0	142.0	07-09-15	18.8	114.6
16-06-15	19.3	172.7	28-07-15	18.7	135.0	08-09-15	18.5	92.5
17-06-15	19.2	246.5	29-07-15	18.7	214.8	09-09-15	18.3	210.9
18-06-15	19.1	173.4	30-07-15	18.7	233.6	10-09-15	18.1	200.0
19-06-15	19.0	167.9	31-07-15	18.8	239.8	11-09-15	17.9	200.0
20-06-15	18.9	157.4	01-08-15	18.8	267.2	12-09-15	17.7	70.6
21-06-15	18.8	123.0	02-08-15	18.9	271.9	13-09-15	17.4	139.8
22-06-15	18.7	187.8	03-08-15	18.9	288.7	14-09-15	17.2	82.9
23-06-15	18.6	101.9	04-08-15	19.0	171.1	15-09-15	17.0	69.8
24-06-15	18.5	280.0	05-08-15	19.0	251.6	16-09-15	16.8	32.2
25-06-15	18.4	314.8	06-08-15	19.1	275.5	17-09-15	16.6	43.3
26-06-15	18.5	198.6	07-08-15	19.1	275.9	18-09-15	16.3	149.3
27-06-15	18.6	305.6	08-08-15	19.2	290.2	19-09-15	16.1	123.1
28-06-15	18.7	176.6	09-08-15	19.2	250.8	20-09-15	15.9	106.7
29-06-15	18.8	287.4	10-08-15	19.3	173.4	21-09-15	15.7	110.9
30-06-15	18.9	340.2	11-08-15	19.3	173.4	22-09-15	15.5	99.9
01-07-15	19.0	332.1	12-08-15	19.4	138.8	23-09-15	15.2	93.9
02-07-15	19.1	261.6	13-08-15	19.4	261.9	24-09-15	15.0	34.6
03-07-15	19.2	312.2	14-08-15	19.5	159.3	25-09-15	14.8	135.3
04-07-15	19.3	301.0	15-08-15	19.5	106.0	26-09-15	14.6	156.9
05-07-15	19.4	191.8	16-08-15	19.6	117.9	27-09-15	14.5	184.5
06-07-15	19.5	309.8	17-08-15	19.6	32.5	28-09-15	14.3	121.8
07-07-15	19.6	212.6	18-08-15	19.6	75.0	29-09-15	14.2	164.2
08-07-15	19.7	160.3	19-08-15	19.7	195.8	30-09-15	14.0	170.0
09-07-15	19.8	235.6	20-08-15	19.7	251.7	01-10-15	13.8	169.1
10-07-15	20.0	323.8	21-08-15	19.8	154.4	02-10-15	13.7	168.9
11-07-15	20.1	281.5	22-08-15	19.8	241.8	03-10-15	13.5	126.9
12-07-15	20.2	116.9	23-08-15	19.9	224.8	04-10-15	13.3	109.3
13-07-15	20.3	99.0	24-08-15	19.9	149.3	05-10-15	13.2	78.7

Date	T water	Radiation [w/m2]	Date	T water	Radiation [w/m2]	Date	T water	Radiation [w/m2]
06-10-15	13.0	69.4	17-11-15	11.8	23.8	29-12-15	8.5	16.0
07-10-15	12.8	34.3	18-11-15	11.4	39.8	30-12-15	8.3	36.9
08-10-15	12.6	78.9	19-11-15	11.0	17.8	31-12-15	8.2	33.2
09-10-15	12.5	125.2	20-11-15	10.6	30.1	01-01-16	8.0	36.5
10-10-15	12.3	131.4	21-11-15	10.5	36.6			
11-10-15	12.1	127.4	22-11-15	10.4	35.0			
12-10-15	12.0	120.8	23-11-15	10.4	39.9			
13-10-15	11.8	82.2	24-11-15	10.3	5.4			
14-10-15	11.6	21.8	25-11-15	10.3	24.3			
15-10-15	11.5	20.4	26-11-15	10.2	52.5			
16-10-15	11.3	17.7	27-11-15	10.1	16.0			
17-10-15	11.1	13.7	28-11-15	10.1	38.0			
18-10-15	11.0	37.6	29-11-15	10.0	11.5			
19-10-15	10.8	33.2	30-11-15	10.0	8.9			
20-10-15	10.6	49.0	01-12-15	9.9	13.2			
21-10-15	10.5	31.5	02-12-15	9.9	16.1			
22-10-15	10.5	38.4	03-12-15	9.8	20.4			
23-10-15	10.6	41.7	04-12-15	9.7	47.8			
24-10-15	10.7	36.0	05-12-15	9.7	22.2			
25-10-15	10.8	87.8	06-12-15	9.6	15.5			
26-10-15	10.8	110.1	07-12-15	9.6	22.6			
27-10-15	10.9	97.5	08-12-15	9.5	29.3			
28-10-15	11.0	43.9	09-12-15	9.4	45.9			
29-10-15	11.2	77.4	10-12-15	9.4	15.4			
30-10-15	11.2	74.1	11-12-15	9.3	11.7			
31-10-15	11.3	92.6	12-12-15	9.3	16.8			
01-11-15	11.3	49.9	13-12-15	9.2	27.0			
02-11-15	11.3	87.3	14-12-15	9.2	19.0			
03-11-15	11.3	72.8	15-12-15	9.1	28.0			
04-11-15	11.4	28.6	16-12-15	9.0	8.9			
05-11-15	11.4	27.0	17-12-15	9.0	28.9			
06-11-15	11.4	22.9	18-12-15	9.0	23.3			
07-11-15	11.5	25.5	19-12-15	9.0	13.5			
08-11-15	11.5	42.2	20-12-15	9.0	17.2			
09-11-15	11.5	31.1	21-12-15	9.0	27.3			
10-11-15	11.5	13.7	22-12-15	9.8	3.6			
11-11-15	11.6	20.5	23-12-15	9.6	31.9			
12-11-15	11.6	58.6	24-12-15	9.4	28.5			
13-11-15	11.6	55.4	25-12-15	9.3	17.0			
14-11-15	11.7	30.1	26-12-15	9.1	30.8			
15-11-15	11.7	18.4	27-12-15	8.9	5.6			
16-11-15	11.7	12.0	28-12-15	8.7	40.4			

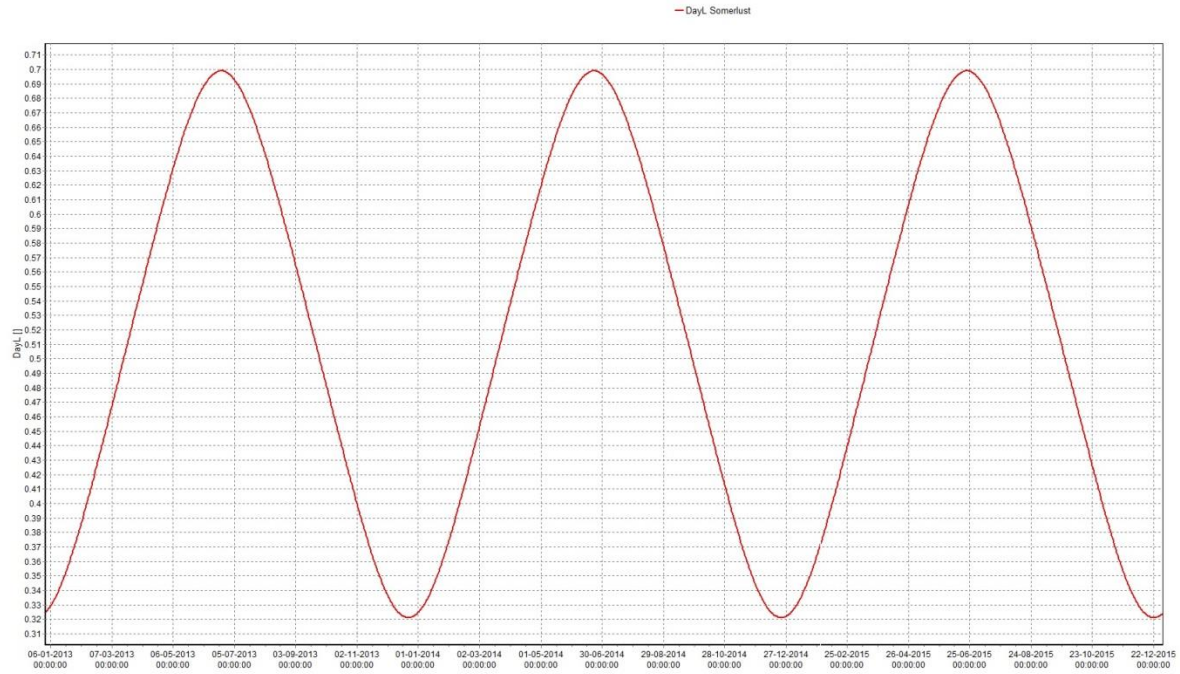

Figure 49 Day length over time used in this model

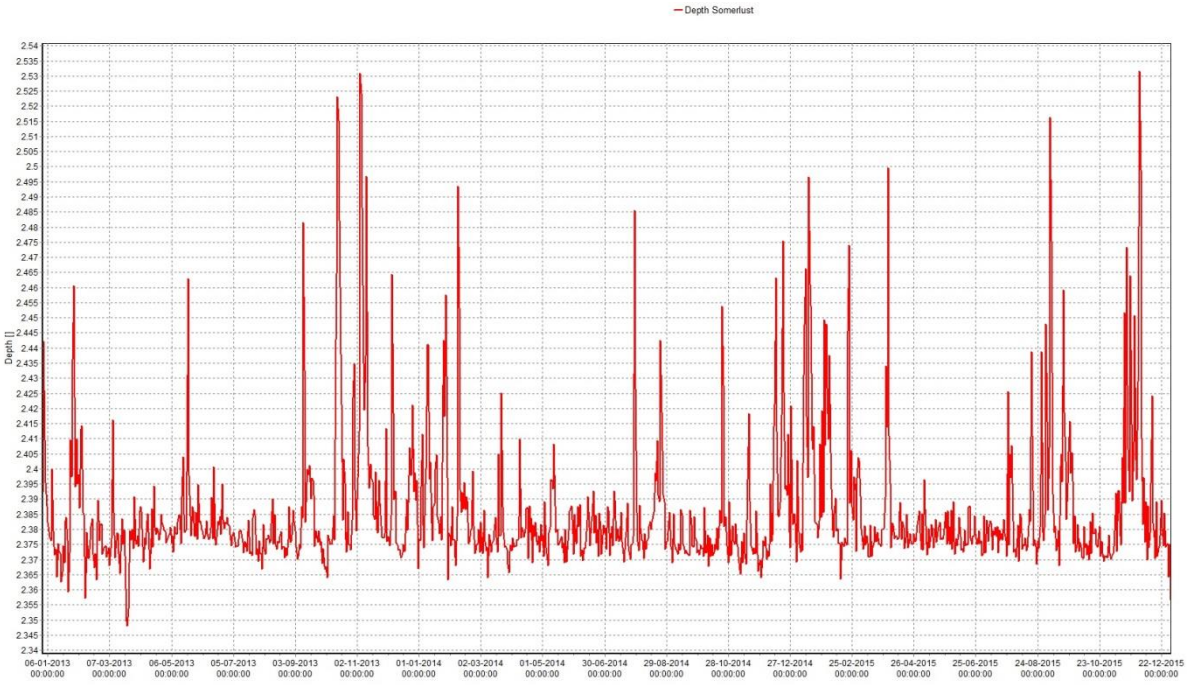

Figure 50 Water depth over time at location Somerlust

As a conclusion, the first part of the formula, namely the temperature and salinity mortality rate is plotted in Figure 51. As can be seen, the mortality rate is gradually increasing with an increasing temperature. Two Celcius degrees is set as the critical value for decay of *E coli*.

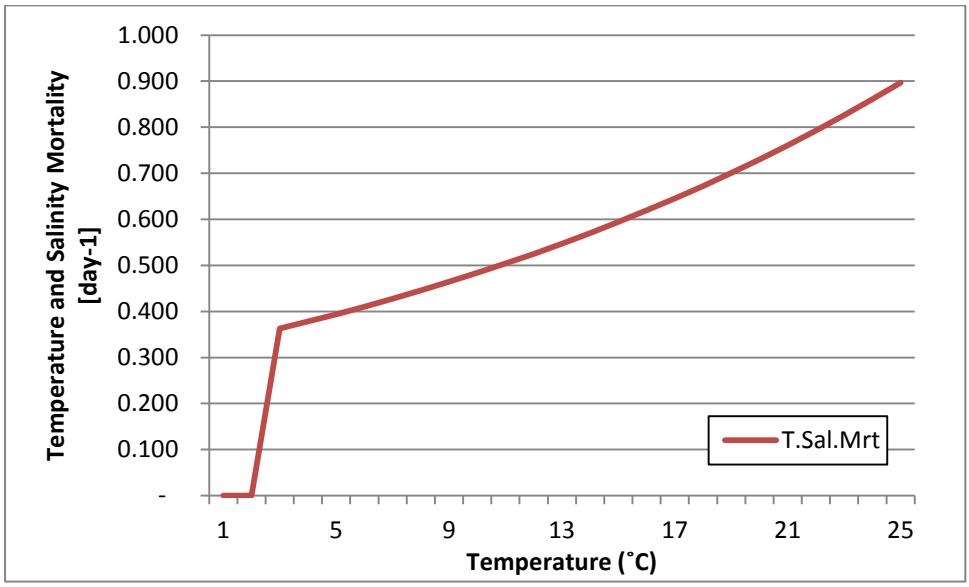

Figure 51 Temperature and Salinity mortality rates plotted against the water temperature

Additionally the mortality rate due to radiation is added to get the total mortality rate per timestep. As the radiation is variable over time a simple table is made to see what the effect is of different radiation values (Table 24).

Table 24 Additional mortality rate due to difference in radiation

Rad (W/m2)	Mrt.Rad
0	0
25	0.01505
50	0.0301
75	0.04515
100	0.0602
125	0.07525
150	0.090299
175	0.105349
200	0.120399
225	0.135449
250	0.150499
275	0.165549
300	0.180599
325	0.195649
350	0.210699

The final total mortality rate, assessed with this formula is shown in Figure 52. This plot matches with the findings of Reddy *et al.* (1981) as they state that the first order die-off rate in a simplified formula would be 0.99 with 20°C and 0.50 with 15°C.

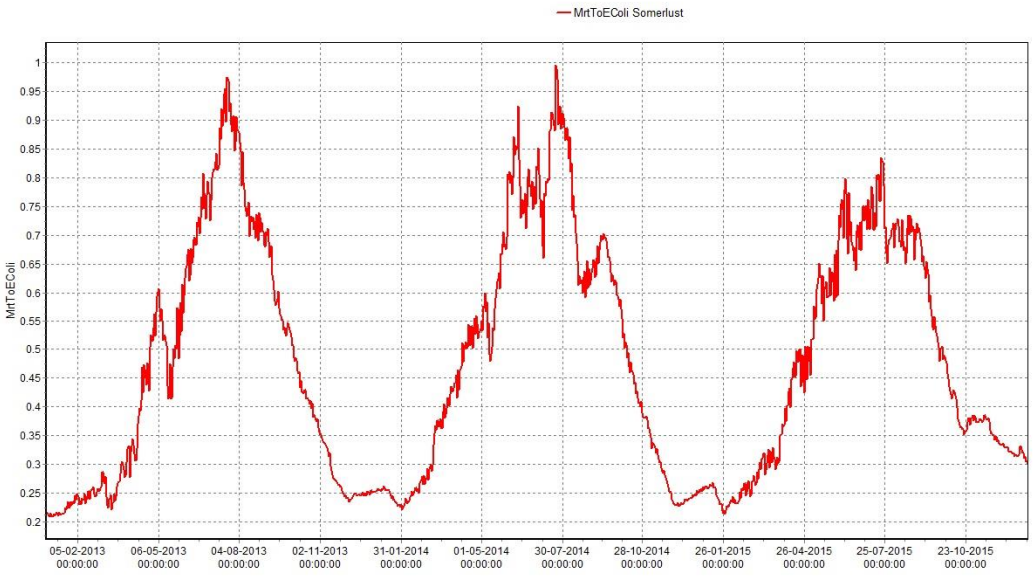

Figure 52 Decay rates per day of *E coli* modelled in SOBEK over time

2. Formula and tables used in chapter 2.6 to determine the effect of E coli to human health

Doorduyn *et al.* (2012) states that the general monthly risk of getting GI problems -thus without swimming in surface water- is five percent. As all the other studies give their chance of getting GI problems in one week after the swim event, the monthly risk is transferred into a risk per week with the following formula:

$$P_{sick_{month}} = 1 - \left(1 - P_{sick_{week}}\right)^{\frac{52}{12}}$$

Solving this formula, results in a weekly chance of getting sick in general of 1.18 percent.

Table 25 Measurements of *E coli* bacteria during the City Swim of 2015

ACS 06/09/2015	Location	CFU/100mL
	Start	4400
	Mid	7100
	End	11000
	Average	7500

Table 26 Concluding table corresponding to the final Figure 10 in Chapter 2.6

Reference	Chance of getting GI problems [%]	Water quality framed as "..."	*E coli* concentrations in water (CFU/100mL) linked to framing	C min	C max	% min	% max
Doorduyn *et al.* (2012)	1.18	-	0	-	-	-	-
Stuurgroep Water (2013)	7.75	approved	500	500	999	7	8.5
STOWA (2009)	11	just sufficient	1000	1000	1800	-	-
GGD Amsterdam (2016)	31	polluted	7500	4400	11000	-	-

3. Discharges at the Berlage-brug of the new and initial datafile

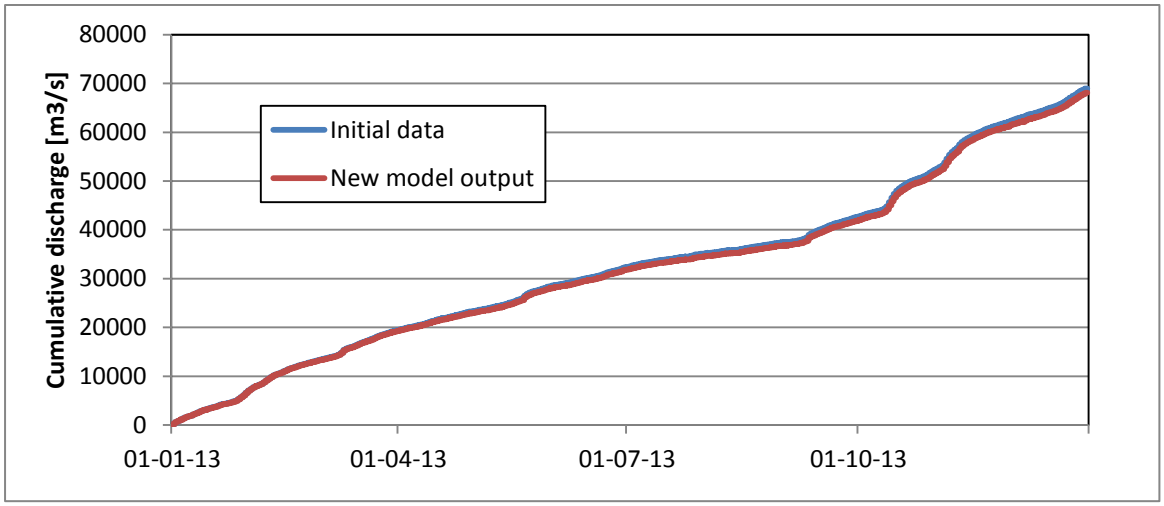

Figure 53 Discharges at the Berlage-brug of the new and initial datafile

4. E coli concentration input for polders

The *E coli* concentrations for polders were found in literature as burden (CFU) to the surface water during the whole swim-runoff-season per hectare, soil type and land use (Mol *et al.,* 2005) (Table 23).

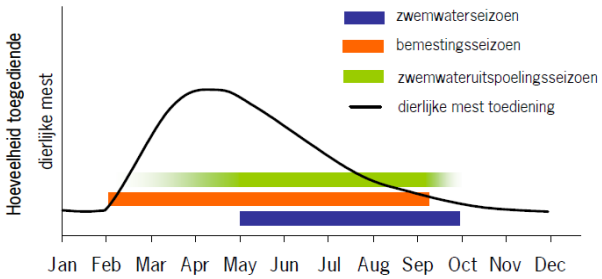

Figure 54 Explanation of swim-runoff-season, designed by Mol *et al.* (2005)

The soil type around Amsterdam is peat and the land is mainly grazed by cows, therefore the CFU/(ha, swim-runoff-season) is $2.3.10^{10}$. As the swim season has 153 days the total burden per ha per day is $1.5.10^{8}$. With this number the CFU/day per polder is calculated (Table 27).

Table 27 Concentrations per day per polder

Polder	Area (ha)	Concentration (CFU/day)
Middelpolder	58	$8.72.10^{9}$
Duivendrecht	320	$4.81.10^{10}$
Holendrecht	200	$3.01.10^{10}$
Waardassacker	600	$9.02.10^{10}$
Horstermeer	600	$9.02.10^{10}$
BijlmerSouth	not grazed anymore	$0.00.10^{0}$
Bijlmer	not grazed anymore	$0.00.10^{0}$
Groot Mijdrecht	1000	$1.50.10^{11}$

The data of Table 27 were transferred into CFU/100mL, the unit which is used as input in SOBEK, by converting those data with the average discharge per day (Table 28). The *hourly* discharge per polder was known by Waternet, which was combined in this research to average discharge over the day.
Additional to the CFU/100mL per day per polder, there was quickly looked into the rainfall and time of fertilization. For Amstelveen, no concrete information on the sewer overflows was known by Waternet. Yet, it is known that the sewer overflows discharge close to the polder pumping stations. Therefore an additional log CFU/100mL is added on those days where the precipitation per hour was higher than 10milimeters. For the additional contamination due to fertilization, a rough estimation is made. Following a farmer in the Netherlands, farmers fertilize their grassland immediately when they are allowed to (mid Febr), once at the end of the season (end Augustus) and once or twice in the middle (around June/July). As the middle of February is not yet in the swim-runoff-season (Figure 54), this time is not taken into account. For the other three cases, a log CFU/100mL is added for those days on all polders.

Table 28 Calculation table for Duivendrecht polder as example to show how to transformation of numbers is done

Data	Average discharge m3/s	m3/day	L/day	100mL/day	CFU/day	CFU/100mL
01-12-12	0.1967	$1.70.10^{4}$	$1.70.10^{7}$	$1.70.10^{8}$	$4.81.10^{10}$	$2.83.10^{2}$
02-12-12	0.3629	$3.14.10^{4}$	$3.14.10^{7}$	$3.14.10^{8}$	$4.81.10^{10}$	$1.53.10^{2}$
03-12-12	0.1721	$1.49.10^{4}$	$1.49.10^{7}$	$1.49.10^{8}$	$4.81.10^{10}$	$3.24.10^{2}$
04-12-12	0.2596	$2.24.10^{4}$	$2.24.10^{7}$	$2.24.10^{8}$	$4.81.10^{10}$	$2.14.10^{2}$
05-12-12	0.1429	$1.23.10^{4}$	$1.23.10^{7}$	$1.23.10^{8}$	$4.81.10^{10}$	$3.90.10^{2}$
…	…	…	…	…	…	…

5. Runoff areas per separated sewer overflow

Table 29 Runoff areas per separated sewer overflows obtained from QGIS, numbers corresponding with Figure 55.

Separated SO	Runoff area (m^2)
1	84600
2	900
3	148050
4	4500
5	4320
6	2700
7	84600
8	55350
9	3240

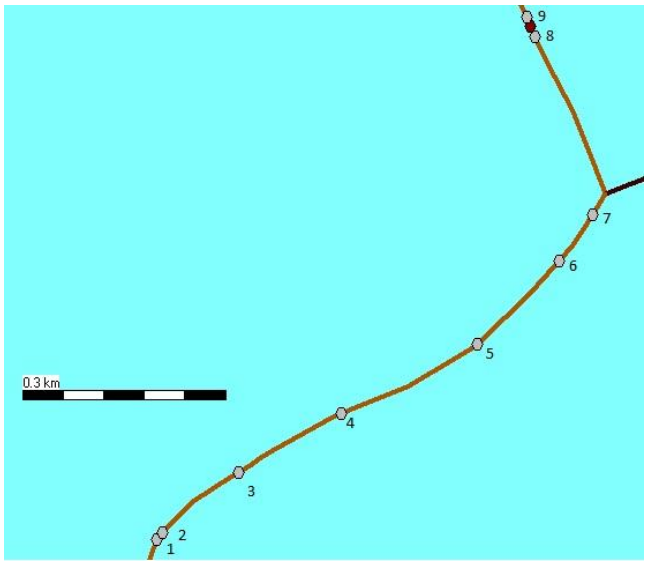

Figure 55 Location and numbers of separated sewer overflows

6. Calculation of the discharges of the combined sewer overflows

As described in chapter 2.4.3 the calculations for the discharges of the combined sewer overflows were done by combining the overflow status, water level in the sewer, threshold levels of the overflows, overflow width's and discharge calculated with a rainfall-runoff model of Jan Willem Voort (Waternet). The first three items could be found in FEWS, however not for all CSO's those data were always available. The overflow width's was obtained out of QGIS with a map of the whole sewer system of Amsterdam (Table 30). The data of the overflow status, water level in the sewer and the threshold level of the overflows were combined into first of all the information if the overflow was flowing and if so, how high the water had reached above the threshold level.The latter was used as an input value for the following formula in which the overflow width was also added;

$$D = 1.8 * w * h^{\frac{3}{2}}$$

With: D Discharge (m3/s)
w Width of the sewer overflow (m)
h Water height in the sewer above the threshold level (m)

The rainfall-runoff model of Voort is seen as less accurate, however, when adding precipitation, runoff area (Table 30) and a buffer height of the overflow (7mm), the discharges could be calculated for every day needed. Therefore is this method used when the other data were not available.

Table 30 Runoff areas and width per combined sewer overflows obtained from QGIS, names corresponding with Figure 56.

Name combined SO	Global runoff area [m^2]	Width [mm]
Amsteldijk 824	125000	4240
Amsteldijk 811	125000	4600
Amsteldijk 101	125000	3350
Weesperzijde 69	65000	1840
Weesperzijde 2	65000	3070
Weesperzijde 3	65000	3460
Weesperzijde 4	65000	18770

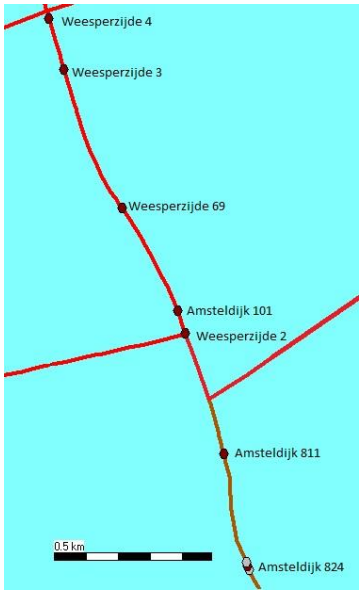

Figure 56 Location and names of the different combined sewer overflows

When all those data is combined, using yes/no formulas in Excel, one general discharge is obtained with this self-designed method. In such a way a discharge is calculated for a period and overflows were no discharges were known. As can be seen in Figure 57 most times when the status of Weesperzijde shows an overflow status, the three different ways of calculating the discharges cover each other and get most of the status events. Some differences still can be found, but in agreement with Waternet, this method can now be used in periods where no measurements are available.

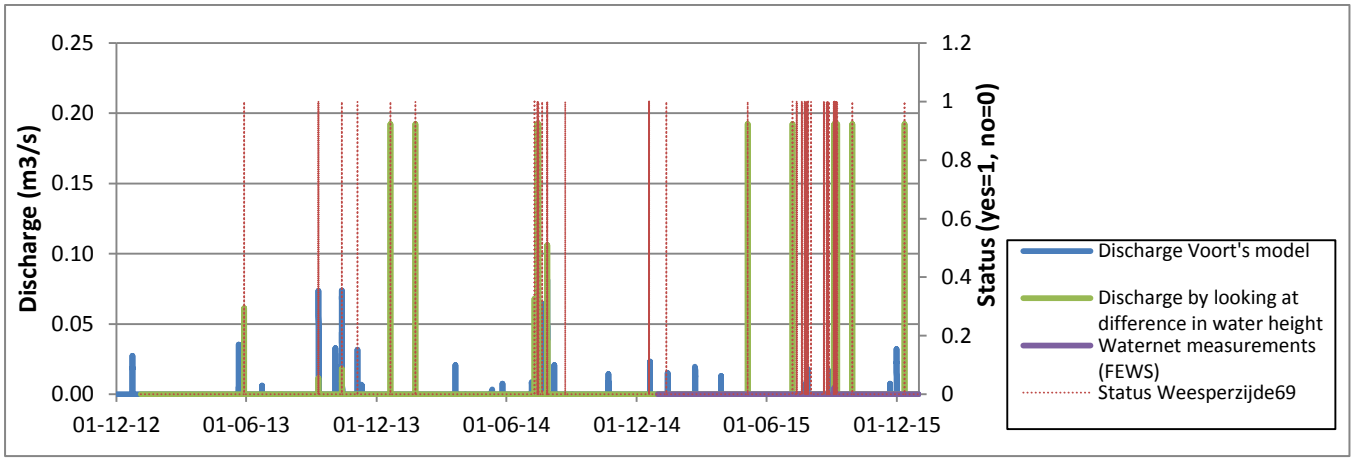

Figure 57 All the data combined for calculating the discharges of the combined SO in as example Weesperzijde69

7. Fraction calculation for location Somerlust

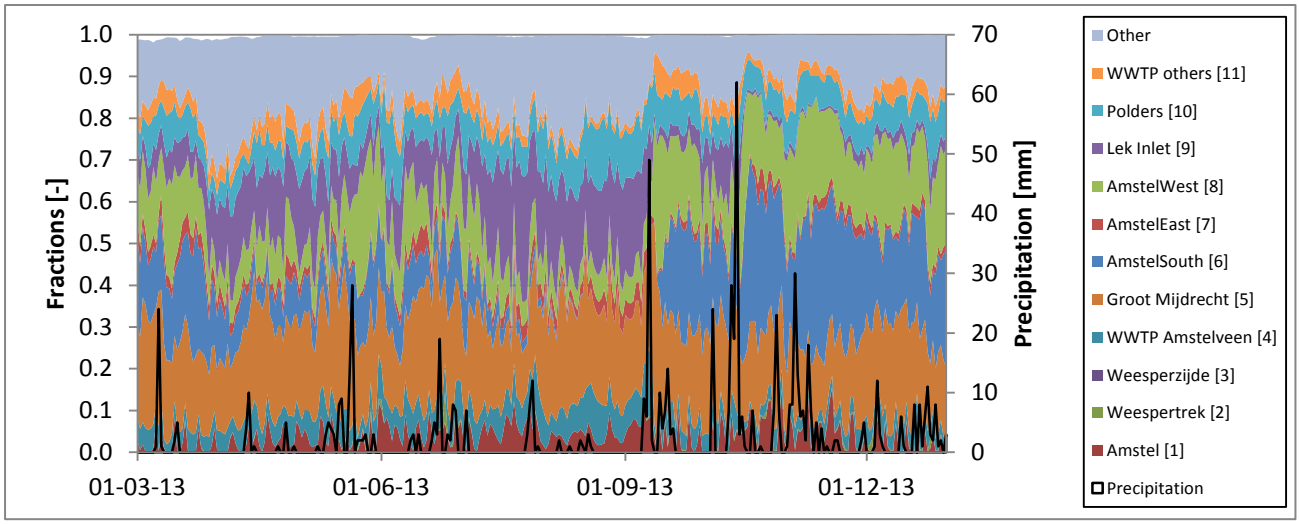

Figure 58 Fraction calculation for location Somerlust year 2013

Note that Figure 58 start at the first of March instead of January; this is done as first the 'initial' water of Somerlust had to flow away and for the time span which was needed for the other water to reach Somerlust. The influence of the initial water can still be found in the bit of 'missing' water to complete the 100 percent.

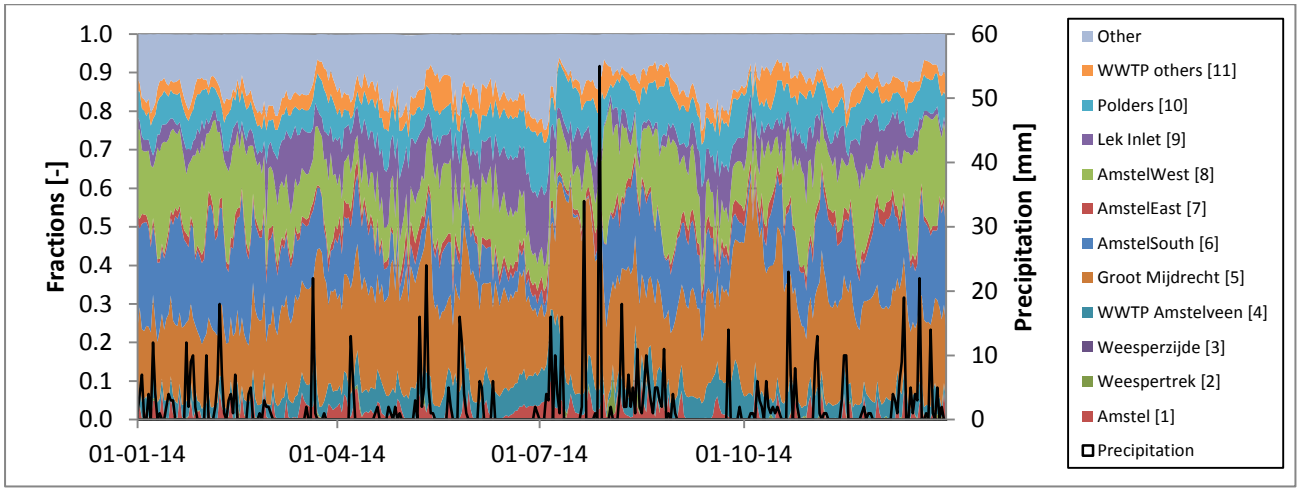

Figure 59 Fraction calculation for location Somerlust year 2014

Table 31 Detailed table with fraction and ages of the water corresponding (2013)

Source	Year	Fraction [min] [-]	Fraction [max] [-]	Fraction [average summer] [-]	Age [min] [days]	Age [max] [days]	Age [average summer] [days]
Groot Mijndrecht	2013	0.11	0.38	0.24	3	24	14
Amstel South	2013	0	0.18	0.07	16	81	42
Amstel West	2013	0.06	0.42	0.16	2	13	8
Lek Inlet	2013	0.02	0.34	0.19	15	31	23
Muiden	2013	0.01	0.17	0.09	1	15	9
Amstel East	2013	0.02	0.18	0.07	3	19	11
WWTP Amstelveen	2013	0.02	0.16	0.07	0.5	11	5.5
HDSR	2013	0.07	0.29	0.12	4	24	17
HolendrechtBullenwijk	2013	0	0.03	0.009	0.5	10	5.5
DuivendrMiddenpolder	2013	0	0.09	0.02	0.5	19	6
Von Liebigweg	2013	0	0.03	0.0003	0	260	27

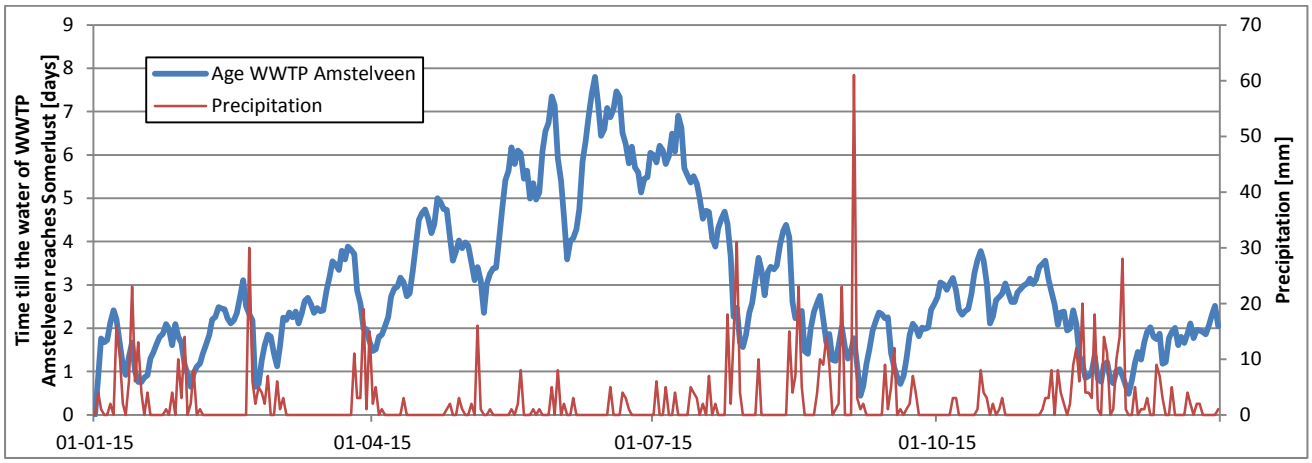

Figure 60 Travel time from the water of WWTP Amstelveen till Somerlust plotted together with the rainfall (2015)

8. Source analysis Somerlust summer 2016

Table 32 Results of the q-PCR analysis for source determination of faecal bacteria at Somerlust (2016)

		Human	Ruminant	Horse	Dog	Birds
Date	Location	Bacteroides				Helicobacter
25-04-16	Somerlust	$5.80.10^{4}$	<	-	<	<
17-05-16	Somerlust	$1.30.10^{4}$	<	-	<	<
30-05-16	Somerlust	$1.20.10^{5}$	$1.40.10^{3}$	-	<	<
13-06-16	Somerlust	$8.40.10^{4}$	<	-	<	<
27-06-16	Somerlust	$1.30.10^{5}$	$1.10.10^{4}$	-	<	<
11-07-16	Somerlust	$3.00.10^{5}$	$3.60.10^{3}$	-	<	<
25-07-16	Somerlust	$1.30.10^{5}$	<	-	$1.00.10^{4}$	<
08-08-16	Somerlust	$7.80.10^{4}$	<	-	<	<
22-08-16	Somerlust	$5.00.10^{6}$	$1.10.10^{4}$	-	$6.60.10^{3}$	<
05-09-16	Somerlust	$2.50.10^{5}$	<	-	<	<
19-09-16	Somerlust	$3.00.10^{5}$	<	-	$2.50.10^{4}$	<

9. Location tHuis aan de Amstel, where the samples are taken in 2014, compared to Somerlust

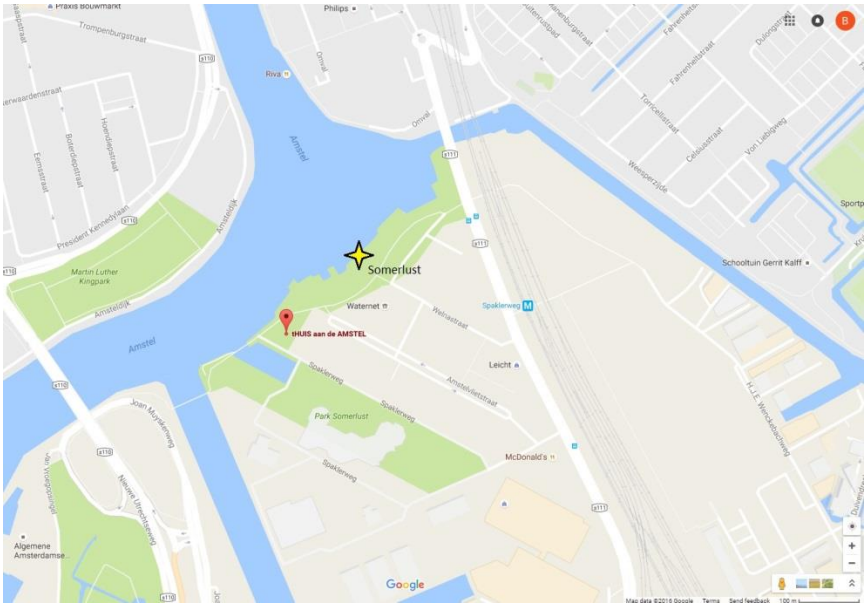

Figure 61 Location tHuis aan de Amstel compared to Somerlust

10. Fraction calculations of the E coli concentration at Somerlust and their origin

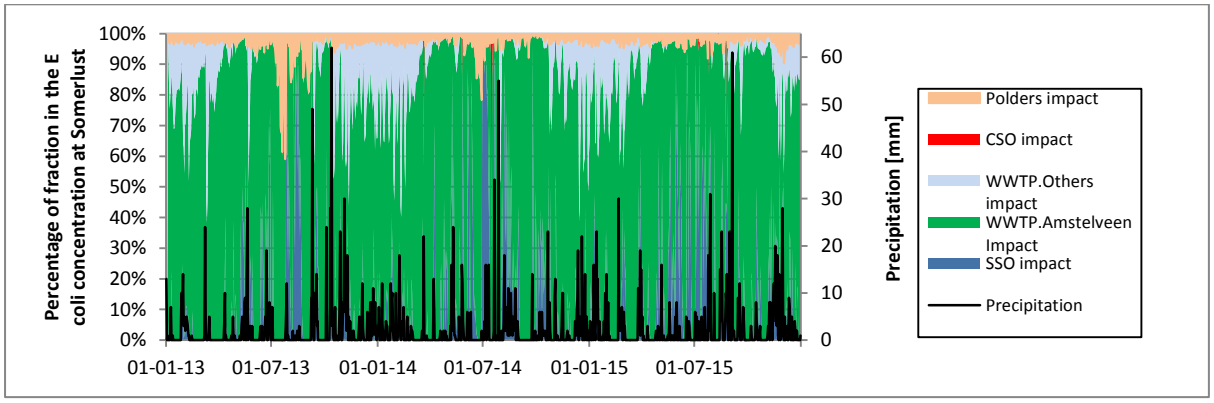

Figure 62 Figure with percent of each of the defined fractions in the *E coli* concentration at Somerlust including precipitation

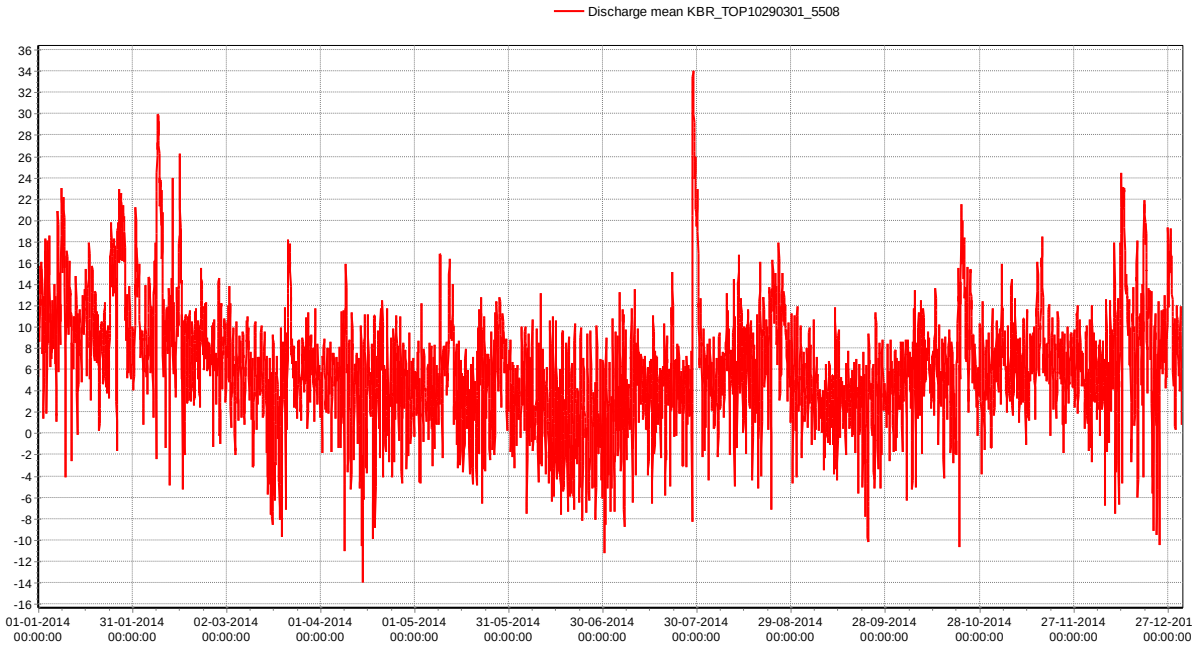

Figure 63 Hourly discharges in 2014 at the Berlagebrug close to the locations of the CSOs

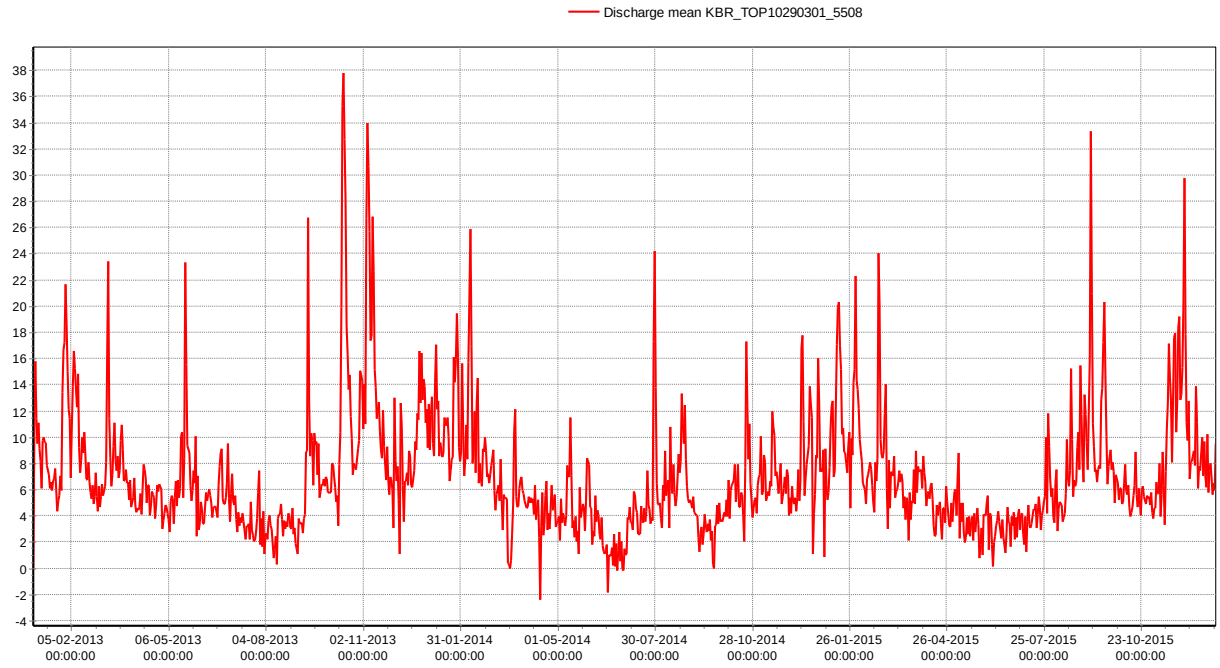

Figure 64 Daily discharges at the Berlagebrug close to the locations of the CSOs

11. E coli concentration at Somerlust in the summer of 2013 with fractions and precipitation

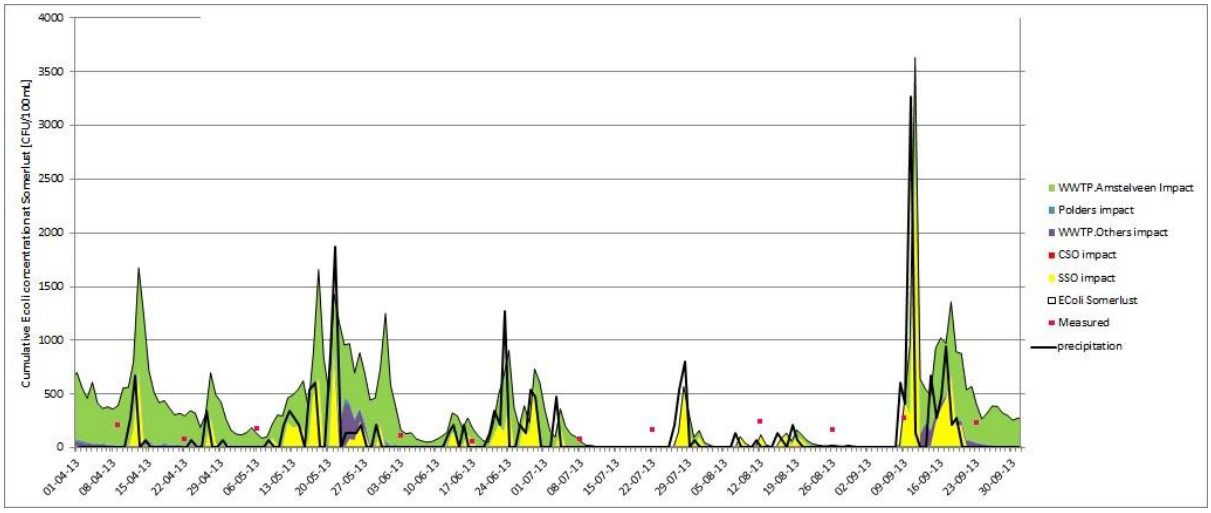

Figure 65 *E coli* concentration at Somerlust in the summer of 2013 with fractions and precipitation